Supporting Information

Triplet-Triplet Annihilation Upconversion in Laponite/PVP Nanocomposites: Absolute Quantum Yields up to 23.8% at Solid-State and Application to Anti-counterfeiting

Lingling Wei,[a] Chunying Fan,[b] Ming Rao,[a] Fanrui Gao,[a] Cheng He,[a] Yujiao Sun,[a] Sijia Zhu,[a] Qiuhui He,[a] Cheng Yang[a] and Wanhua Wu[a]*

[a] Key Laboratory of Green Chemistry & Technology of Ministry of Education, College of Chemistry, State Key Laboratory of Biotherapy, and Healthy Food Evaluation Research Center, Sichuan University, Chengdu 610064, China

[b]School of Pharmacy, Health Science Center, Xi'an Jiaotong University, Xi'an 710061 (China)

Contents

1.0 General S2
2.0 The detailed preparation process of the nanocomposite gels S9
3.0 Synthesis and gel preparation S12
4.0 NMR and MS spectra of the UC components S22
5.0 Characterization of the hydrogels S49
6.0 Photophysical property details of the UC dyes pair S52
7.0 Upconversion details in hydrogels S60
8.0 Characterization of dried gel S49
9.0 Upconversion details in dried gels S70
10.0 Reference S74

1.0 General

All reagents and solvents for synthesis were used as received without further purification. Solvents were dried and distilled before use. Platinum (II) octaethylporphyrin (PtOEP), 9,10-diphenylanthracene (DPA), Laponite XLG ($Mg_{5.34}Li_{0.66}Si_8O_{20}$ $(OH)_4Na_{0.66}$), Surfactant Triton X-100, Monomer N-Vinyl-2-Pyrrolidinone (NVP) and initiator 2,2-Azobis(2-Methylpropionitrile) (AIBN) and 1-Iododecane were obtained from commercial suppliers. Other sensitizers and annihilators were synthesized according to modified procedures of the literature method.[1-4]

^1H NMR and ^{13}C NMR spectra were recorded at room temperature on Bruker AMX-400 (operating 400 MHz for ^1H NMR and 101 MHz for ^{13}C NMR) with TMS as the internal standard. Thermogravimetric analysis (TG) was recorded using a DTG-60 instrument, and the samples were heated under nitrogen gas at a rate of 10 °C/min. HRMS data were measured with a waters-Q-TOF Premiers (ESI) and a MALDI-TOF-MS spectrometer. UV-vis spectra were obtained on JASCO V-650. Fluorescence spectra and Fluorescence lifetime decay were taken on Fluoromax-4 spectrofluorometer. Absolute quantum yields were taken on a Horiba Fluorolog TCSPC spectrometer equipped with a calibrated integrating sphere system. DLS and Zeta potential experiments were recorded using a Malvern Zeta / sizer Nano ZS90. Scanning Electron Microscopy (SEM) images were recorded on JSM-5900LV. Transmission electron microscopy (TEM) images were recorded on JEOL JEM-F200. The monomer conversion ratio was obtained by gas chromatography (GC-2010). FTIR spectra was taken on IRTracer100. Differential Scanning Calorimetry (DSC) curves was obtained on DSC214 and the samples were heated under nitrogen gas at a rate of 10 °C/min. X-ray diffraction (XRD) spectra was obtained on X' Pert Pro MPD DY129.

TTA upconversion quantum yield and efficiencies of the involved photophysical steps:

For TTA-UC emission measurements, diode pumped solid state (DPSS) lasers (532 / 589 nm) were used for the upconversion and diameter of the laser spot was ca. 1 mm. The upconversion quantum yields (Φ_{UC}) of the UC hydrogel was measured by a relative method, using the prompt fluorescence of Rhodamine B (Φ_F = 89 % in ethanol) as the standard. The uponversion quantum yields were calculated with equation (1):

$$\Phi_{UC} = \Phi_{std} \frac{A_{std}}{A_{sam}} \frac{I_{sam}}{I_{std}} \left(\frac{\eta_{sam}}{\eta_{std}}\right)^2 \qquad \text{equation (1)}$$

where A, I, and η represent the absorbance, integrated photoluminescence intensity and the refractive index of the solvent, respectively, the subscript sam and std represent the sample and standard, respectively.

The Φ_{UC} for the dry gel was obtained by two methods: the absolute method and the relative method. For the absolute method, a Horiba Fluorolog TCSPC spectrometer equipped with a calibrated integrating sphere system was used and an external space laser with a laser spot diameter of ca. 1 mm was used as the excitation source. Four-curve method was adopted to avoid the influence of the scattered laser. In order to reduce the negative influence of the self-absorption, the thickness of investigated sample was controlled to be 0.5-1mm. Two batches of samples with different sample thickness were prepared and the two batches of samples was distinguished by the absorption difference between the blank and the sample. The absorption differences for Batch 1 samples were controlled to <5%, and for Batch 2, were ca. 4%~10%. The specific steps are as follows: Step1: the laser beam is directed into the sphere to obtain excitation spectra of blank (wavelength range: 522-542 nm), filter was used to make sure the maximum intensity of excitation below 10^6 CPS. A similar hydrogel without UC components doping was used as the blank to assure the same same scattering of light with that of the sample and the blank was newly measured for every sample; Step 2: Remove the filter and adjust the wavelength range (380 - 525 nm) to get emission spectra of blank; Step 3: After the sample was placed in the sample holder, the excitation

spectra of sample was measured at the same condition as that of the blank (wavelength range: 527 - 537 nm); Step 4: The emission spectra of sample at the wavelength range of 380 - 525 nm was obtained at the same conditions of the blank. The quantum yield of the sample was calculated directly with the software on the instrument, without further data processing. A schematic diagram about four-curve method and a typical original spectrum showing the measurement of absolute UC quantum yield were shown in the part 7 (Fig. S99 and S100) and the original data were summarized in Table S1:

Table S1. Absolute UC quantum yields in solid matrix achieved in the present study.

Samples[a]		QY[b] (%)	Abs Error[c]	La[d]	Lc[e]	$D_{Abs.}$[f] (%)	Ea[g]	Ec[h]
Batch 1	Sample 1	26.3	2.77	1.11E6	1.12E6	0.9	4.25E6	5.36E5
	Sample 2	21.6	1.64	1.10E6	1.12E6	1.8	4.80E6	5.35E5
	Sample 3	22.1	2.69	1.26E6	1.28E6	1.6	3.56E6	6.50E5
	Sample 4	22.7	4.10	1.12E6	1.13E6	0.9	2.49E6	6.04E5
	Sample 5	18.6	3.59	1.33E6	1.34E6	0.8	2.22E6	6.52E5
	average	**22.3**						
Batch 2	Sample 6	27.7	0.81	1.04E6	1.09E6	4.6	1.44E6	5.45E5
	Sample 7	24.3	0.59	1.17E6	1.28E6	8.6	2.42E6	7.21E5
	Sample 8	23.3	0.39	1.04E6	1.13E6	8.0	2.10E7	6.09E5
	Sample 9	22.8	0.35	1.19E6	1.29E6	7.8	2.39E7	7.20E5
	Sample 10	21.1	0.62	1.04E6	1.1E6	5.5	1.11E7	5.92E5
	average	**23.8**						

[a] the samples were nanocomposite dry gels doped with **PtOEP** and **DPAS** which were prepared independently. [b] absolute UC quantum yield. [c] Absolute error of measurement; [d] L_a is the number of photons in the excitation wavelength region (527 nm - 537 nm) with the sample present in the sphere; [e] Lc is the number of photons in the excitation wavelength region (527 nm - 537 nm) with the blank present in the sphere; [f] absorption difference between the blank and the sample, calculated by $D_{Abs} = (Lc-La)/Lc$; [g] Ea is the number of photons in the emission wavelength region (380 nm -

525 nm) with the sample present in the sphere; [h] Ec is the number of photons in the emission wavelength region (380 nm - 525 nm) with the blank present in the sphere.

A relative method was also employed to determine the Φ_{UC} of the dry gel using the absolute quantum yield of **PtOEP** in dry gel as the standard (Φ = 37.65%, $C_{\mathbf{PtOEP}}$ = 10 μM) and the Φ_{UC} was calculated with equation (1). The concentrations of the sample and standard were carefully controlled to be the same, thus the ratio of the absorbance between the sample and the standard can be equal to the thickness. The thickness of the solid samples was measured with a vernier caliper. Also, the refractive index was reorganized to be the same. The results of ten independent samples were listed in Supplementary Table 2, and the average value was in accordance with results determined with the absolute method.

Table S2. UC quantum yields calculated by relative method in solid matrix achieved in the present study.

Samples	Thickness[a]	QY[b] (%)
PtOEP	1 mm	37.65
Sample 1	0.5 mm	27.2
Sample 2	0.5 mm	26.2
Sample 3	0.5 mm	24.5
Sample 4	0.7 mm	24.2
Sample 5	0.5 mm	23.6
Sample 6	0.5 mm	23.3
Sample 7	0.5 mm	22.3
Sample 8	0.5 mm	22.2
Sample 9	0.5 mm	21.1
Sample 10	0.7 mm	20.9
average	23.6	

[a] the thickness of samples. [b] UC quantum yield calculated by the relative method. (Note: using the absolute quantum yield of **PtOEP** in dry gel as the standard (Φ = 37.65 %, C_{PtOEP} = 10 μM).)

The efficiencies of all the involved photophysical steps were quantitatively analyzed. The quantum yield of photo-upconversion through TTA is actually the product of the efficiencies of all the involved photophysical steps:

$$\Phi_{UC} = \frac{1}{2}\Phi_{(S,ISC)}\Phi_{TTET}\Phi_{TTA}\Phi_{A,F} \qquad \text{equation (2)}$$

Where $\Phi_{S,ISC}$ is the quantum yield of intersystem crossing (ISC) of the sensitizers, herein, Pt complexes with efficient ISC were used as sensitizers,$\Phi_{ISC,S}$ was designated as 100%;Φ_{TTET} is the quantum efficiency of triplet energy transfer from the sensitizer to the annihilator which can be estimated by equation (3):

$$\Phi_{UC} = 1 - \frac{\Phi_P}{\Phi_{P0}} \qquad \text{equation (3)}$$

Where Φ_p and Φ_{p0} represent the phosphorescence quantum yield of sensitizers with and without the annihilators, respectively.

$\Phi_{A,F}$ is the fluorescence quantum yield of the annihilator. In the present study, $\Phi_{A,F}$ was determined by the relative method using DPA as the standard (Φ_F = 95% in ethanol).

Φ_{TTA} is the quantum efficiency of the TTA between two annihilators in their triplet states and can be quantitatively calculated using eq (3).

Gas Chromatography Analysis for the Determination of Monomer Conversion Rate

The monomer conversion rate was obtained using the internal standard method. 1-Iododecane as the internal standard.

The preparation steps of the control group are as follows: To 20.0 μL of NVP was injected into 2.0 mL acetone solvent, then 1-Iododecane (10.0 μL) was added as internal standard. The mixture solution was treated to ultrasonic for 5 min to assure thoroughly mixing. Then 10 μL of the mixture was injected into GC to analysis.

The preparation steps of the experimental group are as follows: To 1.0 mL solution of NVP monomer was added 5.2 mg initiator (AIBN) to obtain a mother solution (Quality ratio: NVP: AIBN = 200:1). The quality ratio of NVP and AIBN was the same as in hydrogel preparation. Every time, 20.0 μL mother solution was heated at 70 °C for given time, then the polymerization was terminated by lowering the temperature. 2.0 mL acetone was added to dissolve the unreacted NVP, and 10.0 μL 1-Iododecane was added as the internal standard. The obtained mixture was treated to ultrasonic for 5 min to assure thoroughly mixing, then 10 μL of the mixture was injected into GC to analysis.

The amount of unreacted monomer can be obtained by GC analysis by the peak area ratio of monomer NVP (Ai) and internal standard (As) (eq (4)), the conversion rate of monomer (C/%) was calculated through the total amount minus the amount of unreacted monomer of different polymerization time.

$$C/_{\%} = 1 - \frac{A_i/_{A_s}}{A_i/_{A_s}} \qquad \text{equation (4)}$$

The results were displayed in table S3 and the Figure were shown in Fig. S79.

Isothermal Adsorption Experiment: Firstly, we prepared a clay dispersion with a mass fraction of 1% in water by exposing to ultrasonic for 10 minutes, to which different concentrations of **DPAS** from 10 μM to 700 μM was added. The dispersion was further stirred at room temperature for approximately 24 h to achieve an adsorption equilibrium. The expersion was then centrifuged and the supernatant was collected to measure the UV-Vis spectra (JASCO, Japan) to determine the concentration of free **DPAS** (the equilibrium concentration of **DPAS** , Ce, mg L^{-1}), by using a quartz cuvette with 2 mm optical path. The absorbance at the wavelength (λ) of 379 nm was used to determined the concetration according to a calibration curve of absorbance as a function of **DPAS** concentration. The adsorbed amount of **DPAS**, Q_e (mg g^{-1}) was then determined according to equation (5) where C_{clay} (mg L^{-1}) is the concentration of Laponite in the sample and C_0 is the initial concentration of **DPAS**.

$$Q_e = \frac{C_0 - C_e}{C_{clay}} \times 1000 \qquad \text{equation (5)}$$

The adsorption capacity (Q_e) of **DPAS** by nanosheets was determined to be 19.7 mg/g according to the adsorption isotherms curves (Fig.S102).

Calculation of the Ratio of Acceptors Absorbed per Nanosheet.

• the diameter and thickness of a single clay nanoparticle were 30 nm and 1~2 nm, respectively.

• the surface area of single clay nanosheet: $2\pi r^2 + \pi dh = 1.5\sim1.6 \times 10^{-15}\ m^2$

• the surface area of the commercial Laponite XLG was 370 m^2/g, which was easily available from the supplier. We used 40 mg clay for preparing the hydrogel, thus the numbers of nanoparticles of this system is $9.2\sim9.8 \times 10^{15}$.

•mol mass of absorbed acceptors (n_a) = $Q_e \times m / M = 19.7 \times 40 \times 10^{-6} / 432.47 = 1.8 \times 10^{-6}$ mol;

• number of absorbed acceptors (N_a) = $n_a\ NA \approx 1.8 \times 10^{-6} \times 6 \times 10^{23} \approx 11 \times 10^{17}$;

• the ratio of acceptor molecules absorbed per nanosheet : Na / Nc ≈ 112~119;

• the circumference of each clay: πd = 94.2 nm;

• the distance between each two acceptors: 94.2/112 ~94.2/119 ≈ 7.9~8.4 Å, an average value of 8.2 Å was used.

Jablonski diagram of the TTA-UC process

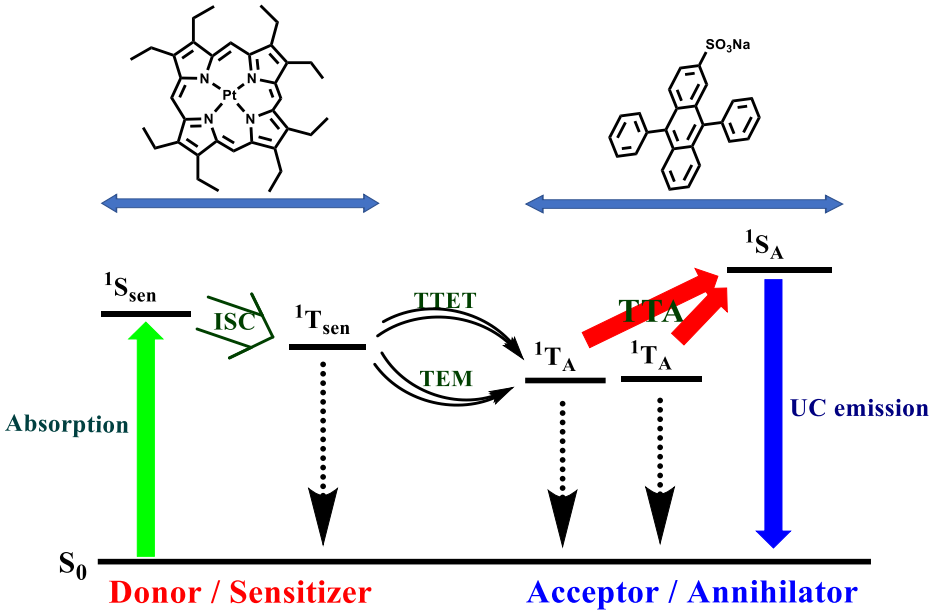

Fig. S1 Jablonski diagram of the TTA-UC process. S_0 represents the ground state, ^{1}Ssen and ^{1}Tsen represent singlet and triplet excited state of the Donor / Sensitizer, respectively. ^1S_A and ^1T_A represent singlet and triplet excited state of the Acceptor / Annihilator, respectively. ISC represent the intersystem-crossing, TTET is triplet-triplet energy transfer, TEM is triplet energy migration, and TTA is triplet-triplet annihilation, respectively. Up-arrow (green), down-arrow (blue) and dotted-arrow (black) represent absorption, emission and nonradiative transition, respectively.

Summary of the upconversion quantum yield ever achieved in solid state

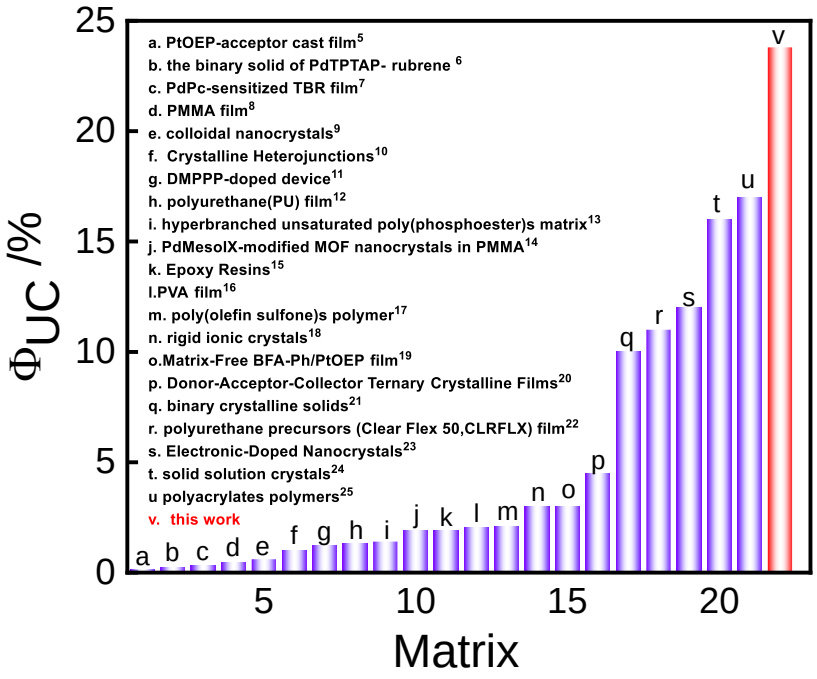

Fig. S2 Summary of maximum UC quantum yield ever reported in solid matrix since 2012. Note: the quantum yields have been unified with theoretical maximum of 50%. Note: in ref 12, the theoretical maximum for calculating UC efficiency was not clear, the reported UC quantum yield was used directly.

2.0 The detailed procedures for preparing nanocomposite gels.

Preparation of the nanocomposite XLG/PVP hydrogels

XLG/PVP UC hydrogel was prepared by using N-vinyl pyrrolidone (NVP) as monomer, azodiisobutyronitrile (AIBN) as initiator and Laponite XLG ($Mg_{5.34}Li_{0.66}Si_8O_{20}$ $(OH)_4Na_{0.66}$) as cross-linking agent and reinforcer. The UC components were added in the precursor solution before polymerization. Using XLG/PVP UC hydrogel doped with **PtOEP** and **DPAS** as an example:

As schemed in Fig. S3, under air atmosphere, 42.0 mg Laponite XLG was suspended in 815 μL water (mass fraction: 4.0 %) to give a thick solution; AIBN (26.0 mg) was dissolved in NVP (5.0 mL), of which 100 μL was injected into the thick solution, then the surfactant Triton X-100 (50 μL) was added to achieve a precursor

solution. The mother solution of the UC components **PtOEP** and **DPAS** were prepared with DMF, with the concentration of 1 mM and 100 mM, respectively. According to the required concentration of the sensitizer and annihilator, the required volume of the mother solution was calculated and was added to the precursor solution, e.g., for the hydrogel doped with 10 μM **PtOEP** and 2.5 mM **DPAS**, 10 μL and 25 μL of the mother solution were added for **PtOEP** and **DPAS**, respectively. The resulting solution was heated at 70 °C for 10 min until a homogeneous transparent hydrogel was obtained.

Similar procedures were used to prepare hydrogels doped with other UC components, except the mother solution was different. **PtTCPP** was prepared in CH_3OH, with the concentration of 1 mM. **Pt-1** and **Pt-2** were prepared in toluene, with the concentration of 1 mM. The mother solution of the **A-1**, **A-2**, **A-3**, **A-4** were prepared with DMSO, with the concentration of 20 mM.

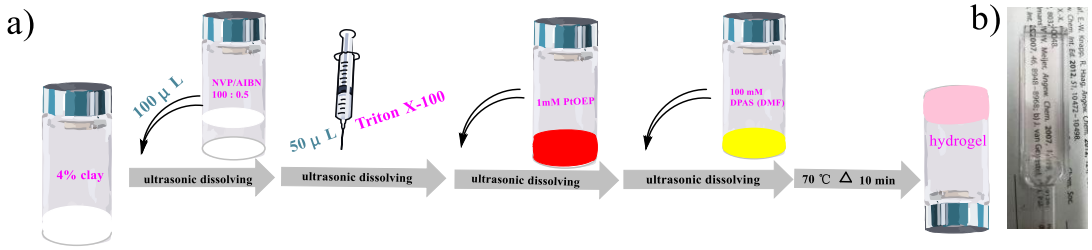

Fig. S3 (a) The graphic illustration of the preparation of XLG/PVP hydrogel doped with **PtOEP** and **DPAS**. (b) A XLG/PVP hydrogel sample doped with 20 μM **PtOEP** and 5 mM**DPAS**.

Preparation of the nanocomposite XLG / PMMA hydrogels

XLG/PMMA UC hydrogel was prepared by using methyl methacrylate (MMA) as monomer, azodiisobutyronitrile (AIBN) as initiator and Laponite XLG as cross-linking agent and reinforcer. Under air atmosphere, 1.04 g MMA was dissolved in water (4.0 mL), 42.0 mg Laponite XLG was suspended in 815 μL water of MMA (mass fraction: 4.0 %) to give a thick solution; AIBN (26.0 mg) was dissolved in 2.0 mL DMF, of which 100.0 mL was injected into the thick solution then the surfactant Triton X-100 (50 μL) was added to achieve a precursor solution. The mother solution of the UC dyes pair **PtOEP** and **DPAS** was prepared with DMF, with the concentration of 1 mM and 100 mM, respectively. For the XLG/PMMA UC hydrogels doped with 10 μM **PtOEP**

and 2.5 mM **DPAS**, 10 μL and 25 μL of the mother solution were added for **PtOEP** and **DPAS**, respectively. The resulting solution was heated at 70 °C for 10 min until a homogeneous transparent hydrogel was obtained.

Preparation of the gelatin hydrogel

Gelatin hydrogel was prepared strictly according to previous report.[26] 250.0 mg gelatin was dissolved in 1.0 mL water (mass fraction: 20.0 %) to give a thick solution; then the surfactant Triton X-100 (25.0 mg) was added to achieve a precursor solution. The mother solution of the UC dyes pair **PtOEP** and **DPAS** was prepared with DMF, with the concentration of 1 mM and 100 mM, respectively. For the gelatin hydrogel doped with 10 μM **PtOEP** and 2.5 mM **DPAS**, 10 μL and 25 μL of the mother solution were added for **PtOEP** and **DPAS**, respectively. The resulting solution was heated at 90 °C for 30 min, after slow cooling to room temperature, the solution undergoes a thermoreversible transition from a liquid to a gel.

Preparation of the dry gel

The XLG/PVP hydrogel doped with 10 μM **PtOEP** and 2.5 mM **DPAS** was molded into different shapes and then was treated to vacuum drying at 55 °C for ~24 h to remove all water, the sample was characterized with thermogravimetric analysis (TG) to show whether all solvent was removed or not (Fig. S94).

Home-made process of information encryption and anti-counterfieting

The dried gels with **PtOEP**/**DPAS** doped or only **DPAS** doped were crushed into powers with an agate mortar. The powders were placed on a white paper with the encrypted information section filling with **PtOEP**/**DPAS** doped gels and the others with **DPAS** doped gels. The images were observed under ambient light, 365 nm UV light and 532 nm laser, respectively. The spot of the laser was expanded from 1 mm to 7.5 cm by 8X expander (N2787-5) coupling with a convex len for fast imaging of the whole picture instead of point-by-point scanning commonly required for TTA-UC emission. The power density of the laser (after expanding) was 1.13 mW cm^{-2}. The images was captured with the camera implanted in a cell phone (iphone 13), and a notch filter (532 nm, NF01-532U-25) was placed before the camera.

3.0 Synthesis

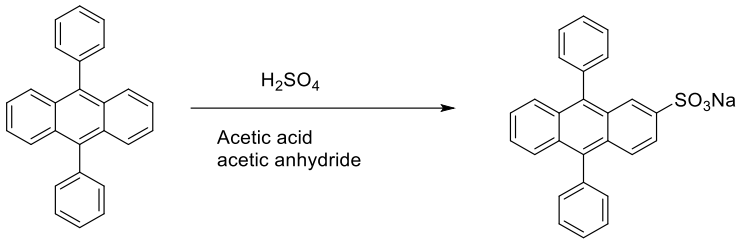

DPAS

Synthesis of Sodium 9,10-diphenylanthracene-2-sulfonate (DPAS)

DPAS was synthesized with modified procedure of the reported method [1]. To an acetic acid (1.8 mL) and acetic anhydride (0.2 mL) solution of 9,10-diphenylanthracene (DPA, 500.0 mg, 1.5 mmol) was added 450 μL concentrated sulfuric acid (98 %). The mixture was stirred in an ice bath for 20 min. Then the mixture was heated to reflux at 120 °C for 1 h. After cooling, 0.9 g NaCl and 8.0 mL H_2O were added, and the mixture was heated to reflux again for another 1 h. After cooling to the room temperature, the resulting mixture was neutralized by adding 5.0 % aqueous solution of NaOH, the generated light-yellow precipitate was collected through membrane filtration. The obtained solid was added 20.0 mL EtOH, the undissolved solid was separated by membrane filtration. The solution was added 60.0 mL water, precipitates was collected, and then was put into 30 % EtOH aqueous solution, the undissolved solid was collected as the product. (182.0 mg, 28.0 %)

^{1}H NMR spectra were recorded, which were in according to literature values.[1] ^{1}H NMR (400 MHz, CD_3OD) δ 8.26 (dd, *J* = 1.4, 0.9 Hz, 1 H), 7.73 - 7.54 (m, 11 H), 7.41 (m, *J* = 10.6, 9.6, 4.6, 3.1 Hz, 6 H).^{13}C NMR (101 MHz, CD_3OD) δ 141.0, 138.7, 138.6, 138.3, 137.1, 130.9, 130.9, 130.7, 130.4, 129.6, 128.5, 128.3, 127.6, 127.5, 127.0, 126.6, 126.5, 125.4, 125.2, 124.3, 121.9, 56.9, 17.0.

HRMS calcd for $[M + H]^+$ m/z = 433.0869, found m/z = 433.0877.

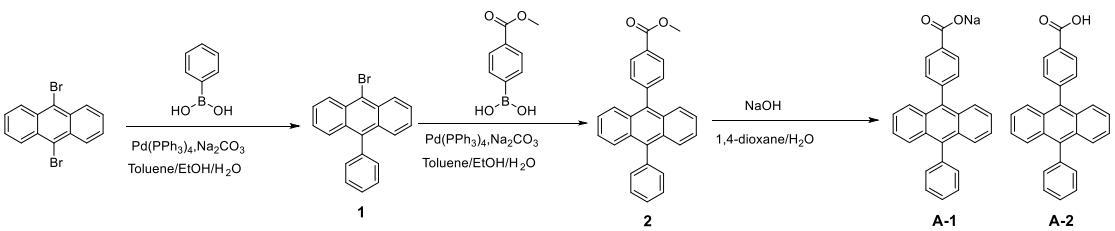

Synthesis of compound 1[2]

Under N_2 atmosphere, 9,10-dibromoanthracene (2.0 g, 6.0 mmol), phenylboronic acid (0.7 g, 6.0 mmol), $Pd(PPh_3)_4$ (0.6 mg, 0.6 mmol) and Na_2CO_3 (2.3 g, 20.0 mmol) was added to a mixed solution of toluene (30.0 mL), ethanol (10.0 mL) and distilled water (12.0 mL). The solution was heated to reflux for 3 h. The solvent was removed under reduced pressure and the resulted residue was subjected to column chromatography on silica gel using PE/CH_2Cl_2 (3:1, v : v) as the eluent to give a white solid of compound 1 (0.6 g, 30.0 %).

^{1}H NMR spectra were recorded, which were in according to literature values.[2] ^{1}H NMR (400 MHz, $CDCl_3$) δ 8.59 (d, *J* = 8.8 Hz, 2 H), 7.62 (dt, *J* = 8.8, 0.9 Hz, 2 H), 7.59 - 7.49 (m, 5 H), 7.41-7.31 (m, 4 H). ^{13}C NMR (101 MHz, $CDCl_3$) δ 138.4, 137.8, 131.1, 131.0, 130.2, 128.4, 127.8, 127.7, 127.4, 126.9, 125.5. MALDI-TOF calcd for [M] m/z = 332.0201, found m/z = 331.7308.

Synthesis of compound 2[2]

Under N_2 atmosphere, compound 1 (0.2 g, 0.6 mmol), 4-(methoxycarbonyl) phenylboronic acid (108.0 mg, 0.6 mmol), $Pd(PPh_3)_4$ (60.0 mg, 0.06 mmol) and Na_2CO_3 (2.3 g, 20.0 mmol) was added to a mixed solution of toluene (6.0 mL), ethanol (2.0 mL) and distilled water (3.0 mL). The mixture was heated to reflux for 3 h. The solvent was removed under reduced pressure and the resulted residue was subjected to column chromatography on silica gel using PE/CH_2Cl_2 (1:1, v: v) as the eluent to give a white solid of compound 2 (116.5 mg, 50.8 %).

^{1}H NMR spectra were recorded, which were in according to literature values.[2] ^{1}H NMR (400 MHz, $CDCl_3$) δ 8.30 (d, *J* = 8.2 Hz, 2 H), 7.74 - 7.68 (m, 2 H), 7.65 - 7.53 (m, 7 H), 7.51 - 7.45 (m, 2 H), 7.35 (dt, *J* = 6.9, 3.2 Hz, 4 H), 4.03 (s, 3 H).^{13}C NMR (101 MHz, $CDCl_3$) δ 167.1, 144.3, 138.9, 137.7, 135.7, 131.5, 131.3, 129.7, 128.4, 127.11, 126.5, 125.4, 125.1, 52.3. HRMS calcd for [M] m/z = 388.1463, found m/z = 388.1474.

Synthesis of compound A-1 and A-2[2]

To mixed solution of 1,4-dioxane (10.0 mL) and distilled water (2.0 mL) was added compound 2 (116.0 mg, 0.3 mmol) and NaOH (0.4 g, 10 mmol). The solution was heated to reflux for 6 h at 90 °C. Then, the solvent was removed under reduced pressure

and then 20 mL water was added, abundant light-yellow precipitation was formed. **A-1** was obtained by direct filtration (69.2 mg, 58.2 %), while **A-2** was obtained by adjusting pH to 7 with HCl before filtration (58.4 mg, 52.0 %).

^{1}H NMR of **A-1** (400 MHz, DMSO-d6) δ 8.21 (d, *J* = 8.2 Hz, 2 H), 7.70 - 7.64 (m, 2 H), 7.64 - 7.56 (m, 7 H), 7.55 (dt, *J* = 6.0, 2.3 Hz, 2 H), 7.50 - 7.40 (m, 6 H).^{13}C NMR of **A-1** (101 MHz, DMSO-d_6) δ 138.5, 137.4, 131.5, 131.4, 130.0, 129.6, 129.4, 129.2, 128.3, 126.9, 126.7, 126.2, 126.1. HRMS calcd for $[M-Na]^-$ m/z = 373.1234, found m/z = 373.1220.

^{1}H NMR spectra were recorded, which were in according to literature values.[2] ^{1}H NMR of **A-2** (400 MHz, DMSO-d_6) δ 13.17 (s, 1 H), 7.70 - 7.64 (m, 2 H), 7.64 - 7.57 (m, 5 H), 7.57 - 7.51 (m, 2 H), 7.45 (ddd, *J* = 13.2, 7.6, 2.5 Hz, 6 H).^{13}C NMR of A-2 (101 MHz, DMSO-d_6) δ 167.7, 138.5, 137.5, 131.8, 131.3, 130.1, 129.6, 129.4, 129.2, 128.3, 126.9, 126.6, 126.3, 126.1. HRMS calcd for [M] m/z = 374.1307, found m/z = 374.1346.

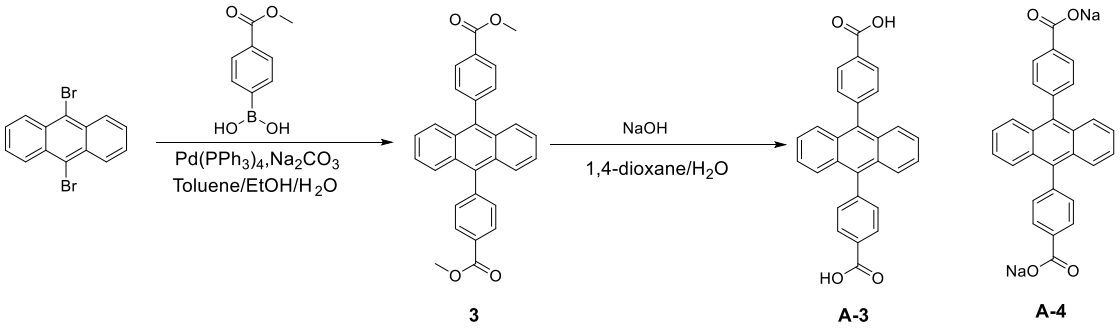

Synthesis of compound 3[2]

Under N_2 atmosphere, 9,10-dibromoanthracene (2.0 g, 6.0 mmol), 4-(methoxycarbonyl) phenylboronic acid (1.3 g, 7.2 mmol), $Pd(PPh_3)_4$ (0.6 mg, 0.6 mmol) and Na_2CO_3 (2.3 g, 20.0 mmol) was added to a mixed solution of toluene (30.0 mL), ethanol (10.0 mL) and distilled water (12.0 mL). The mixture was heated to reflux for 3 h at 100 °C. The solvent was removed under reduced pressure and the resulted residue was subjected to column chromatography on silica gel using PE/CH_2Cl_2 (1:1, v: v) as the eluent to give a white solid of compound 3 (428.2 mg, 32.1 %).

^{1}H NMR spectra were recorded, which were in according to literature values.[2] ^{1}H NMR (400 MHz, $CDCl_3$) δ 8.30 (d, *J* = 8.2 Hz, 4 H), 7.62 (dd, *J* = 6.8, 3.3 Hz, 4 H), 7.60 -

7.55 (m, 4 H), 7.38 - 7.32 (m, 4 H), 4.03 (s, 6 H).^{13}C NMR (101 MHz, $CDCl_3$) δ 167.1, 144.1, 136.3, 131.5, 129.8, 129.6, 129.5, 126.6, 125.5, 52.3. HRMS calcd for $[M + H]^+$ m/z = 447.1591, found m/z = 447.1593.

Synthesis of compound A-3 and A-4[2]

To a mixed solution of 1,4-dioxane (10.0 mL) and distilled water (2.0 mL) was added compound 3 (223.3 mg, 0.5 mmol) and NaOH (0.4 g, 10.0 mmol). The solution was heated to reflux for 6 h at 90 °C. The solvent was removed under reduced pressure, then 20 mL water was added, abundant light-yellow precipitation was formed. A-3 was obtained by direct filtration (117.2 mg, 56.0 %), while A-4 was obtained by adjusting pH to 7 with HCl before filtration (121.6 mg, 52.6 %).

^{1}H NMR spectra were recorded, which were in according to literature values.[2] ^{1}H NMR of **A-3** (400 MHz, DMSO-d_6) δ 13.12 (s, 2 H), 8.27 - 8.18 (m, 4 H), 7.66 - 7.59 (m, 4 H), 7.59 - 7.50 (m, 4 H), 7.51 - 7.41 (m, 4 H).^{13}C NMR of **A-3** (101 MHz, DMSO-d_6) δ 167.7, 143.3, 136.5, 131.7, 130.9, 130.1, 129.3, 126.7, 126.4. HRMS calcd for $[M + Na]^+$ m/z = 485.0737, found m/z = 485.0739.

^{1}H NMR of **A-4** (400 MHz, DMSO-d6) δ 8.22 (d, *J* = 8.3 Hz, 4 H), 7.63 - 7.58 (m, 4 H), 7.56 (dd, *J* = 6.8, 3.3 Hz, 4 H), 7.45 (dd, *J* = 6.9, 3.3 Hz, 4 H). ^{13}C NMR of **A-4** (101 MHz, DMSO-d_6) δ 167.8, 143.1, 136.5, 131.7, 130.1, 129.3, 126.7, 126.4. HRMS calcd for $[M + H]^+$ m/z = 419.1278, found m/z = 419.1280.

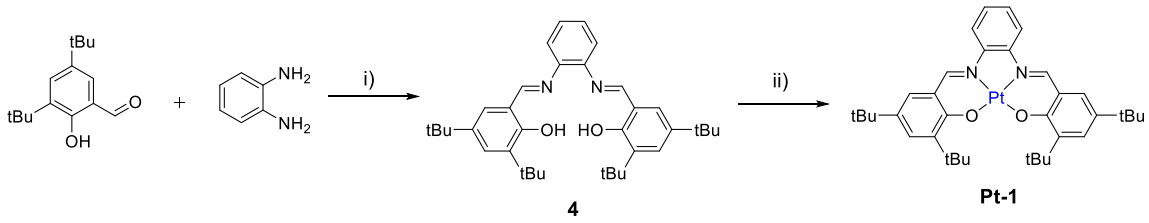

Scheme 1: Reagents and conditions: i) Ethanol, reflux; ii) K_2CO_3, K_2PtCl_4, DMSO, 95 °C.

Synthesis of compound 4[3]

To a 50.0 mL anhydrous EtOH solution of 3,5-di-tert-butylsalicylaldehyde (2.0 g, 8.3 mmol) was added 1,2-phenylenediamine (450.0 mg, 4.2 mmol). The solution was heated to reflux for 12 h. Then the reaction mixture was cooled in the ice bath, to result in the yellow precipitates. The yellow solid was obtained by filtration, the product was purified through recrystallized in EtOH to give compound 4 (1.6 g, 71.0 %).

^{1}H NMR spectra were recorded, which were in according to literature values.[3] ^{1}H NMR (400 MHz, $CDCl_3$): 8.66 (s, 2 H), 7.44 (d, *J* = 2.5 Hz, 2 H), 7.31 (m, 2 H), 7.26 - 7.23 (m, 2H), 7.22 (d, *J* = 2.4 Hz, 2 H), 1.44 (s, 18 H), 1.33 (s, 18 H). ^{13}C NMR (101 MHz, $CDCl_3$) δ 164.7, 158.6, 142.8, 140.3, 137.2, 128.2, 127.9, 127.3, 126.8, 119.8, 118.4, 35.1, 34.2, 31.5, 31.3, 29.4, 29.3. HRMS calcd for $[M + H]^+$ m/z = 541.3789, found m/z = 541.3790.

Synthesis of Pt-1[3]

Compound 4 (500.0 mg, 0.9 mmol) and K_2PtCl_4 (384.0 mg, 1.0 eq) was dissolved in 15.0 mL DMSO, then K_2CO_3 (383.0 mg, 3.0 eq) was added. The mixture was stirred at 95 °C under N_2 atmosphere for 5 h. The reaction mixture was diluted with CH_2Cl_2 and washed with H_2O. The organic layer was collected, and the aqueous layer was extracted with CH_2Cl_2 for 2 times, the combined organic layers concentrated, and the residue was subjected to column chromatography on silica gel using PE/CH_2Cl_2 (3:1, v: v) as the eluent to give a red solid of compound Pt-1 (319.0 mg, 47.0 %).

^{1}H NMR spectra were recorded, which were in according to literature values.[3] ^{1}H NMR (400 MHz, $CDCl_3$) δ 8.83 (s, 2 H), 7.94 (d, *J* = 9.7 Hz, 2 H), 7.67 (s, 2 H), 7.30 (s, 2 H), 7.24 (dd, *J* = 6.6, 3.4 Hz, 2 H), 1.59 (s, 18 H), 1.36 (s, 18 H).^{13}C NMR (101 MHz, $CDCl_3$) δ 164.3, 148.5, 145.3, 141.5, 137.5, 131.0, 127.9, 126.7, 120.8, 114.9, 36.2, 34.0, 31.3, 29.7. HRMS calcd for [M] m/z = 733.3207, found m/z = 733.3259; $[M + H]^+$ m/z = 734.3280, found m/z = 734.3283.

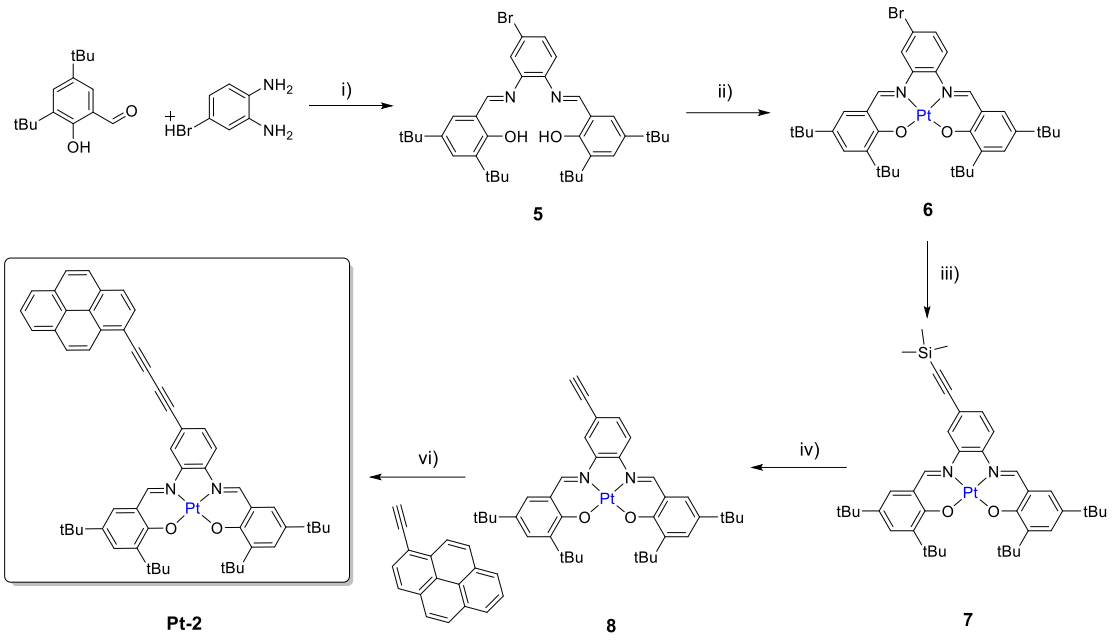

Scheme 2: Reagents and conditions: i) Ethanol, reflux; ii) K_2CO_3, K_2PtCl_4, DMSO, 95 °C; iii) Trimethylsilylacetylene, $Pd(PPh_3)_2Cl_2$, PPh_3, CuI, THF / NEt_3, reflux, 8 h; iv) K_2CO_3, THF / MeOH, r.t.; v) $Pd(PPh_3)_2Cl_2$, PPh_3, CuI, THF / NEt_3; vi) 1-Ethynylpyrene, $Pd(PPh_3)_2Cl_2$, CuI, THF / NEt_3, r.t.

Synthesis of compound 5[3]

To a 150 mL anhydrous EtOH solution of 3,5-di-tert-butylsalicylaldehyde (7.9 g, 33.6 mmol) was added 4-bromo-o-phenylenediamine (3.0 g, 16.0 mmol). The resulting solution was heated to reflux and was stirred for 12 h. The reaction mixture was cooled in the ice bath to result the yellow precipitates. The yellow solid was obtained by filtration, and the product was purified through recrystallized in EtOH to give compound 5 (2.1 g, 21.7 %)

^{1}H NMR spectra were recorded, which were in according to literature values.[3] ^{1}H NMR (400 MHz, $CDCl_3$) δ 8.63 (t, *J* = 6.6 Hz, 2 H), 7.46 (dt, *J* = 5.6, 2.9 Hz, 2 H), 7.42 (dd, *J* = 8.4, 2.1 Hz, 1 H), 7.38 (d, *J* = 2.1 Hz, 1 H), 7.22 (s, 1 H), 7.20 (d, *J* = 2.4 Hz, 1 H), 7.11 (d, *J* = 8.4 Hz, 1 H), 1.43 (s, 18 H), 1.32 (d, *J* = 1.9 Hz, 18 H). ^{13}C NMR (101 MHz, $CDCl_3$) δ 165.4, 165.0, 158.6, 143.9, 141.9, 141.6, 140.6, 140.5, 137.6, 137.3, 131.9, 130.0, 128.7, 128.5, 127.9, 127.0, 126.9, 122.8, 121.1, 120.1, 118.2, 118.2, 35.1, 34.2, 31.5, 31.3, 29.4, 29.3. HRMS calcd for $[M + Na]^+$ m/z = 641.2714, found m/z = 641.2694.

Synthesis of compound 6[3]

Under N_2 atmosphere, compound 5 (2.2 g, 3.5 mmol) and K_2PtCl_4 (1.4 g, 1.0 eq) was dissolved in 30.0 mL DMSO, then K_2CO_3 (1.4 g, 3.0 eq) was added. The resulting solution was stirred at 95 °C for 5 h. The reaction mixture was diluted with CH_2Cl_2 and was washed with H_2O. The organic layer was collected, the aqueous layer was extracted with CH_2Cl_2 for 2 times, and the combined organic layers was concentrated. The resulting residue was subjected to column chromatography on silica gel using PE/CH_2Cl_2 (5:1, v: v) as the eluent to give a red solid of compound 6 (1.3 g, 46.0 %).

^{1}H NMR spectra were recorded, which were in according to literature values.[3] ^{1}H NMR (400 MHz, $CDCl_3$) δ 8.82 (d, *J* = 6.7 Hz, 2 H), 8.11 (d, *J* = 1.9 Hz, 1 H), 7.87 (d, *J* = 9.0 Hz, 1 H), 7.70 - 7.68 (m, 2 H), 7.43 (dd, *J* = 8.8, 1.9 Hz, 1 H), 7.34 (d, *J* = 2.5 Hz, 1 H), 7.31 (d, *J* = 2.5 Hz, 1 H), 1.58 (d, *J* = 1.5Hz, 18 H), 1.35 (d, *J* = 3.9 Hz, 18 H). ^{13}C NMR (101 MHz, $CDCl_3$) δ 164.8, 164.4, 148.6, 148.4, 146.3, 144.4, 141.6, 141.5, 137.9, 137.7, 131.9, 131.5, 131.3, 129.0, 127.9, 127.9, 127. 8, 120.7, 119.8, 117.9, 115.5, 36.2, 36.2, 34.0, 31.3, 31.3, 29.7, 29.3. HRMS calcd for [M] m/z = 811.2312, found m/z = 811.2268.

Synthesis of compound 7[3]

Under N_2 atmosphere, compound 6 (1.0 g, 1.2 mmol) was charged in a Schlenk tube, and was dissolved in 12.0 mL dry THF and 6.0 mL Et_3N, then Pd $(PPh_3)_2Cl_2$ (173.0 mg, 20.0 mmol %), PPh_3 (120.0 mg, 40.0 mmol %) and CuI (94.0 mg, 40.0 mmol %) were added, after strict degassing procedure, trimethylsilylacetylene (TMSA, 1.7 mL, 12.0 mmol) was added. The resulting solution was stirred at 85 °C for 12 h. The solvent was removed under reduced pressure and the resulting residue was subjected to column chromatography on silica gel using PE/CH_2Cl_2 (7: 1, v: v) as the eluent to give a dark purple solid of compound 7 (0.9 g, 88.2 %).

^{1}H NMR spectra were recorded, which were in according to literature values.[3] ^{1}H NMR (400 MHz, $CDCl_3$) δ = 8.83 (s, 1 H), 8.79 (s, 1 H), 8.04 (d, *J* = 1.3 Hz, 1 H), 7.90 (d, *J* = 8.7 Hz, 1 H), 7.67 (dd, *J* = 4.4, 2.6 Hz, 2 H), 7.38 (dd, *J* = 8.6, 1.4 Hz, 1 H), 7.33 (d, *J* = 2.5 Hz, 1 H), 1.57 (d, *J* = 6.6 Hz, 18 H), 1.36 (d, *J* = 3.5 Hz, 18 H), 0.31 (s, 9 H).^{13}C NMR (101 MHz, $CDCl_3$) δ 148.6, 148.5, 141.6, 141.5, 137.7, 131.3, 131.2, 130.0, 128.0,

127.7, 121.2, 120.8, 120.7, 118.2, 114.7, 103.8, 96.4, 36.2, 36.2, 34.0, 31.3, 29.7, 29.6. HRMS calcd for [M] m/z = 829.3602, found m/z = 829.3653.

Synthesis of compound 8[3]

Compound 7 (900.0 mg, 1.1 mmol) and K_2CO_3 (450.0 mg, 3.3 mol, 3.0 eq) were dissolved in the mixed solvent of 20.0 mL THF and 20.0 mL MeOH, the mixture was stirred at room temperature for 40 min. the reaction was monitored by TLC until the complete consumption of the start material. The solvent was removed under reduced pressure and the residue was subjected to column chromatography on silica gel using CH_2Cl_2 as the eluent to give a dark purple solid of compound 8 (700.0 mg, 85.5 %).

^{1}H NMR spectra were recorded, which were in according to literature values.[3] ^{1}H NMR (400 MHz, $CDCl_3$) δ= 8.82 (d, *J* = 4.0 Hz, 2 H), 8.08 (d, *J* = 1.3 Hz, 1 H), 7.93 (d, *J* = 8.7 Hz, 1 H), 7.70 - 7.65 (m, 2 H), 7.39 (dd, *J* = 8.6, 1.5 Hz, 1 H), 7.31 (dd, *J* = 13.8, 2.5 Hz, 2 H), 3.22 (s, 1 H), 1.57 (d, *J* = 4.1 Hz, 18 H), 1.36 (d, *J* = 3.3 Hz, 18 H) ^{13}C NMR (101 MHz, $CDCl_3$) δ 148.7, 137.8, 131.4, 130.1, 127.9, 127. 8, 120.2, 114.7, 36.2, 34.0, 31.2, 29.7. HRMS calcd for [M] m/z = 757.3207, found m/z = 757.3250.

Synthesis of compound Pt-2[3]

Under N_2 atmosphere, 1-ethynylpyrene (3.0 mg, 0.01 mmol) and 8 (10.0 mg, 0.01 mmol) were dissolved in the mixed solvent of THF/Et_3N (5.0 mL/5.0 mL), then $Pd(PPh_3)_2Cl_2$ (1.8 mg, 10.0 mmol %) and CuI (1.0 mg, 20.0 mmol %) was added, and the resulting solution was stirred for 8 h at room temperature. The reaction mixture was diluted with CH2Cl2 and was washed with H_2O. The organic layer was collected, and the aqueous layer was extracted with CH_2Cl_2 for 2 times, the combined organic layers was concentrated, and the residue was subjected to column chromatography on silica gel using PE/CH_2Cl_2 (2:1, v: v) as the eluent to give a red solid of compound Pt-2 (17.9 mg, 46.0 %).

^{1}H NMR spectra were recorded, which were in according to literature values.[3] ^{1}H NMR (400 MHz, $CDCl_3$) δ 8.83 (s, 1 H), 8.76 (s, 1 H), 8.57 (d, *J* = 9.1 Hz, 1 H), 8.18 (d, *J* = 3.2 Hz, 4 H), 8.09 (s, 2 H), 8.05 - 8.02 (m, 2 H), 7.70 (t, *J* = 2.3 Hz, 3 H), 7.35 (t, *J* = 2.1 Hz, 2 H), 7.28 (dd, *J* = 3.8, 2.3 Hz, 2 H), 1.60 (s, 18 H), 1.37 (s, 18 H).^{13}C NMR

(101 MHz, $CDCl_3$) δ 148.6, 141.5, 131.3, 127.9, 126.7, 120.8, 36.2, 31.3, 29.7, 29.7. HRMS calcd for [M] m/z = 981.3833, found m/z = 981.2811.

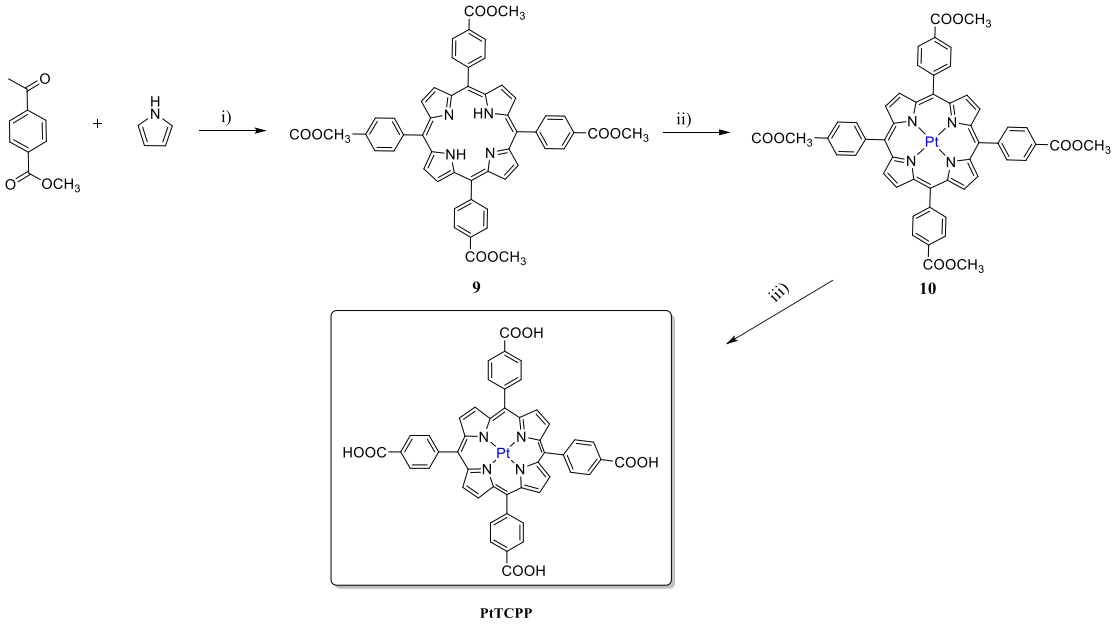

Synthesis of Compound 9[4]

Under N_2 atmosphere, 4-formyl methyl benzoate (2.0 g, 12.0 mmol) was dissolved in 400.0 mL dry dichloromethane, then pyrrole (1.0 mL, 14.0 mmol) was injected. After stirring for 5-10 min at room temperature, 2-3 drops of trifluoroacetic acid were added as catalyst, the mixture was stirred for further 12 h at room temperature. Then DDQ (2.9 g, 12.0 mmol) was dissolved in the freshly distilled THF (10.0 mL), and the solution was added into the reaction system, stirring at room temperature for further 2 h. The solvent was removed under reduced pressure and the residue was subjected to column chromatography on silica gel using gradient eluent from PE/CH_2Cl_2 (1:1 v: v) to DCM/EA (5:1, v: v) to give a red product of 9 (300.0 mg, 12.0 %).

^{1}H NMR spectra were recorded, which were in according to literature values.[4] ^{1}H NMR (400 MHz, $CDCl_3$) δ 8.82 (s, 8 H), 8.45 (d, *J* = 7.7 Hz, 8 H), 8.30 (d, *J* = 7.6 Hz, 8 H), 4.12 (s, 12 H), -2.81 (s, 2 H). ^{13}C NMR (101 MHz, $CDCl_3$) δ 167.3, 146.6, 134.5, 129.8, 128.0, 119.4, 52.5, 29.7. HRMS calcd for $[M + H]^+$ m/z = 847.2763, found m/z =847.2765.

Synthesis of Compound 10[4]

Under N_2 atmosphere, Compound 9 (200.0 mg, 0.2 mmol) and $PtCl_2$ (76.0 mg, 0.3 mmol) were dissolved in 5 mL benzonitrile in a round-bottle flask. The mixture was refluxed at 140 °C for 11 h. after cooling, the solvent was removed under reduced pressure and the residue was subjected to column chromatography on silica gel using PE/CH_2Cl_2 (1:4, v: v) as the eluent to give dark purple product of compound 10 (53.0 mg, 21.5 %).

^{1}H NMR spectra were recorded, which were in according to literature values.[4] ^{1}H NMR (400 MHz, $CDCl_3$) δ 8.72 (s, 8 H), 8.42 (d, *J* = 8.2 Hz, 8 H), 8.23 (d, *J* = 8.2 Hz, 8 H), 4.10 (s, 12 H). ^{13}C NMR (101 MHz, CDCl3) δ 167.2, 145.8, 140.5, 133.9, 130.9, 130.0, 128.1, 121.6, 52.5, 29.7. HRMS calcd for [M + H]+ m/z = 1040.2259, found m/z = 1040.2212.

Synthesis of PtTCPP[4]

Excess potassium hydroxide (28.1 mg, 0.5 mmol) was added into the solution of compound 7 (53.0 mg, 0.05 mmol) in 50.0 mL THF. The mixture was refluxed for 5 h, THF was removed under reduced pressure, then 20.0 mL water was added and conc. HCl was added to tuning pH to 3~4, the formed precipitates was collected through filtration, to give pure product of PtTCPP (40.3 mg, 82.0 %).

^{1}H NMR spectra were recorded, which were in according to literature values.[4] ^{1}H NMR (400 MHz, DMSO-d_6) δ 13.29 (s, 4 H), 8.75 (s, 8 H), 8.36 (d, *J* = 8.2 Hz, 8 H), 8.28 (d, *J* = 8.2 Hz, 8 H). ^{13}C NMR (101 MHz, DMSO-d_6) δ 167.8, 145.0, 140.3, 134.3, 131.7, 131.2, 128.5, 122.1. MALDI-TOF calcd for $[M+H]^+$ m/z =984.1628, found m/z = 984.1938.

4.0 NMR and HRMS spectra of the UC components

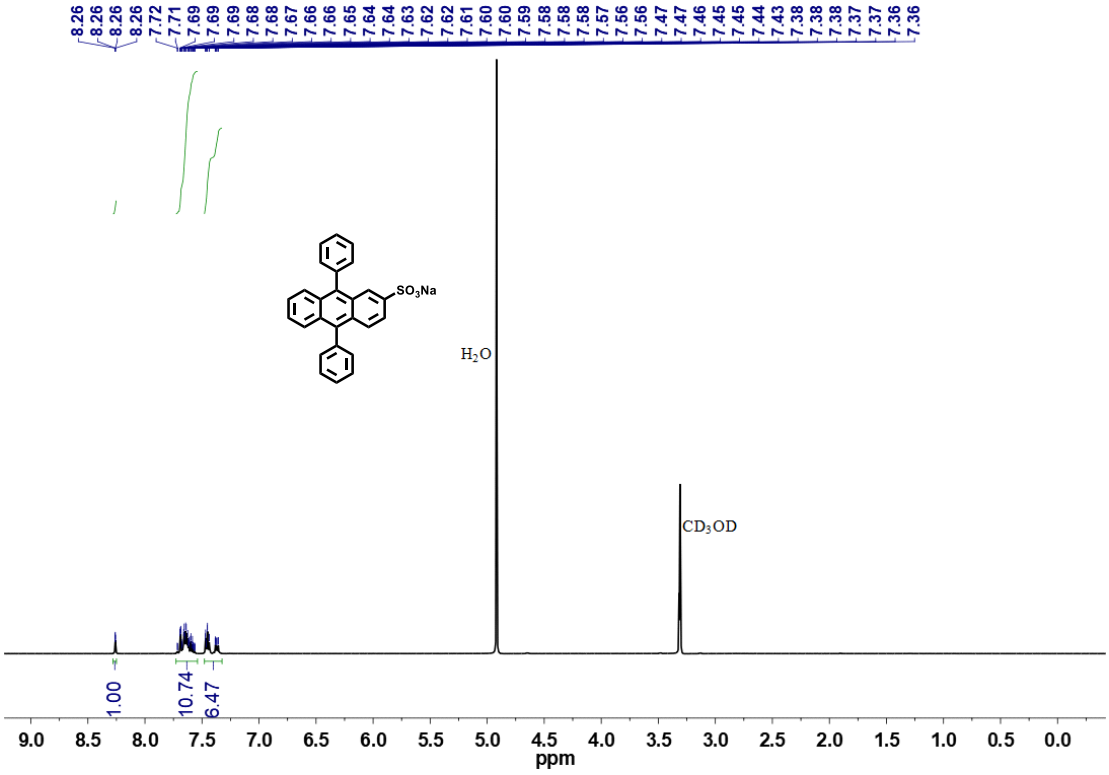

Fig. S4 ^{1}H NMR spectrum of **DPAS** measured in CD_3OD at 25 °C.

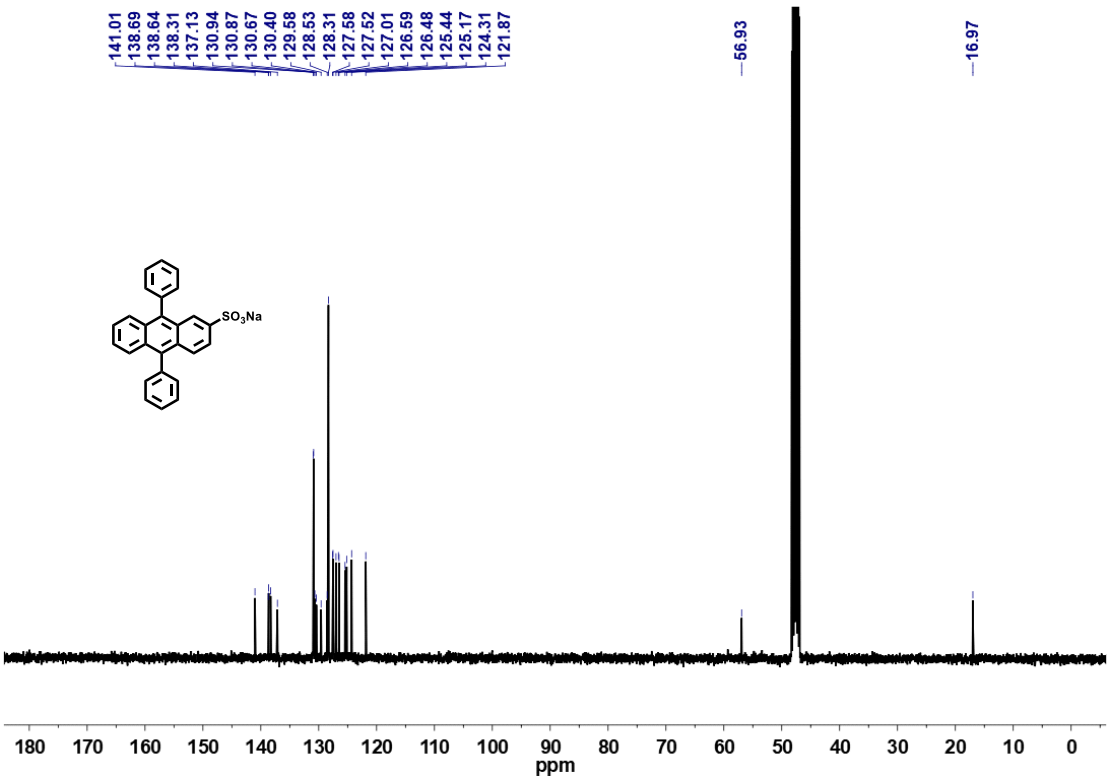

Fig. S5 ^{13}C NMR spectrum of **DPAS** measured in CD_3OD at 25 °C.

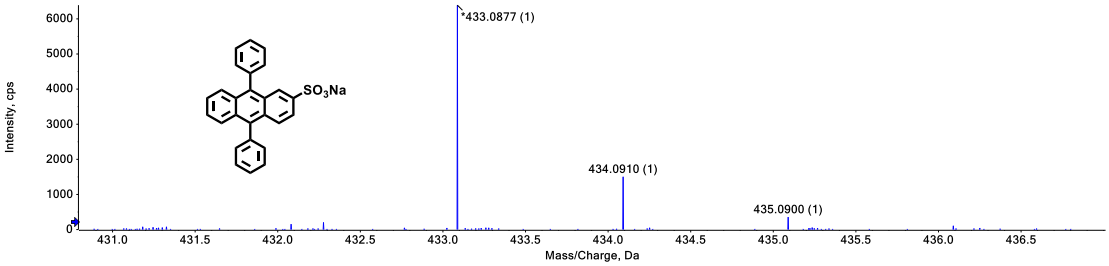

Fig. S6 HRMS spectrum of **DPAS**.

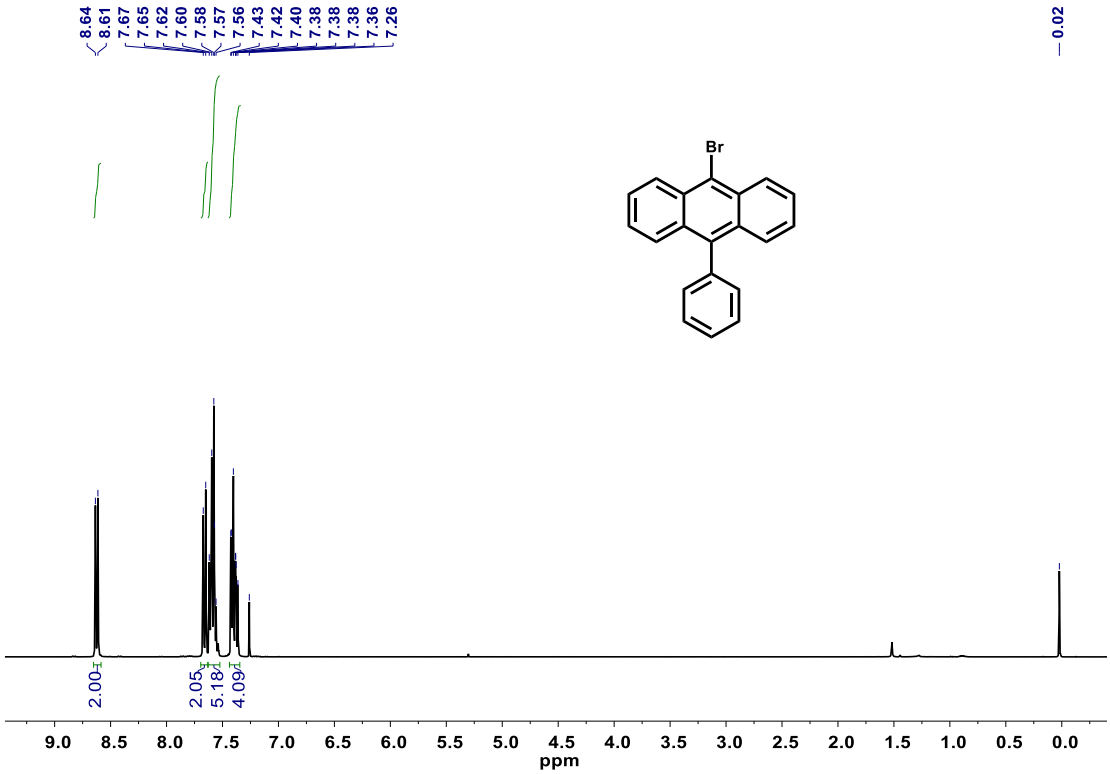

Fig. S7 ^{1}H NMR spectrum of **compound 1** measured in $CDCl_3$ at 25 °C.

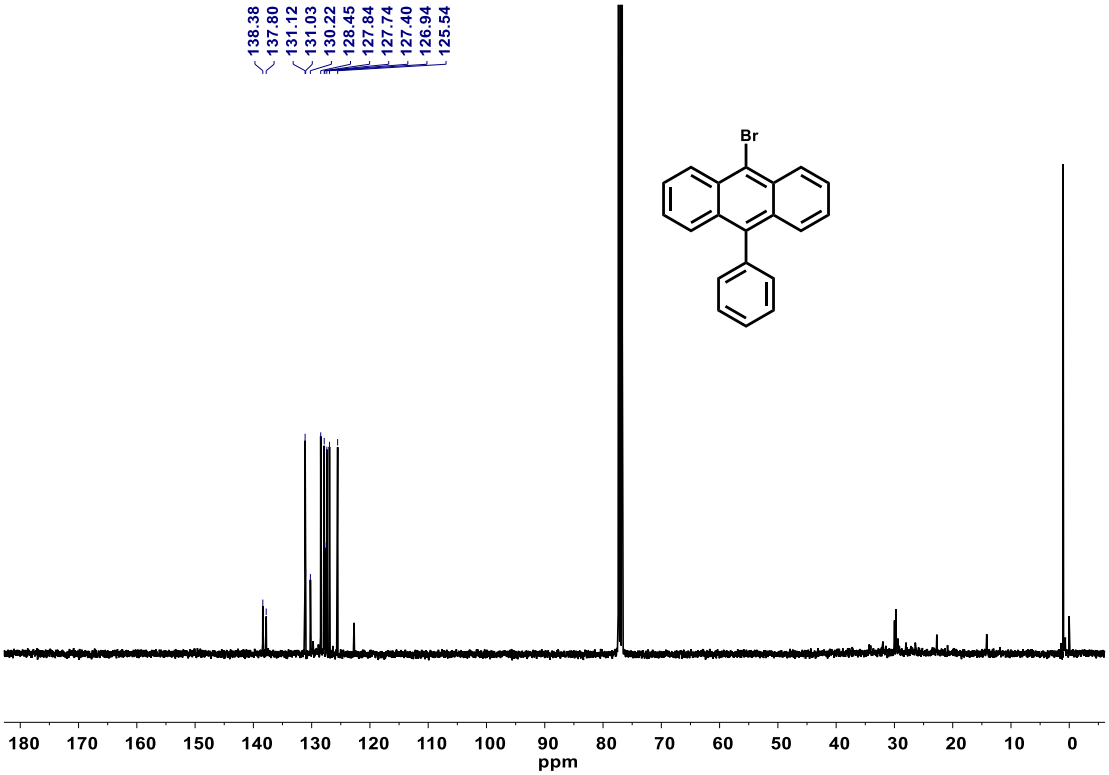

Fig. S8 ^{13}C NMR spectrum of **compound 1** measured in $CDCl_3$ at 25 °C.

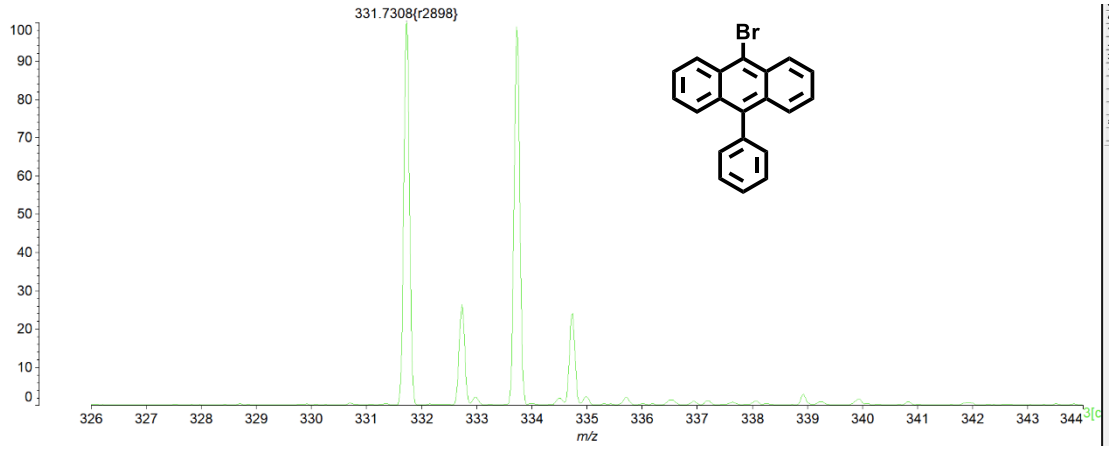

Fig. S9 MALDI-TOF of **compound 1**.

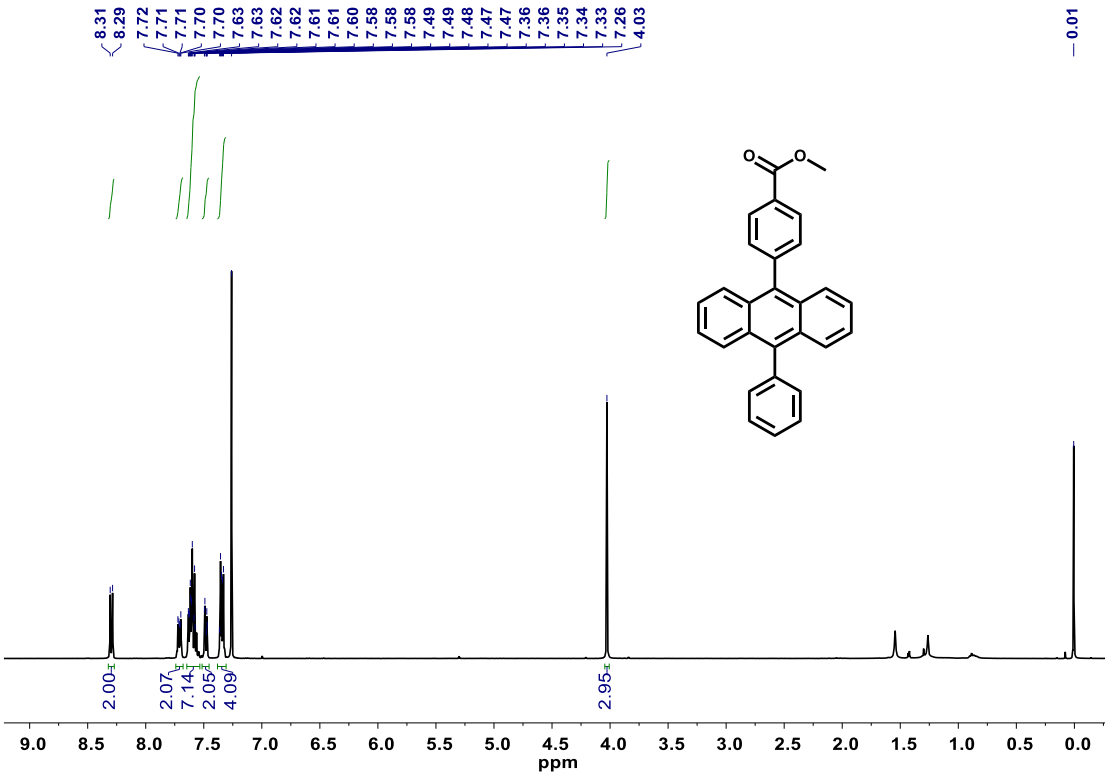

Fig. S10 ^{1}H NMR spectrum of **compound 2** measured in $CDCl_3$ at 25 °C.

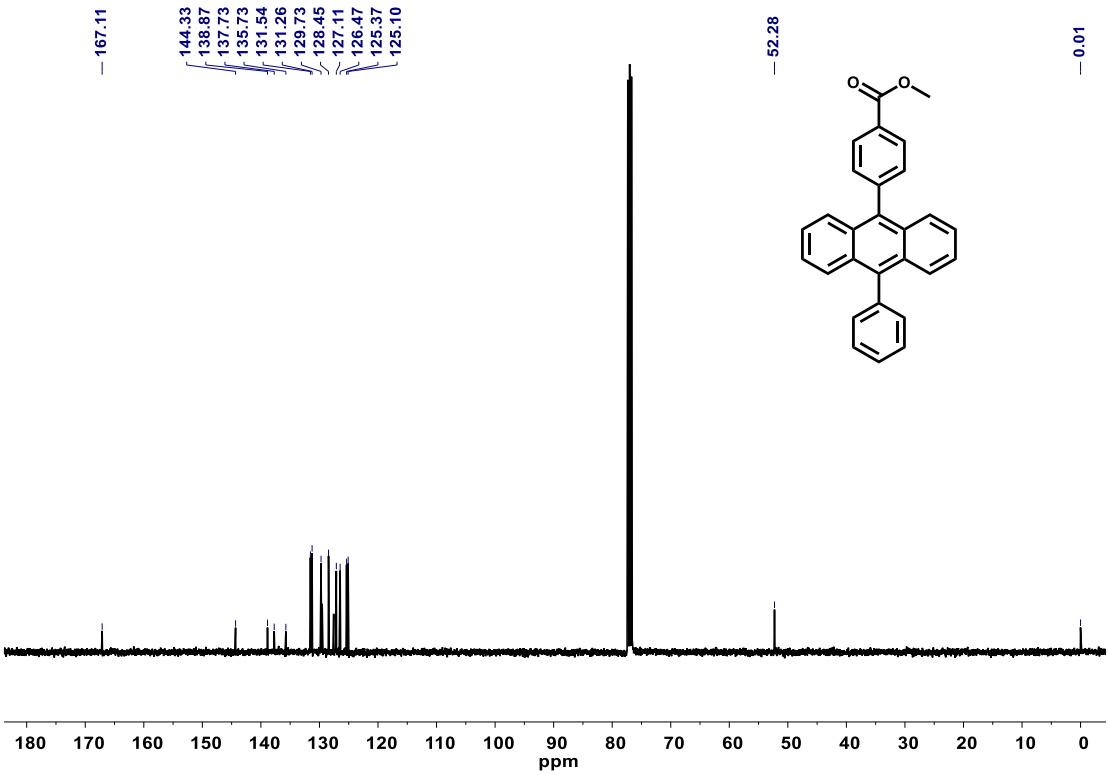

Fig. S11 ^{13}C NMR spectrum of **compound 2** measured in $CDCl_3$ at 25 °C.

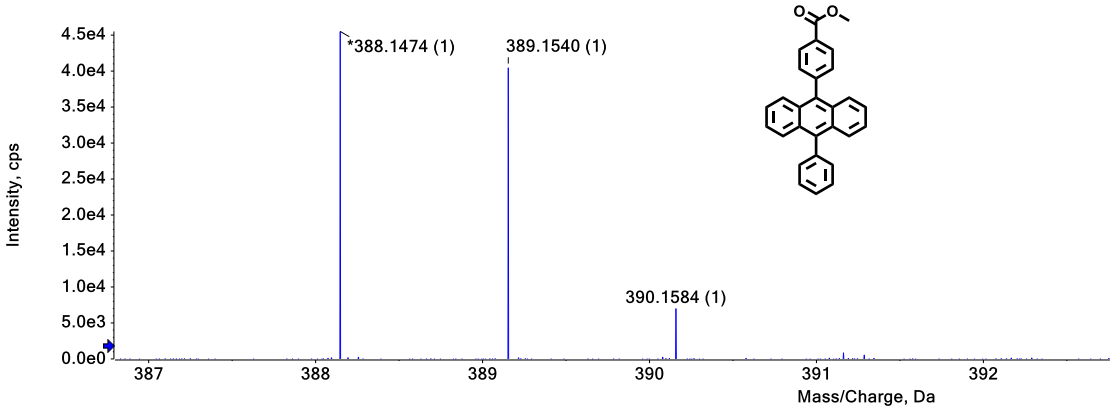

Fig. S12 HRMS spectrum of **compound 2.**

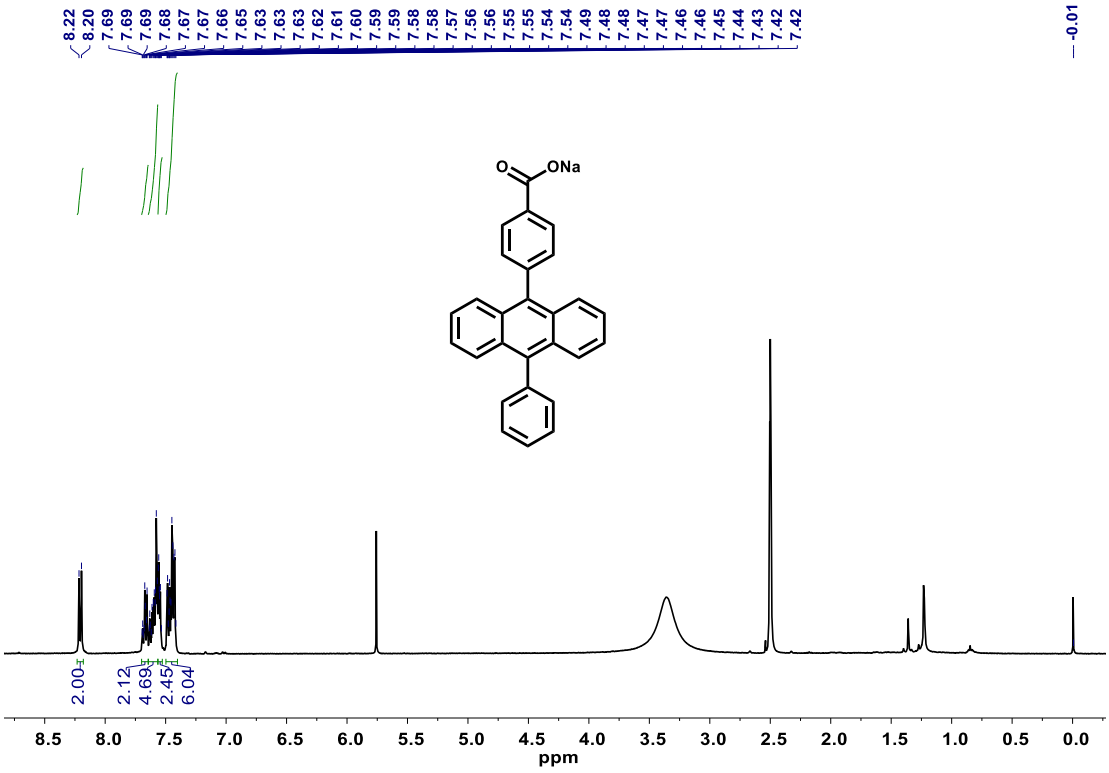

Fig. S13 ^{1}H NMR spectrum of compound **A-1** measured in DMSO-d_6 at 25 °C.

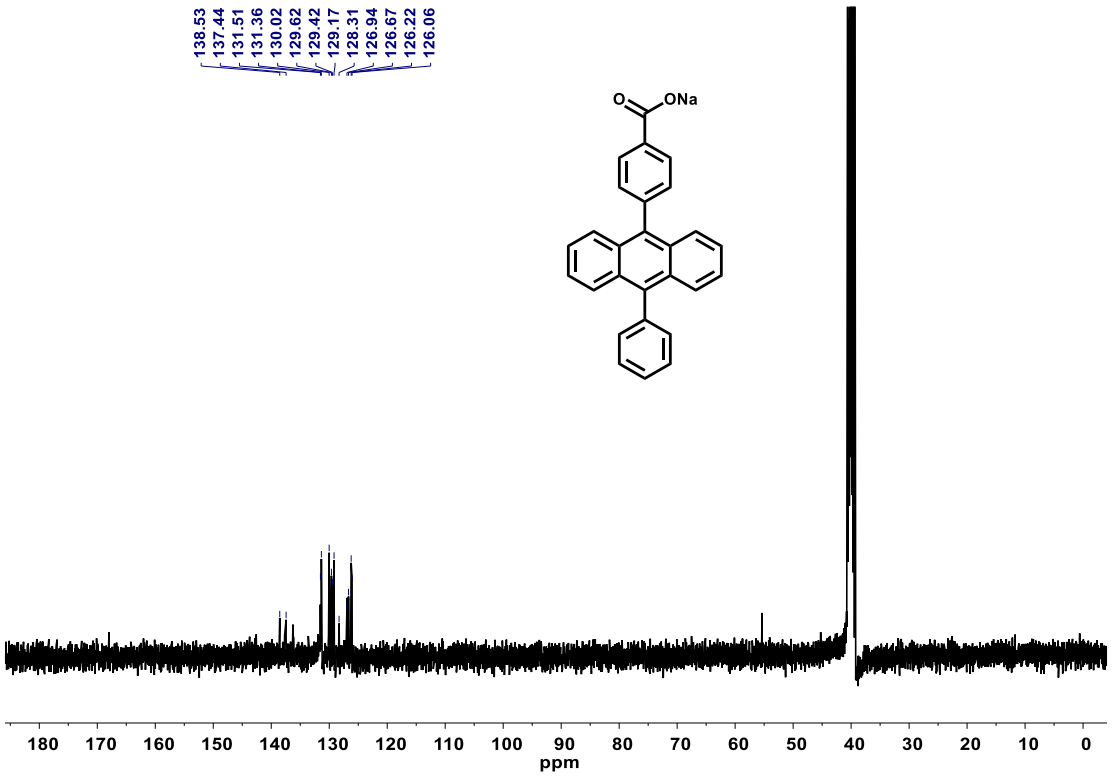

Fig. S14 ^{13}C NMR spectrum of compound **A-1** measured in DMSO-d_6 at 25 °C.

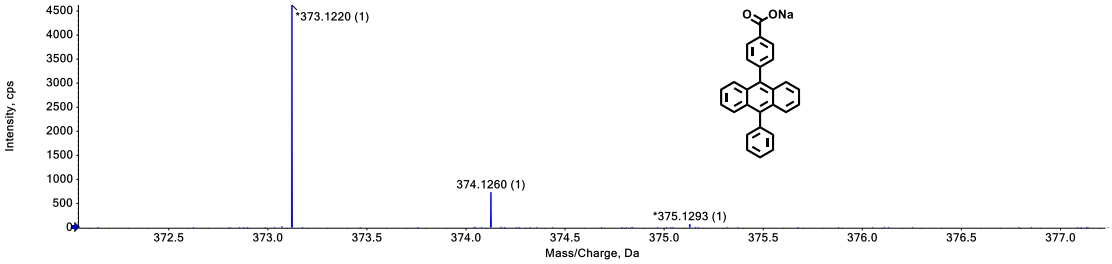

Fig. S15 HRMS spectrum of compound **A-1.**

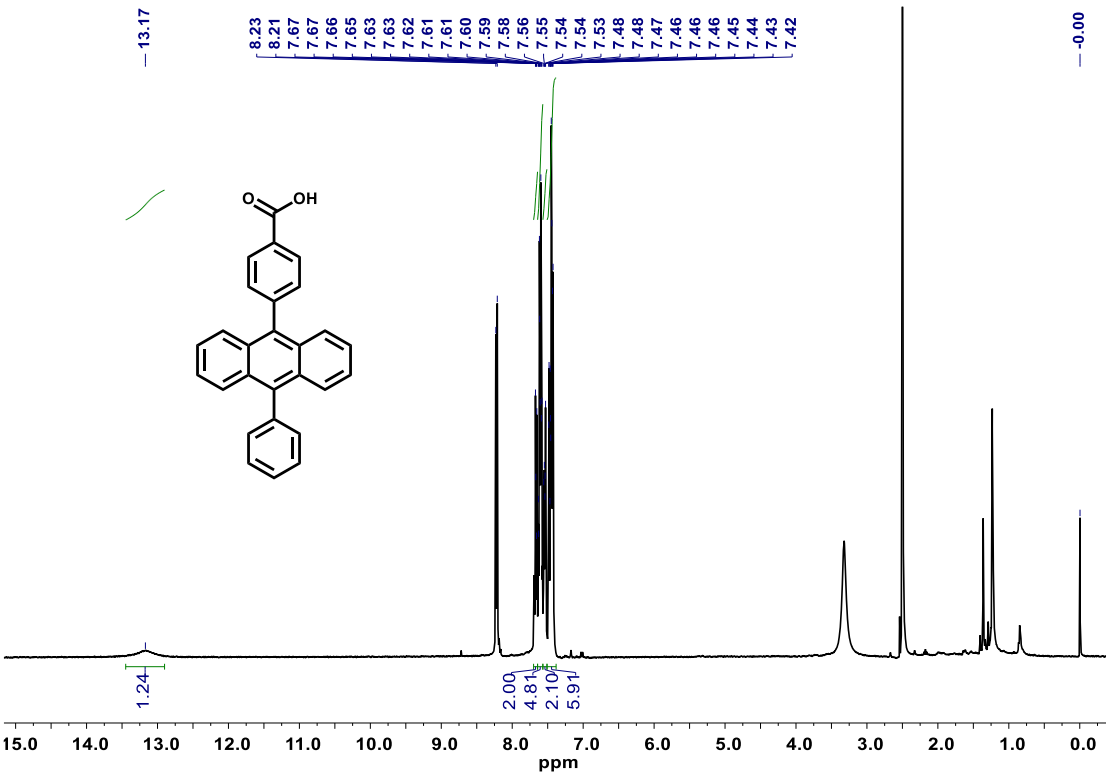

Fig. S16 ^{1}H NMR spectrum of compound **A-2** measured in DMSO-d_6 at 25 °C.

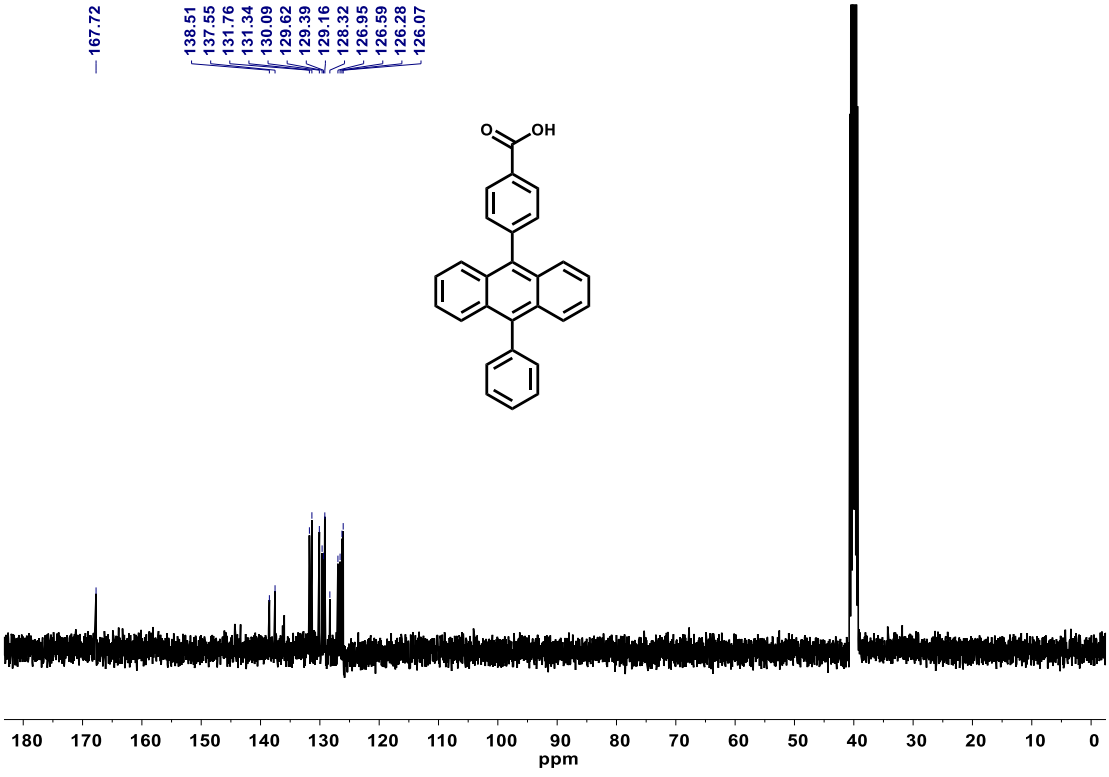

Fig. S17 ^{13}C NMR spectrum of compound **A-2** measured in DMSO-d_6 at 25 °C.

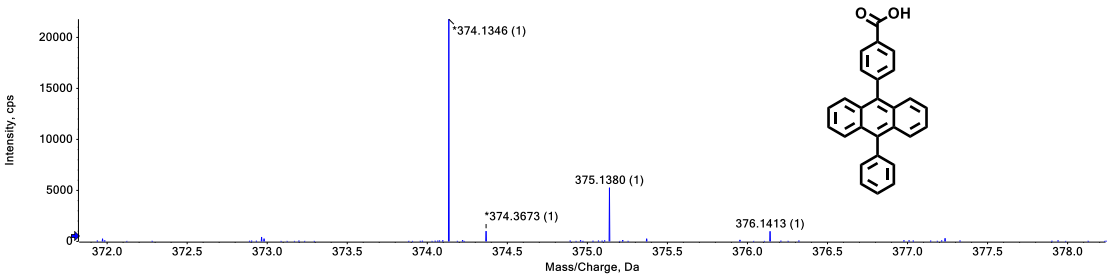

Fig. S18 HRMS spectrum of compound **A-2.**

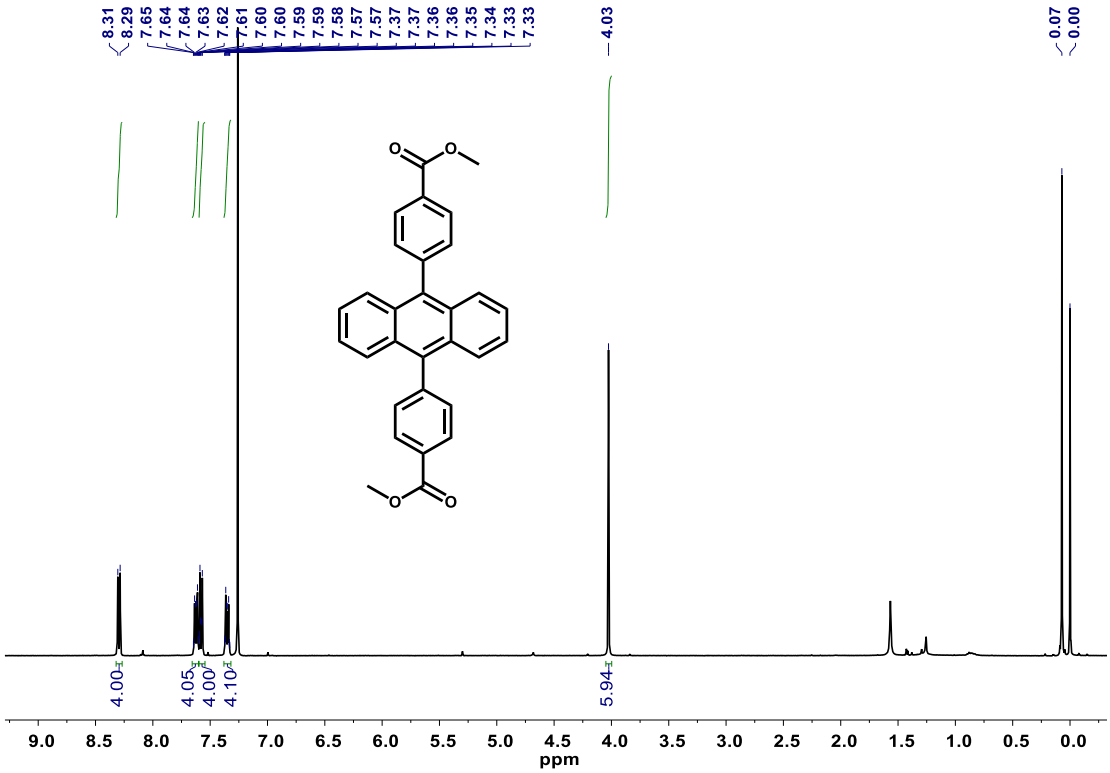

Fig. S19 ^{1}H NMR spectrum of **compound 3** measured in $CDCl_3$ at 25 °C.

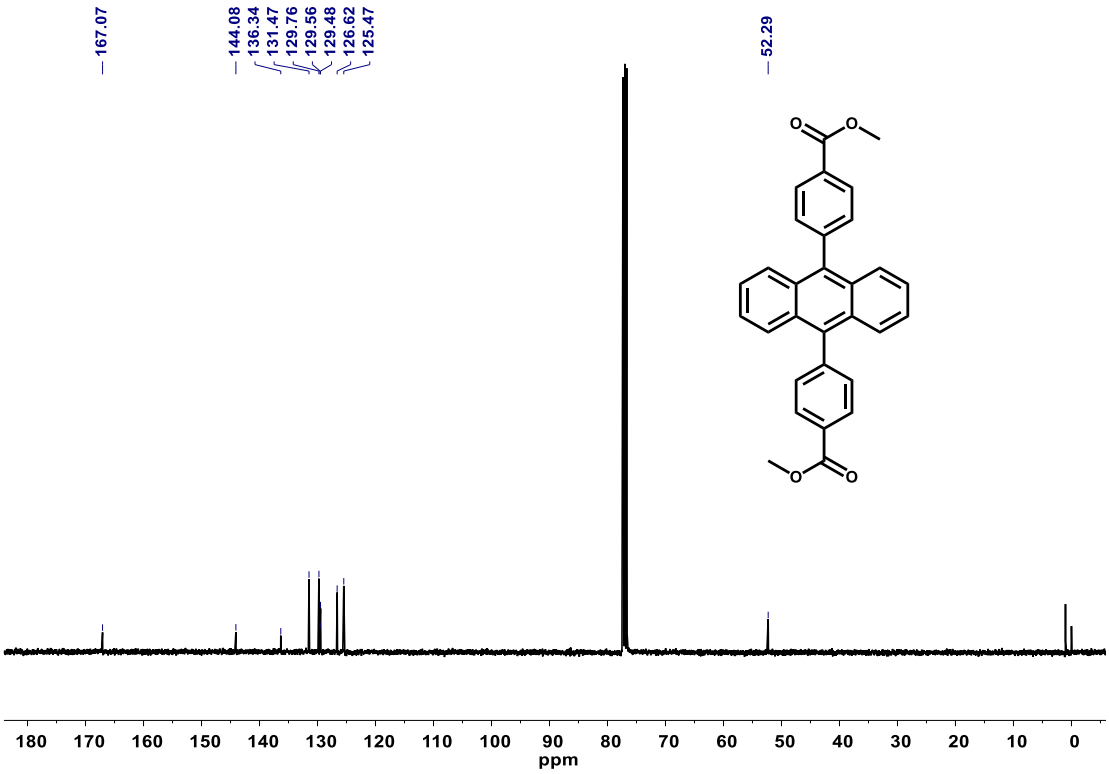

Fig. S20 ^{13}C NMR spectrum of **compound 3** measured in $CDCl_3$ at 25 °C.

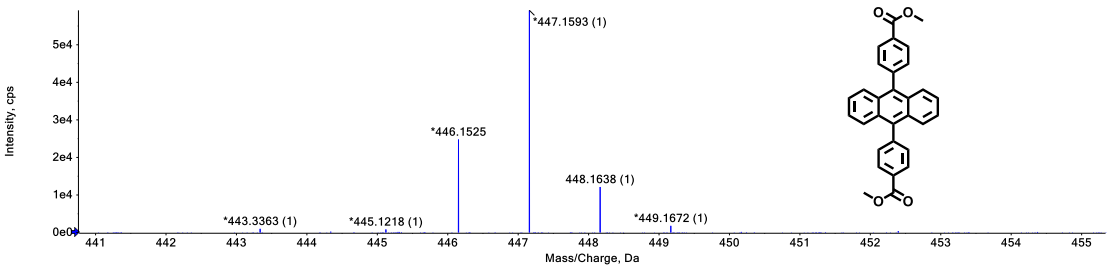

Fig. S21 HRMS spectrum of **compound 3.**

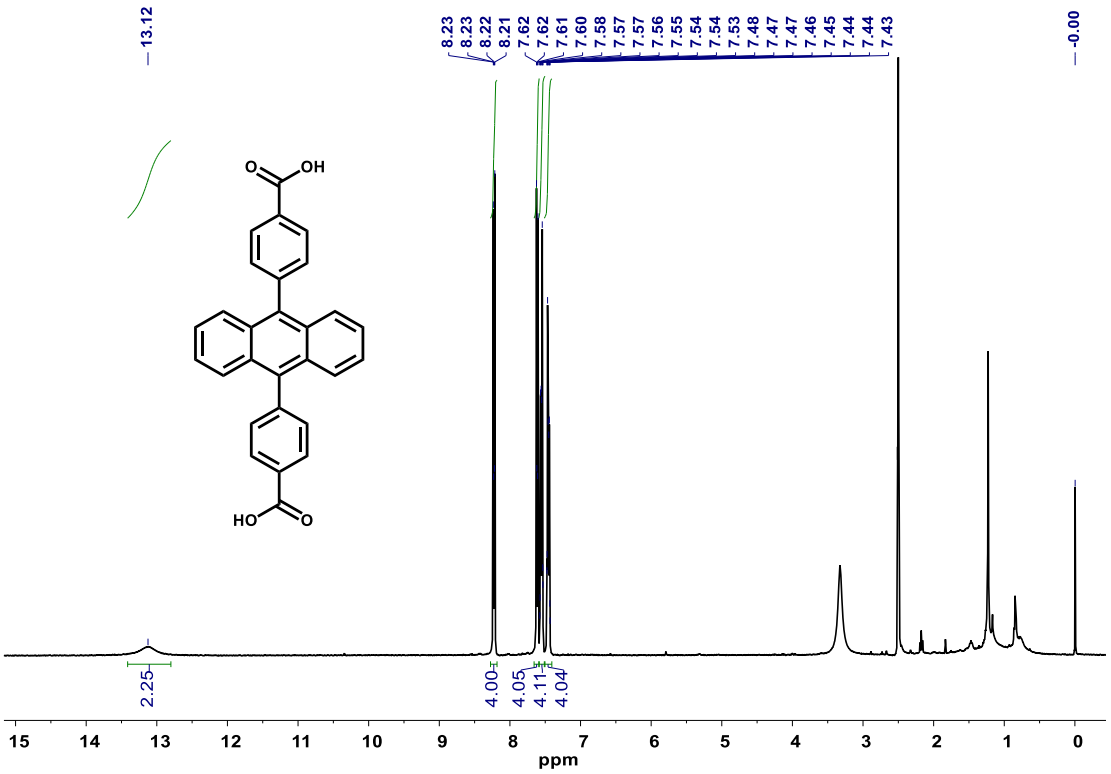

Fig. S22 ^{1}H NMR spectrum of compound **A-3** measured in DMSO-d_6 at 25 °C.

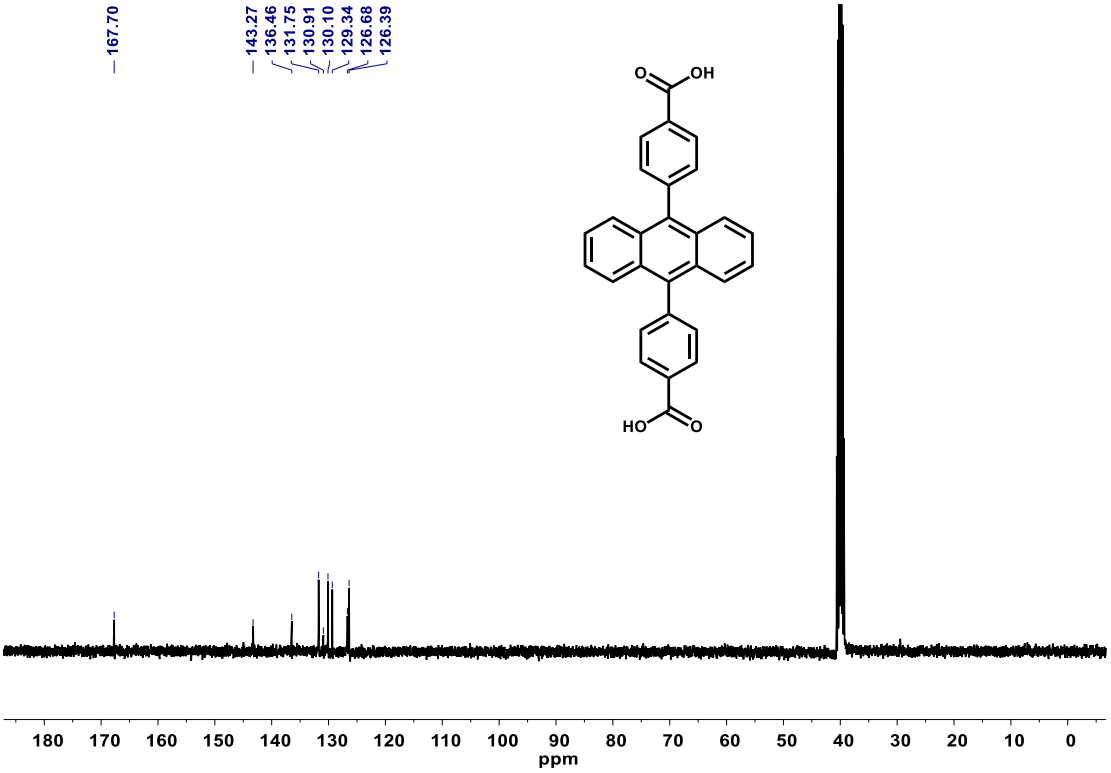

Fig. S23 ^{13}C NMR spectrum of compound **A-3** measured in DMSO-d_6 at 25 °C.

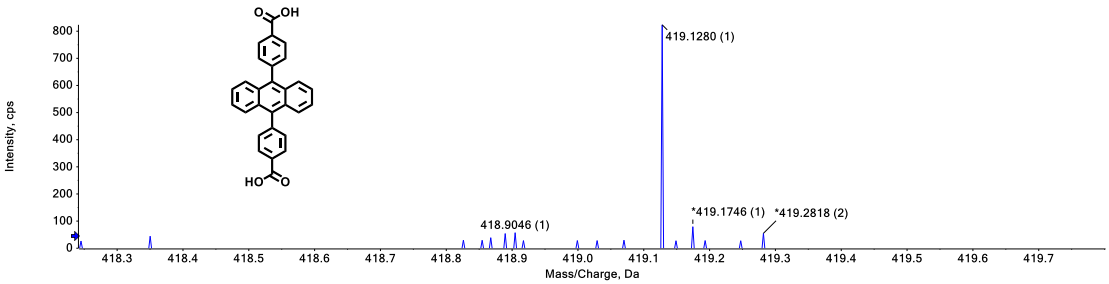

Fig. S24 HRMS spectrum of compound **A-3.**

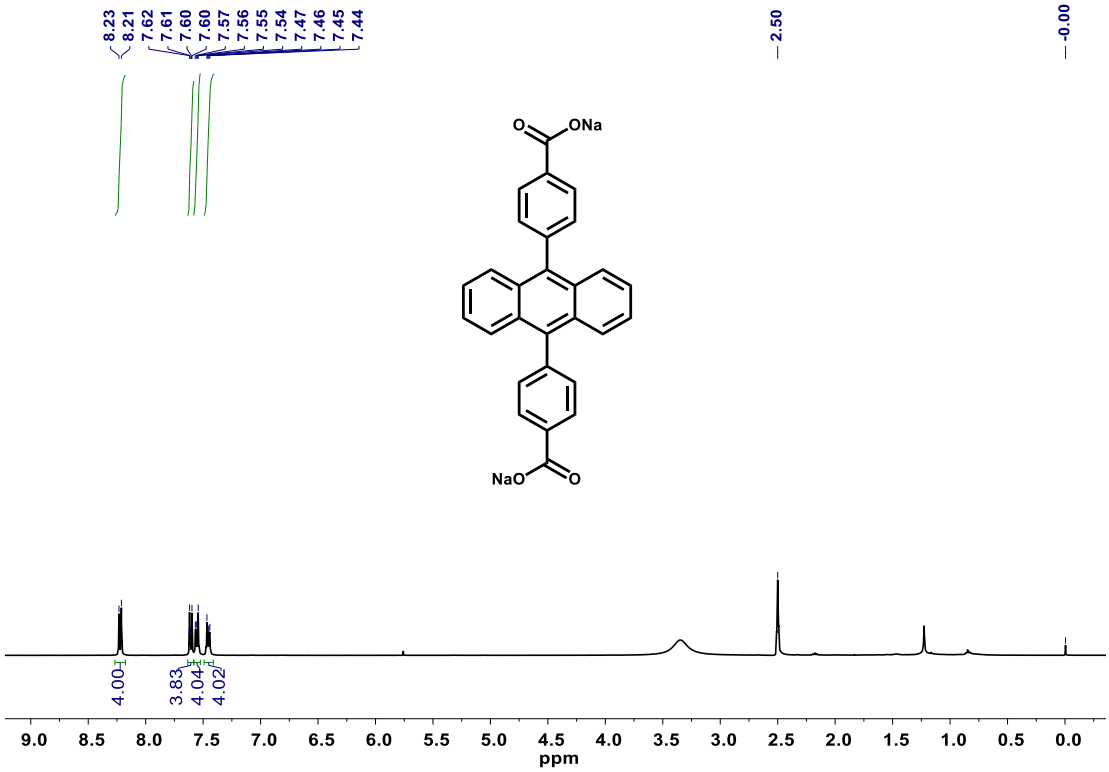

Fig. S25 ^{1}H NMR spectrum of compound **A-4** measured in DMSO-d_6 at 25 °C.

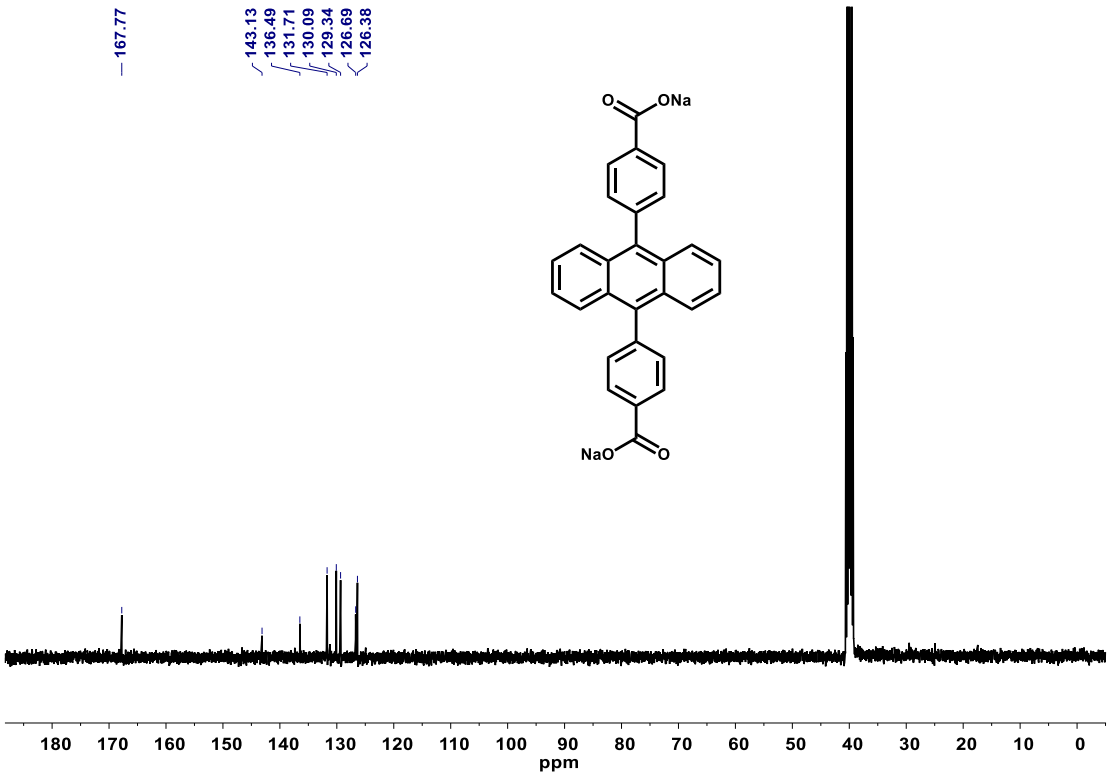

Fig. S26 ^{13}C NMR spectrum of compound **A-4** measured in DMSO-d_6 at 25 °C.

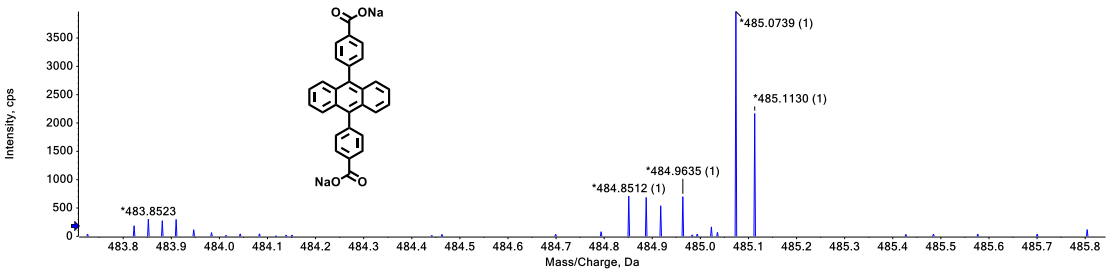

Fig. S27 HRMS spectrum of compound **A-4.**

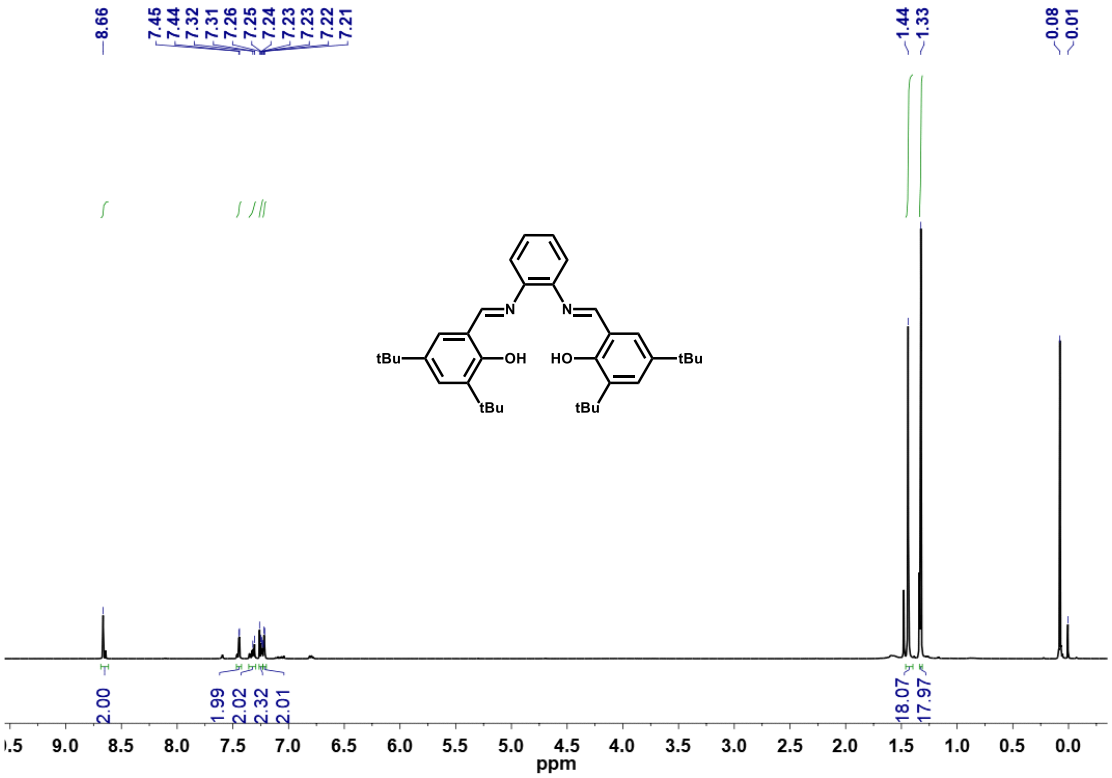

Fig. S28 ^{1}H NMR spectrum of **compound 4** measured in $CDCl_3$ at 25 °C.

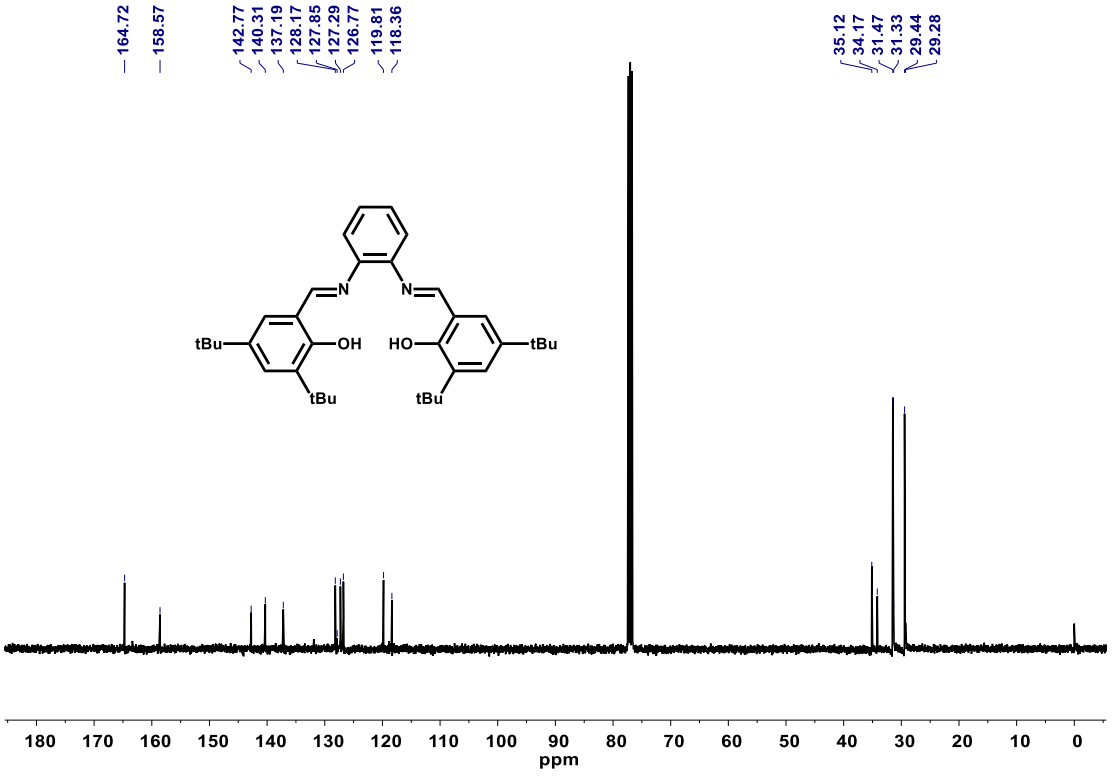

Fig. S29 ^{13}C NMR spectrum of **compound 4** measured in $CDCl_3$ at 25 °C.

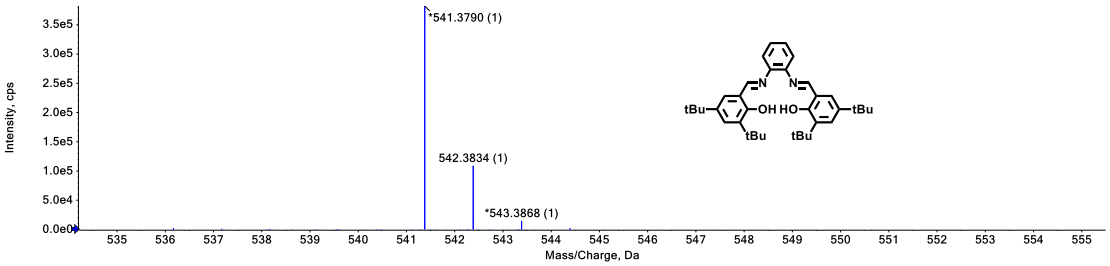

Fig. S30 HRMS spectrum of **compound 4.**

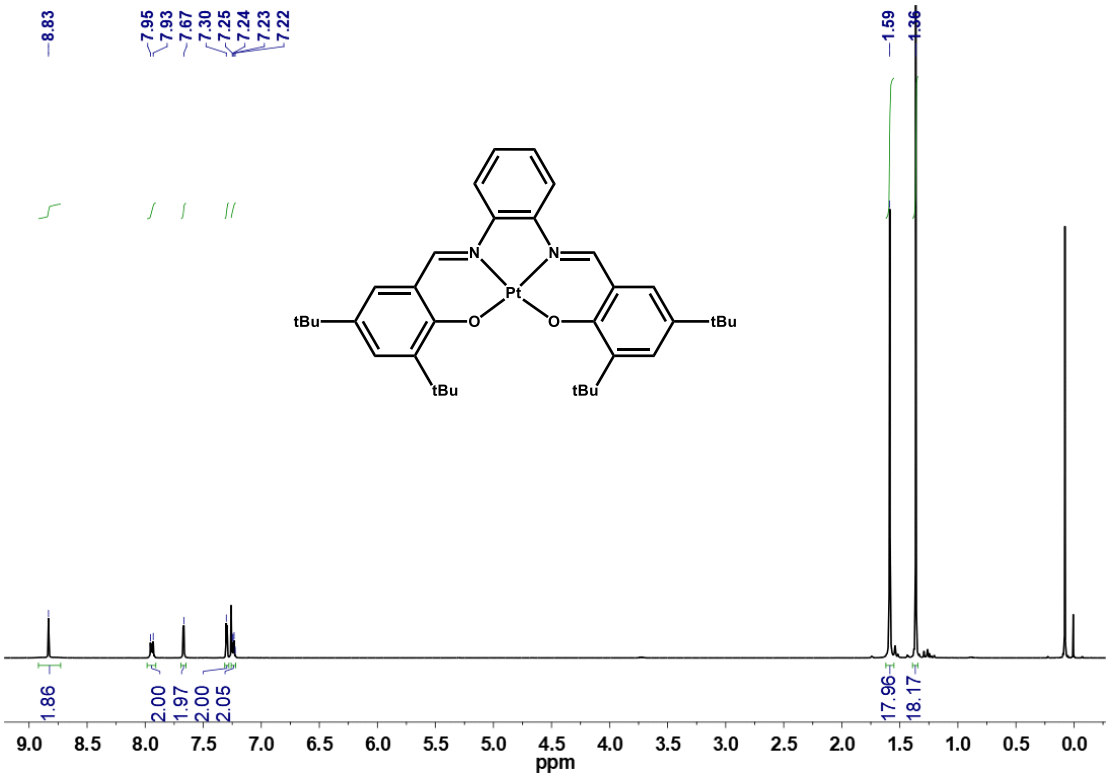

Fig. S31 ^{1}H NMR spectrum of **Pt-1** measured in $CDCl_3$ at 25 °C.

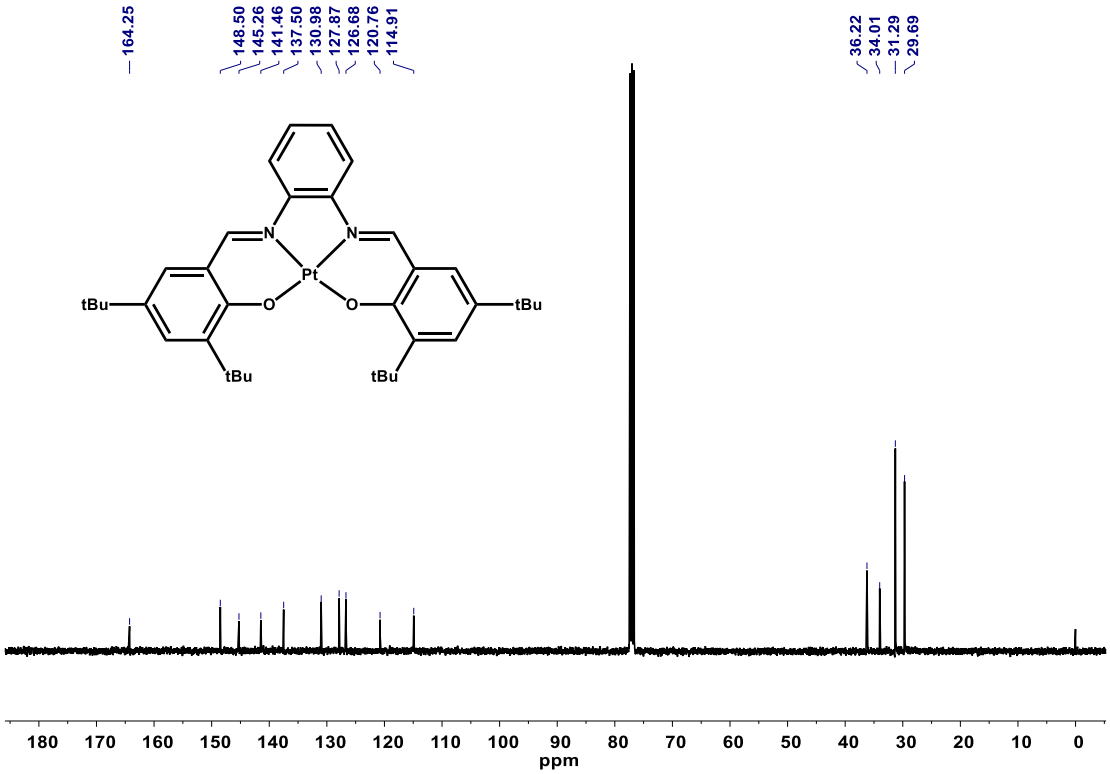

Fig. S32 ^{13}C NMR spectrum of **Pt-1** measured in $CDCl_3$ at 25 °C.

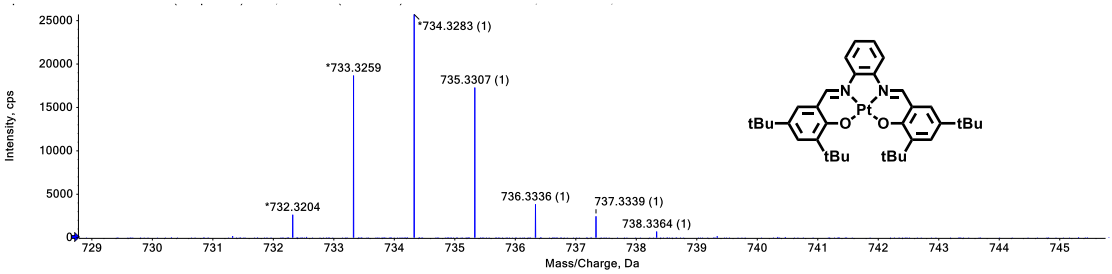

Fig. S33 HRMS spectrum of compound **Pt-1.**

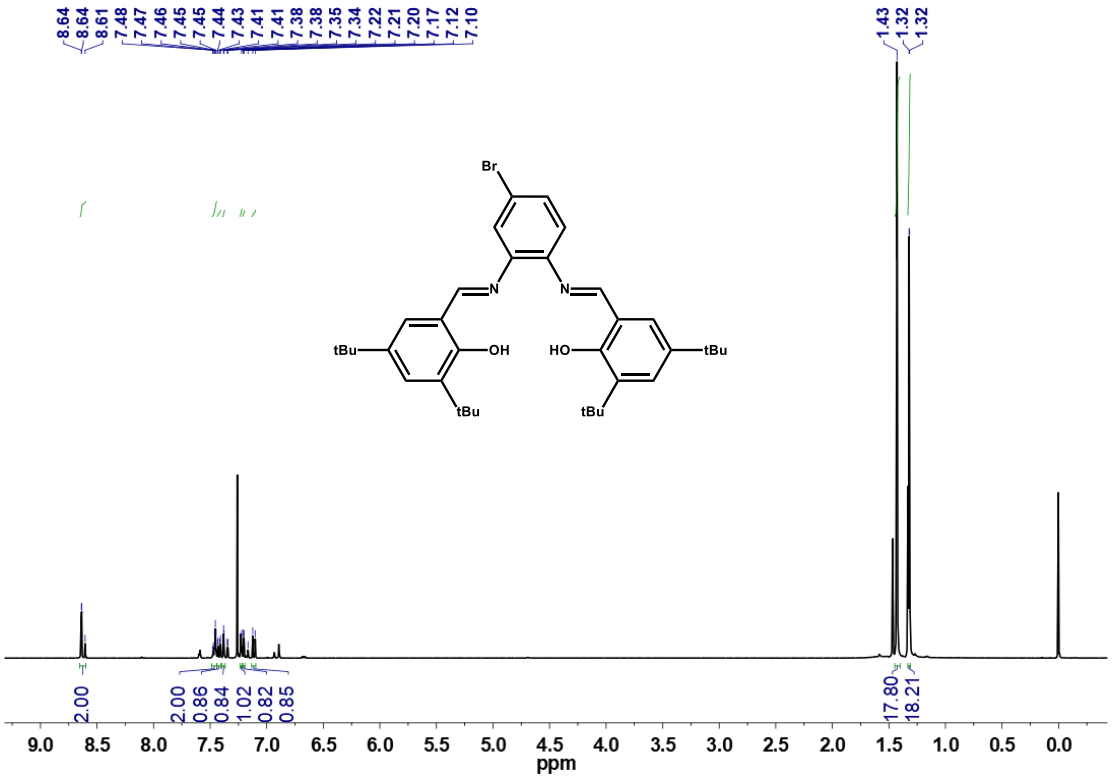

Fig. S34 ^{1}H NMR spectrum of **compound 5** measured in $CDCl_3$ at 25 °C.

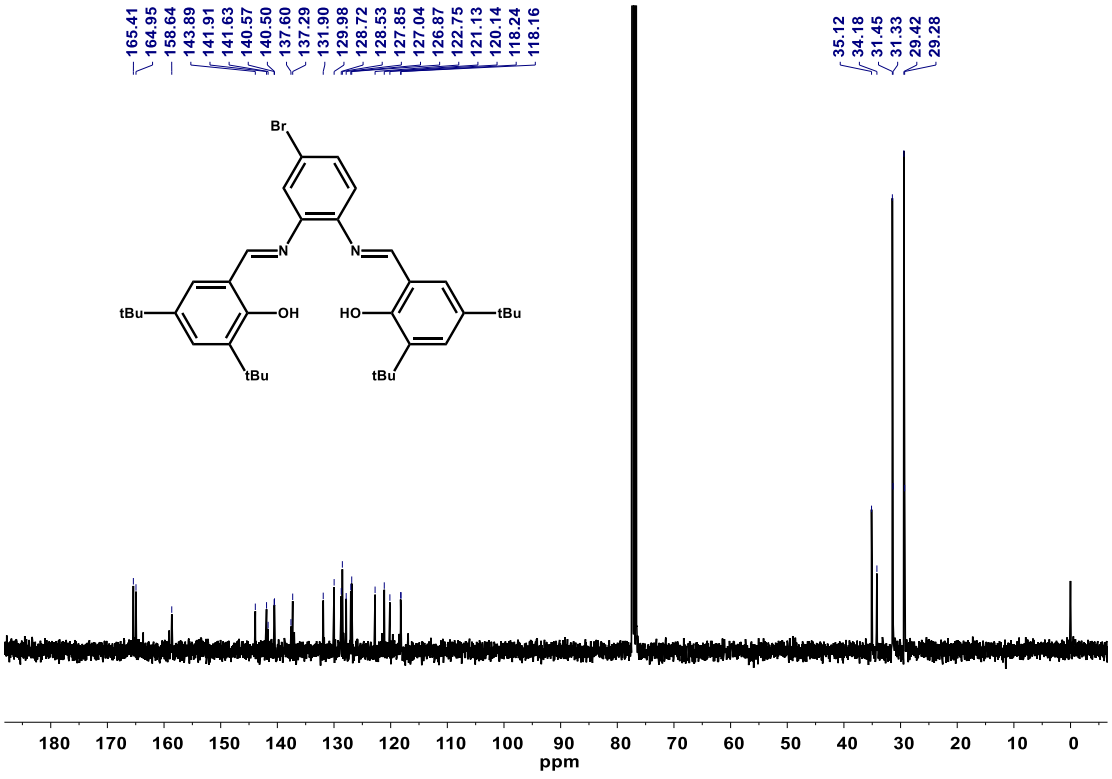

Fig. S35 ^{13}CNMR spectrum of **compound 5** measured in $CDCl_3$ at 25 °C.

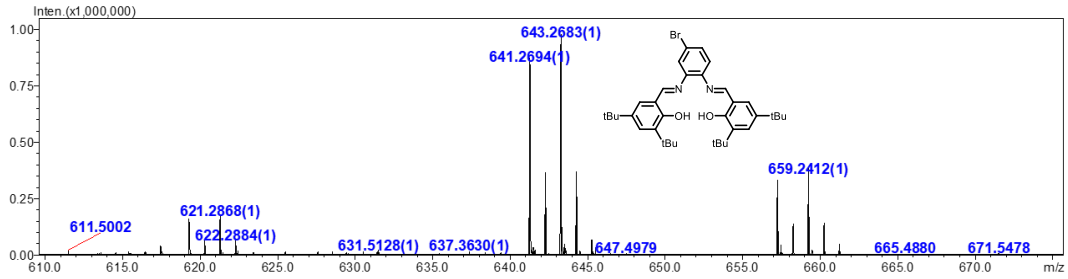

Fig. S36 HRMS spectrum of **compound 5.**

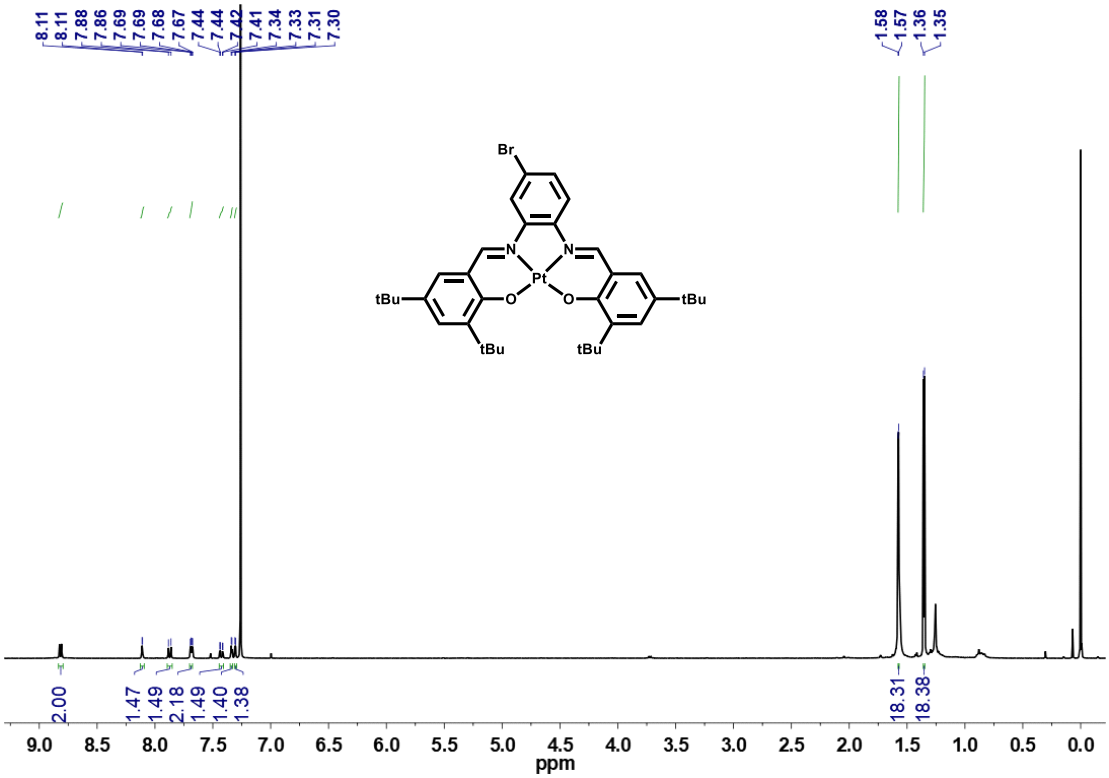

Fig. S37 ^{1}H NMR spectrum of **compound 6** measured in $CDCl_3$ at 25 °C.

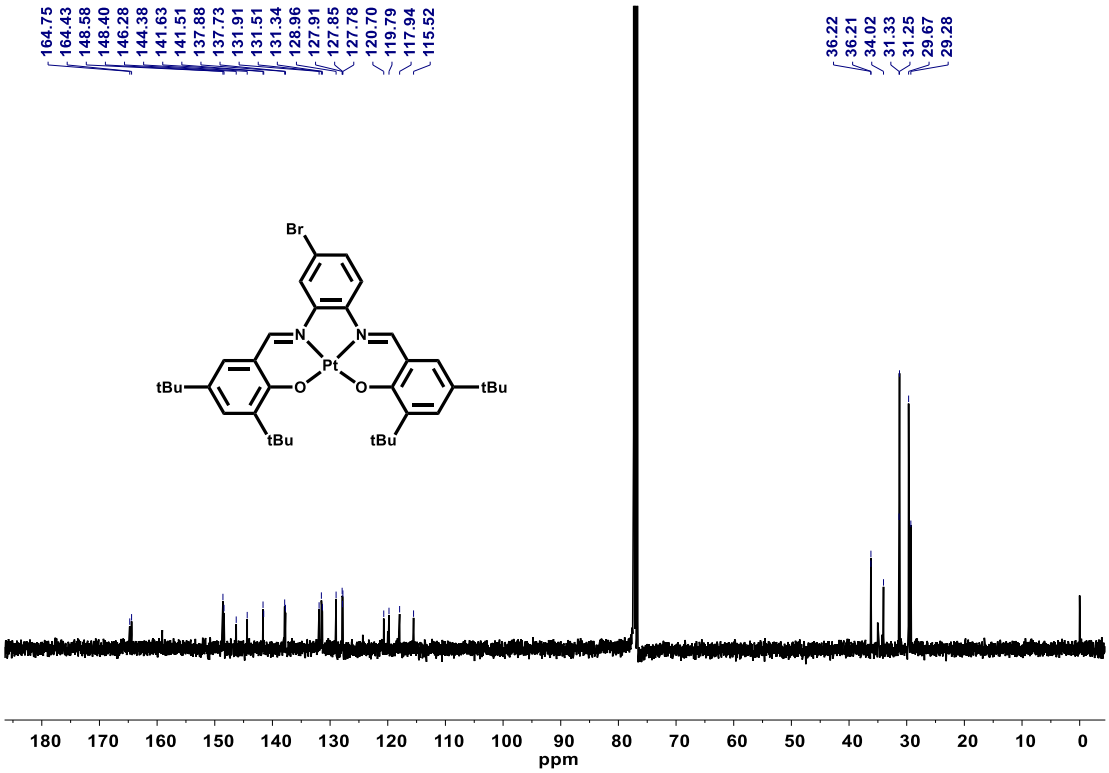

Fig. S38 ^{13}C NMR spectrum of **compound 6** measured in $CDCl_3$ at 25 °C.

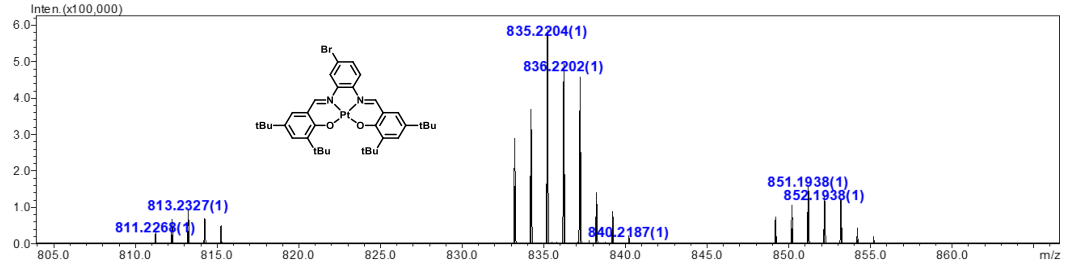

Fig. S39 HRMS spectrum of **compound 6.**

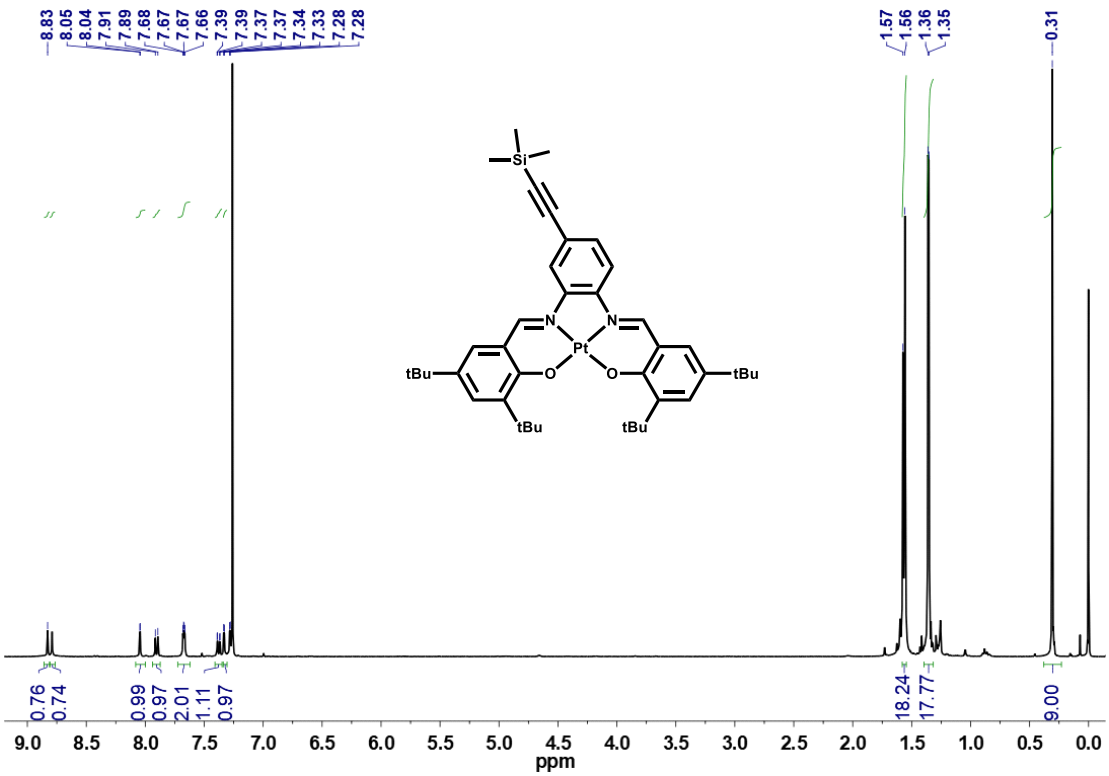

Fig. S40 ^{1}H NMR spectrum of **compound 7** measured in $CDCl_3$ at 25 °C.

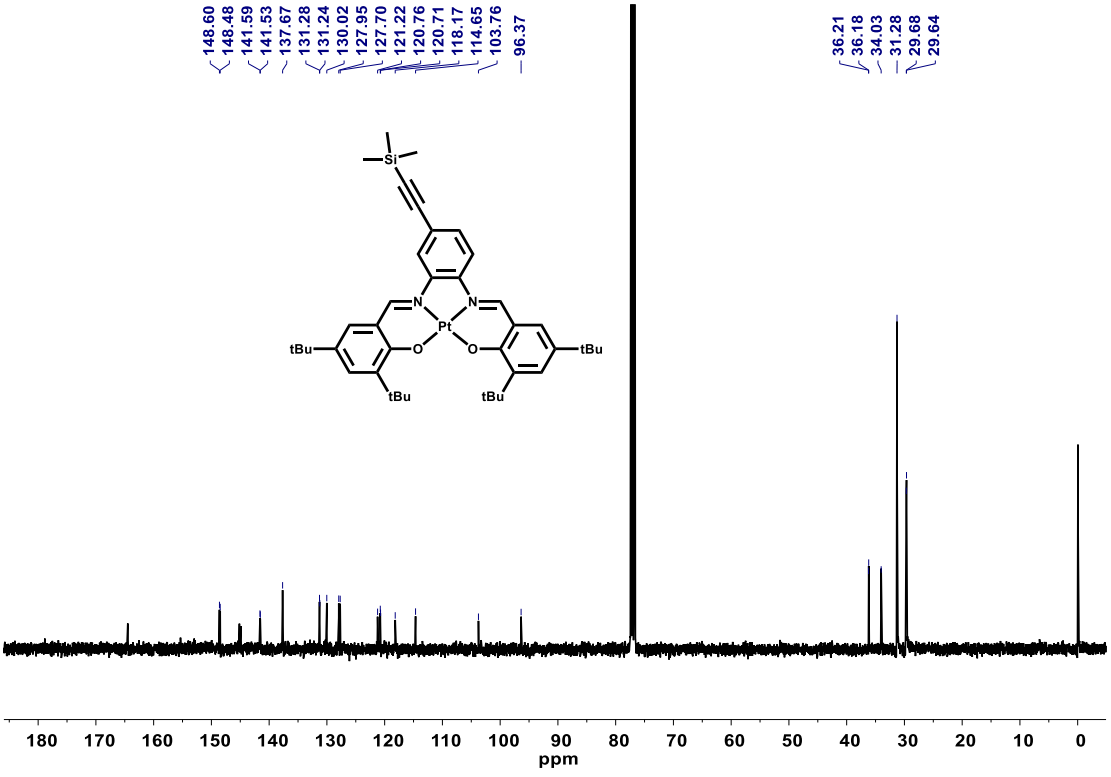

Fig. S41 ^{13}C NMR spectrum of **compound 7** measured in $CDCl_3$ at 25 °C.

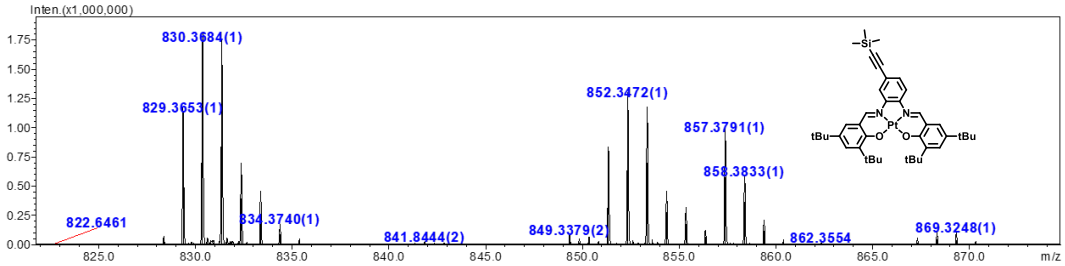

Fig. S42 HRMS spectrum of **compound 7.**

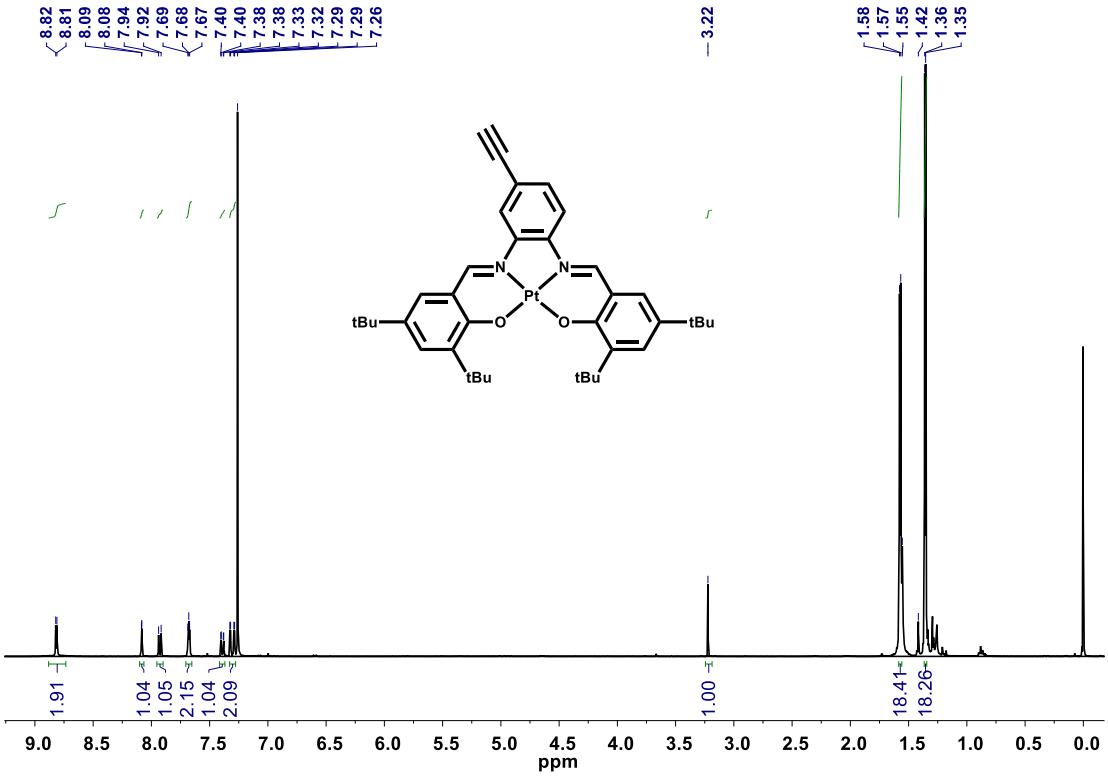

Fig. S43 ^{1}H NMR spectrum of **compound 8** measured in $CDCl_3$ at 25 °C.

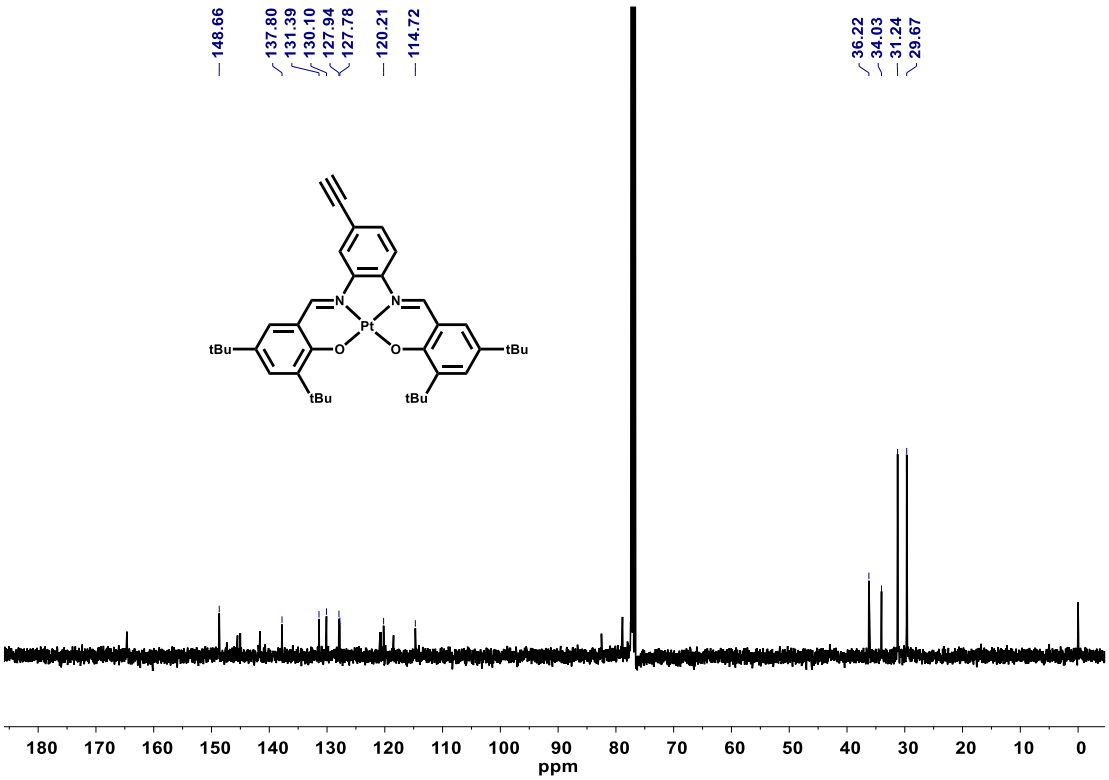

Fig. S44 ^{13}C NMR spectrum of **compound 8** measured in $CDCl_3$ at 25 °C.

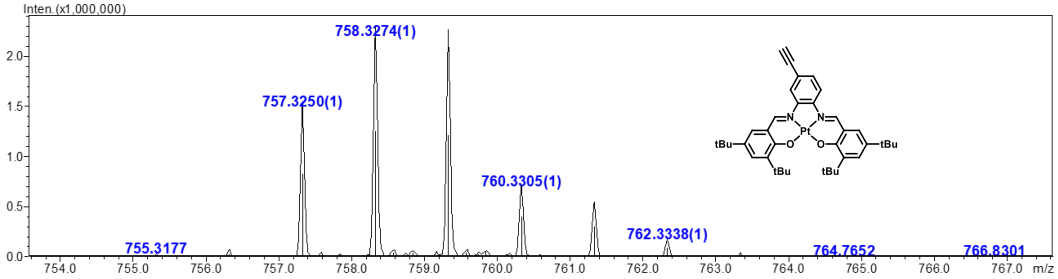

Fig. S45 HRMS spectrum of **compound 8.**

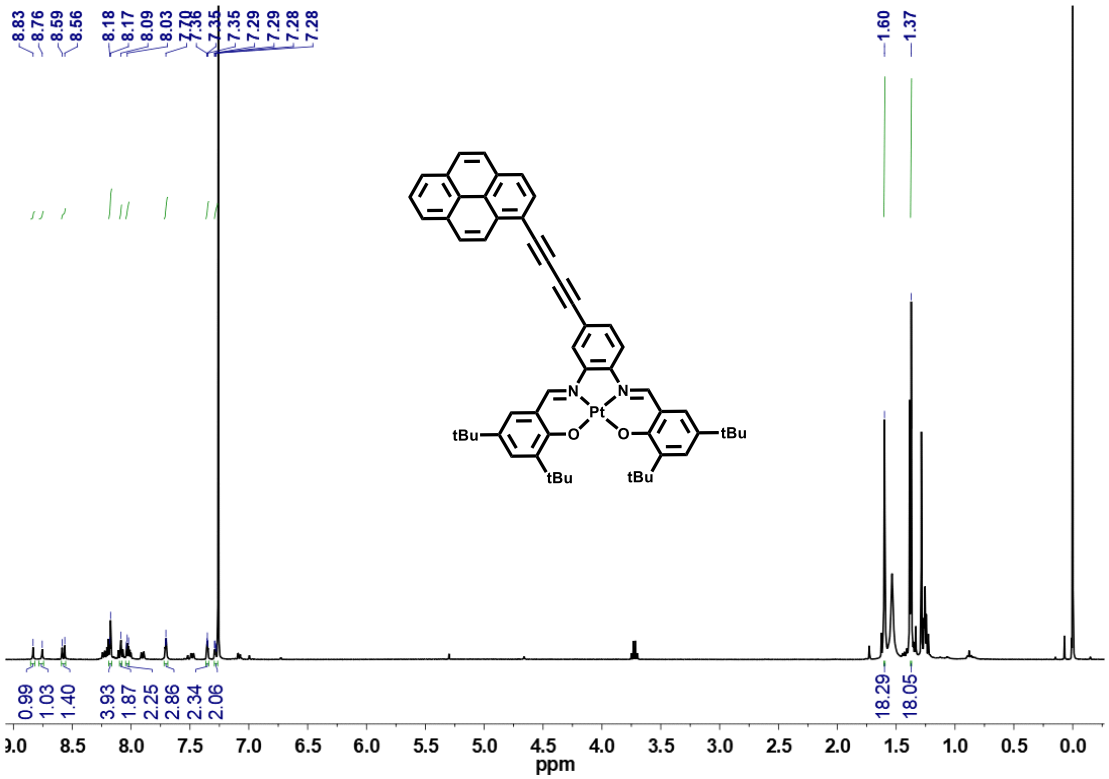

Fig. S46 ^{1}H NMR spectrum of **Pt-2** measured in $CDCl_3$ at 25 °C.

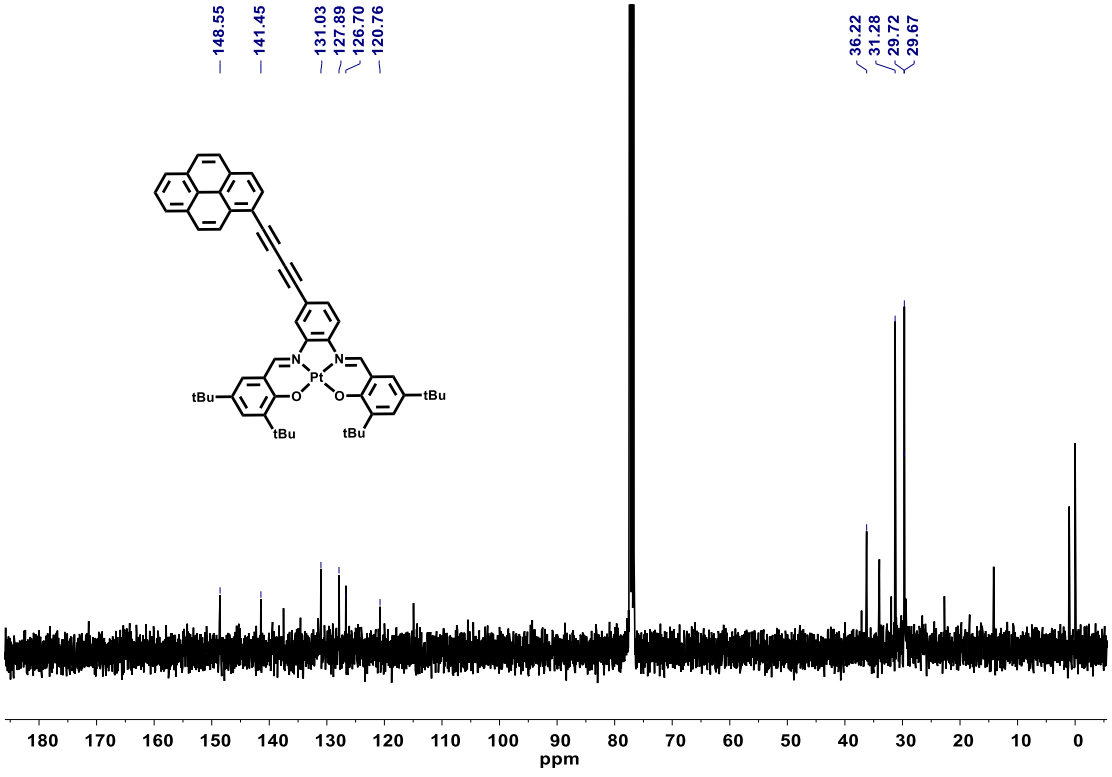

Fig. S47 ^{13}C NMR spectrum of **Pt-2** measured in $CDCl_3$ at 25 °C.

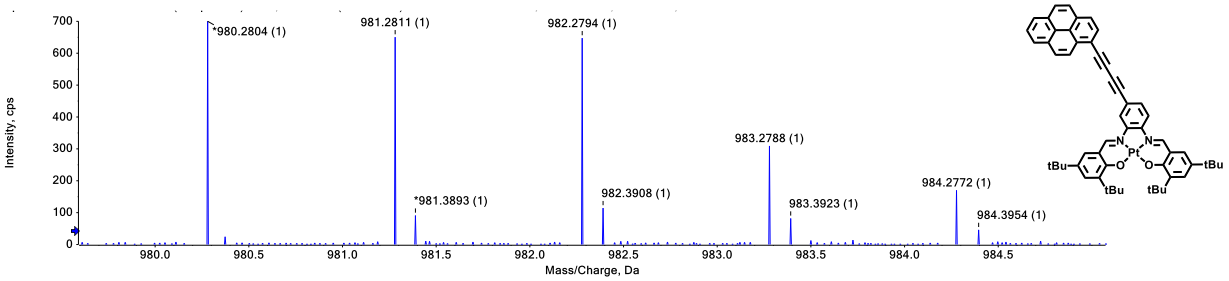

Fig. S48 HRMS spectrum of compound **Pt-2.**

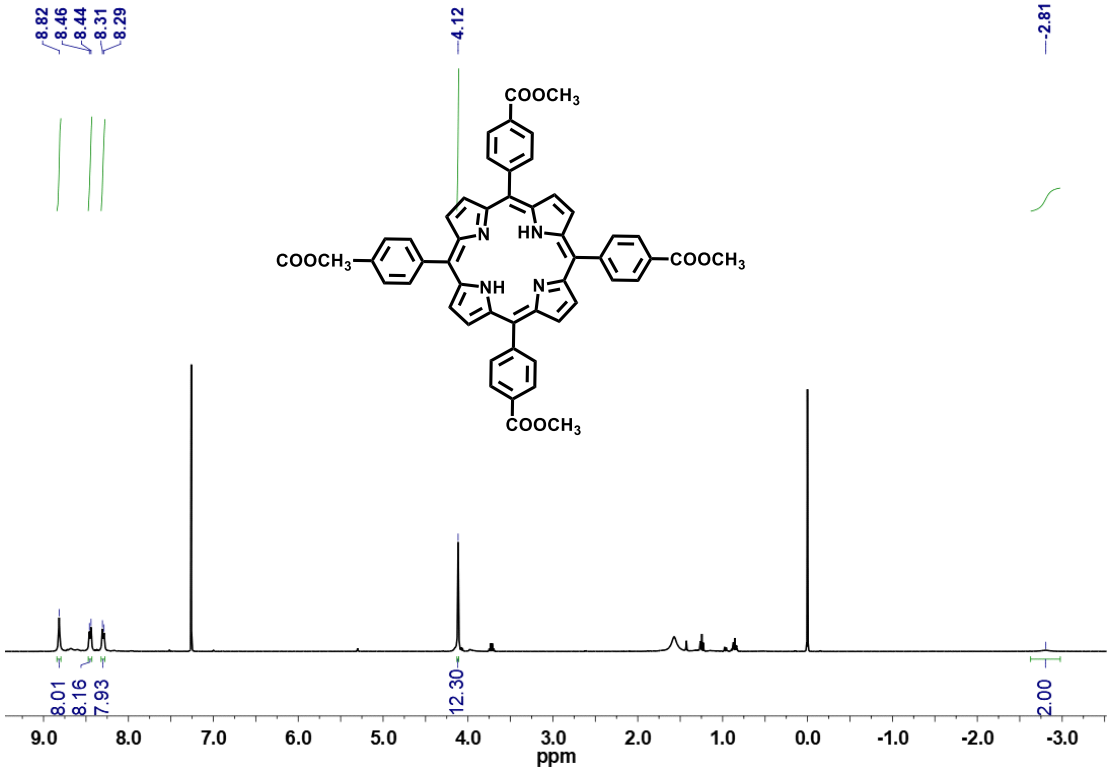

Fig. S49 ^{1}H NMR spectrum of **compound 9** measured in $CDCl_3$ at 25 °C.

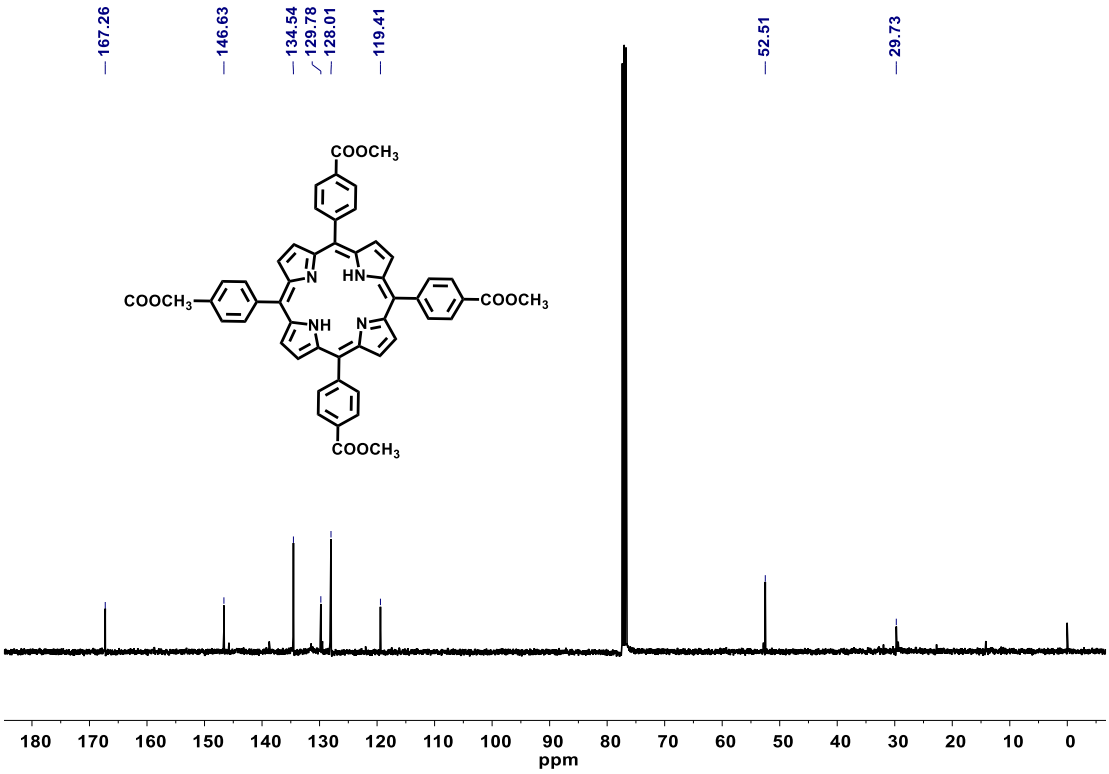

Fig. S50 ^{13}C NMR spectrum of **compound 9** measured in $CDCl_3$ at 25°C.

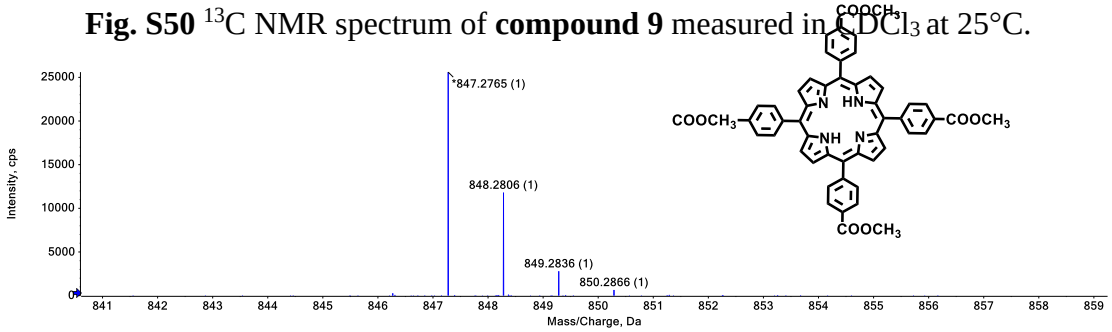

Fig. S51 HRMS spectrum of **compound 9.**

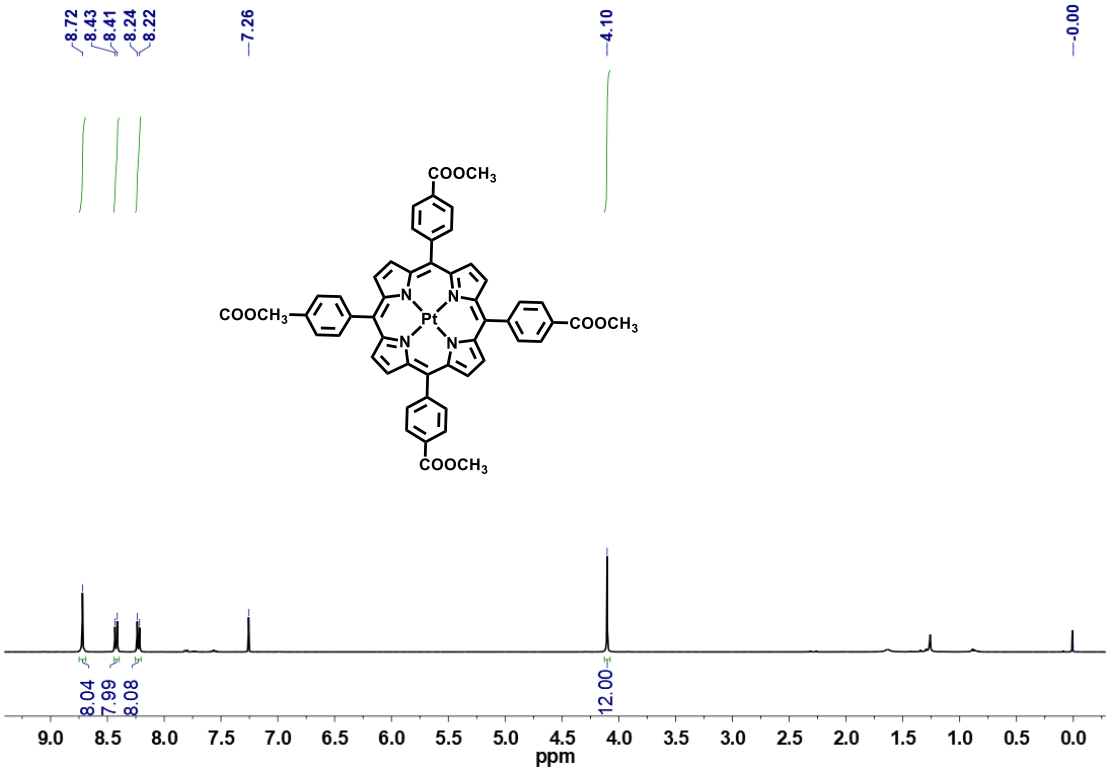

Fig. S52 ^{1}H NMR spectrum of **compound 10** measured in $CDCl_3$ at 25 °C.

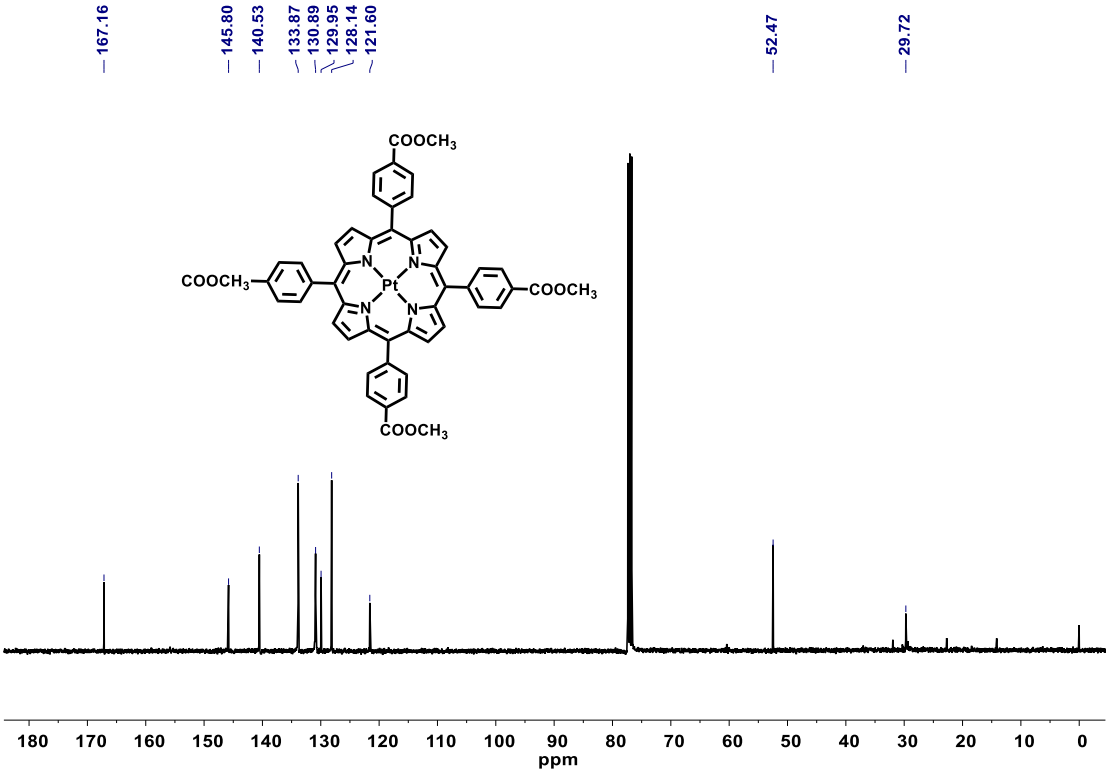

Fig. S53 ^{13}C NMR spectrum of **compound 10** measured in $CDCl_3$ at 25 °C.

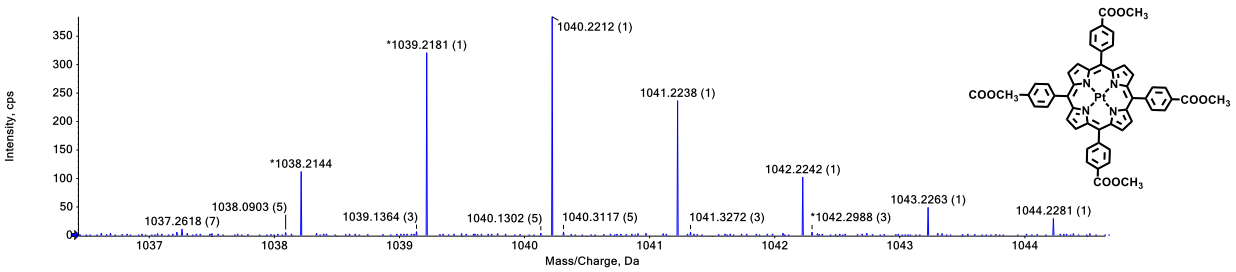

Fig. S54 HRMS spectrum of **compound 10.**

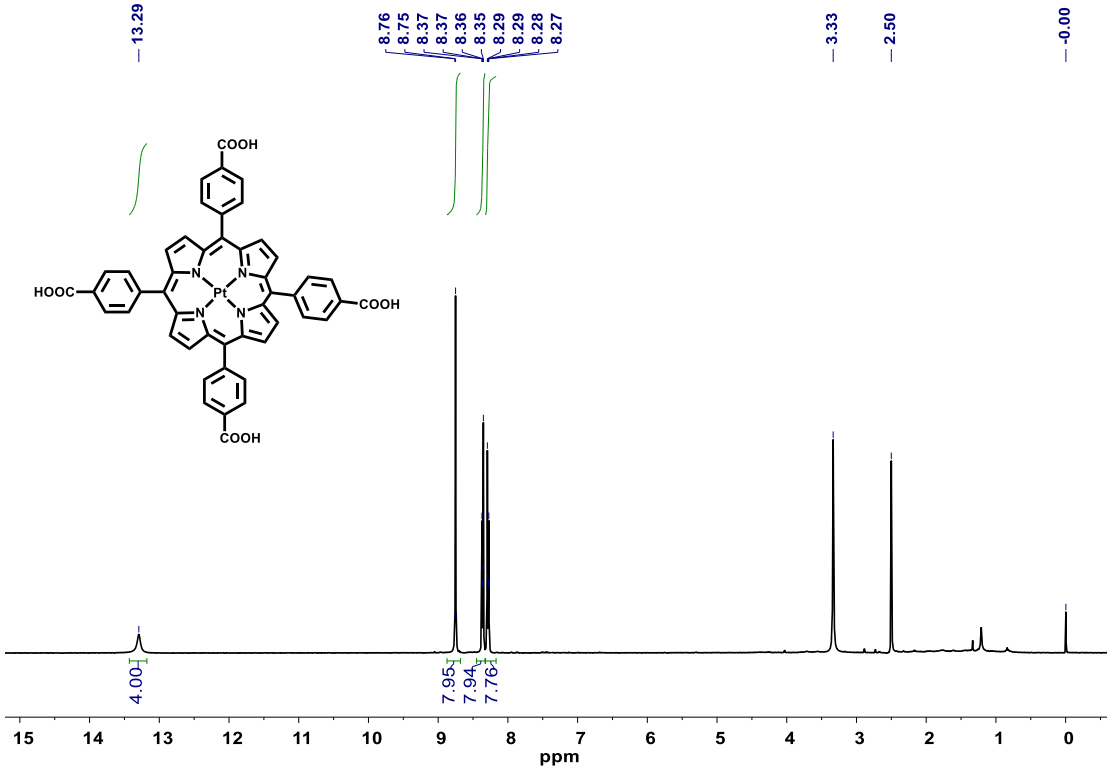

Fig. S55 ^{1}H NMR spectrum of **PtTCPP** measured in DMSO-d_6 at 25 °C.

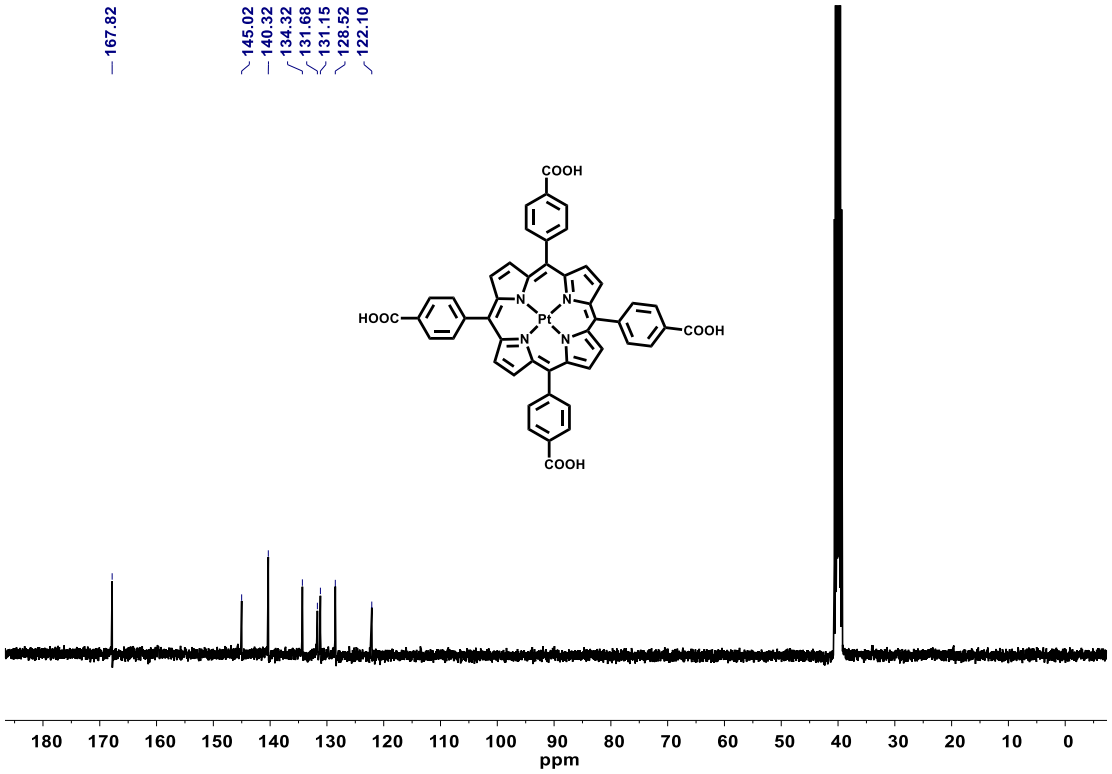

Fig. S56 ^{13}C NMR spectrum of **PtTCPP** measured in DMSO-d_6 at 25 °C.

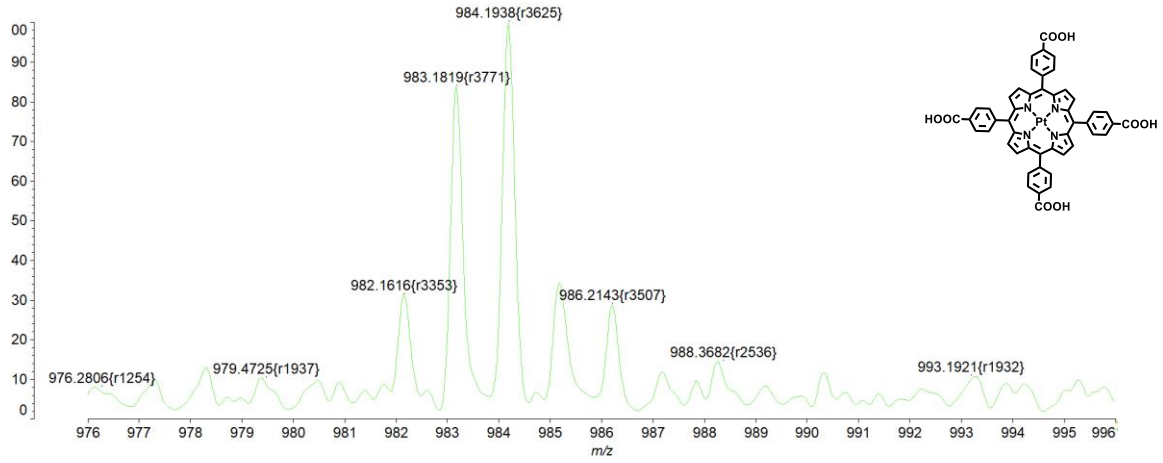

Fig. S57 MALDI-TOF of compound **PtTCPP.**

5.0 Characterization of the hydrogels

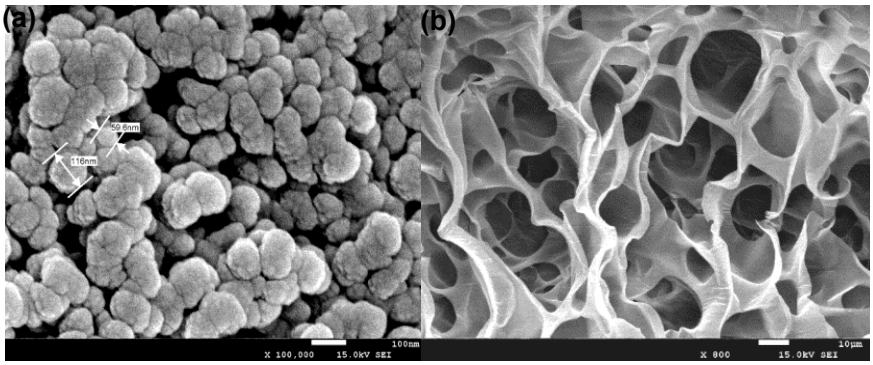

Fig. S58 SEM images of (a) 4.0 % clay solutions; (b) XLG/PVP hydrogel in the absence of **PtOEP** and **DPAS** dyes pair.

Table S3 The original data of monomer conversion rate.

Polymerization time / min	A_i[a]	A_s[b]	A_i/A_s	Conversion / %
0	17768172	8509047	2.088151	0.00
4	15689123	8613608	1.821435	12.77
10	13058639	8877831	1.470927	29.56
12	10170056	8944659	1.136998	45.55
16	7292858	9031908	0.807455	61.33
20	5345228	9082144	0.588543	71.82
24	3992849	8939076	0.446674	78.61
28	2369483	8447550	0.280494	86.57
32	1716804	8514870	0.201624	90.34
36	1339459	8589472	0.155942	92.53
40	1022290	8515828	0.120046	94.25
45	740978	8550588	0.086658	95.85
50	690719	8496565	0.081294	96.11

[a] the peak aera of monomer; [b] the peak of standard. (1-Iododecane as the internal standard)

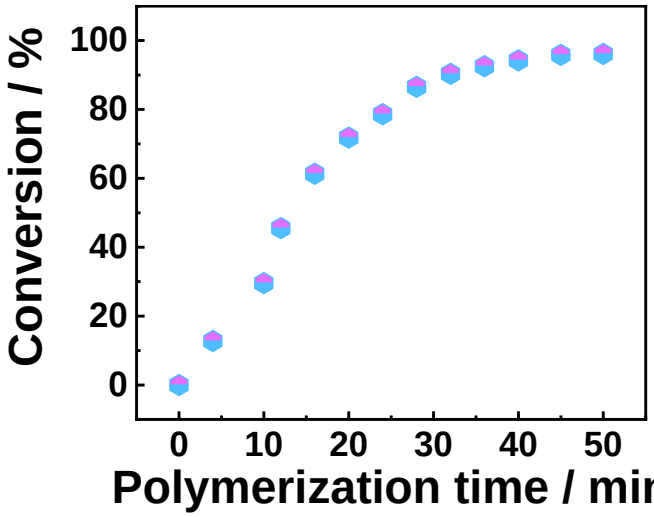

Fig. S59 Dependence of the conversion of monomer (NVP) on different polymerization time.

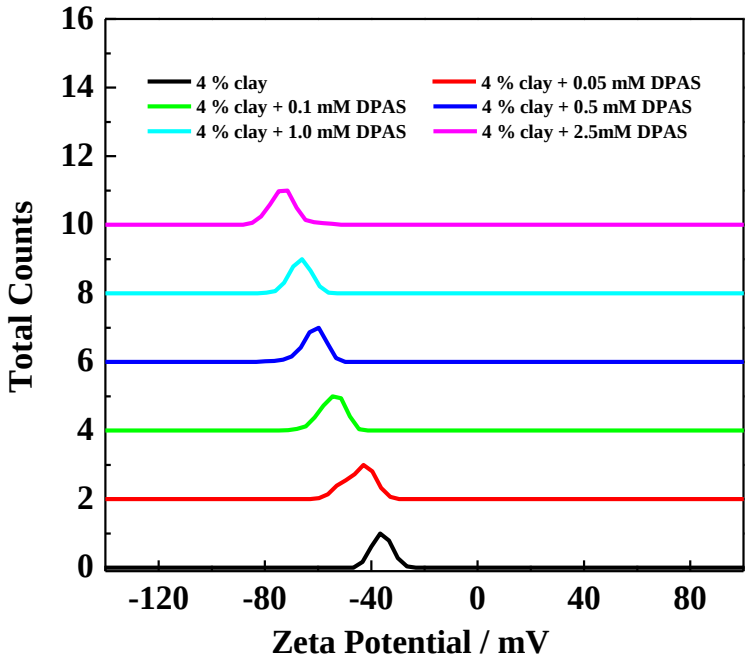

Fig. S60 Zeta potential of 4.0 wt% clay solution in the presence of different concentrations of **DPAS**.

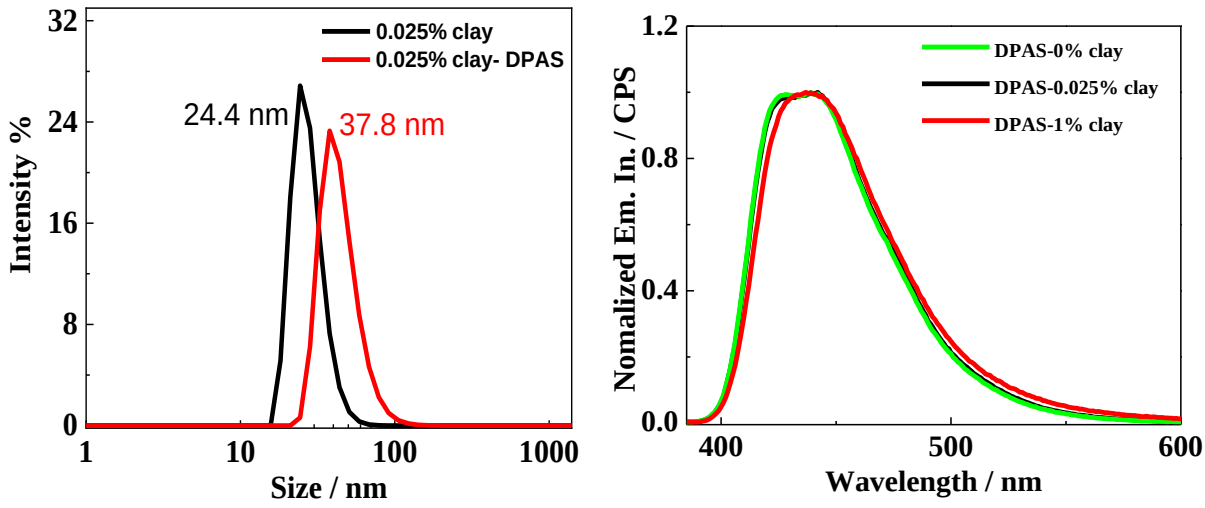

Fig. S61 (a) DLS of 0.025 % clay solutions in the presence of **DPAS**. ([**DPAS**] = 5 μM) and (b) Emission spectra of **DPAS** in the presence of different concentrations of clay solutions.

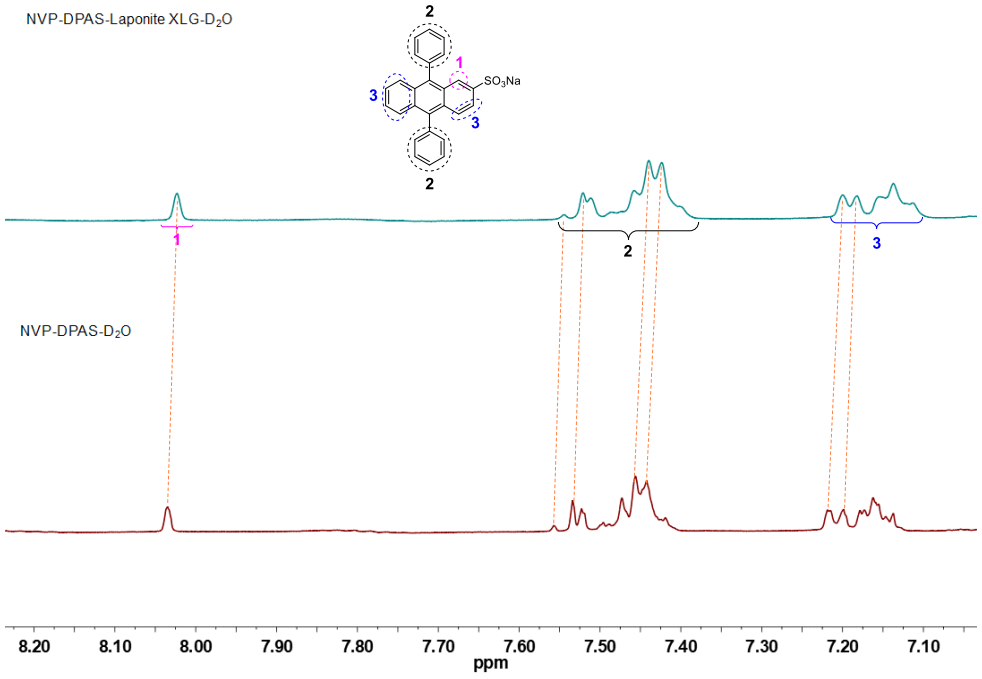

Fig. S62 ^{1}H NMR spectrum of **DPAS** in NVP before (down) and after adding the Laponite XLG nanosheets, measured in D_2O at 25 °C.

6.0 Photophysical property details of the UC dyes pair

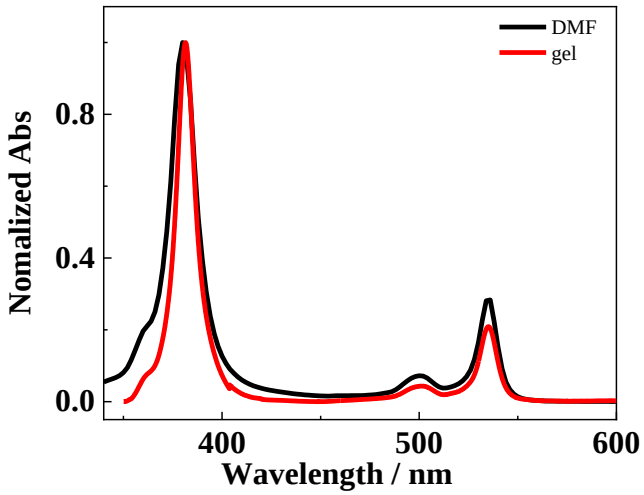

Fig. S63 Normalized absorption spectra of **PtOEP** in XLG/PVP hydrogel (red) and in DMF (black). (**[PtOEP]** = 10 μM).

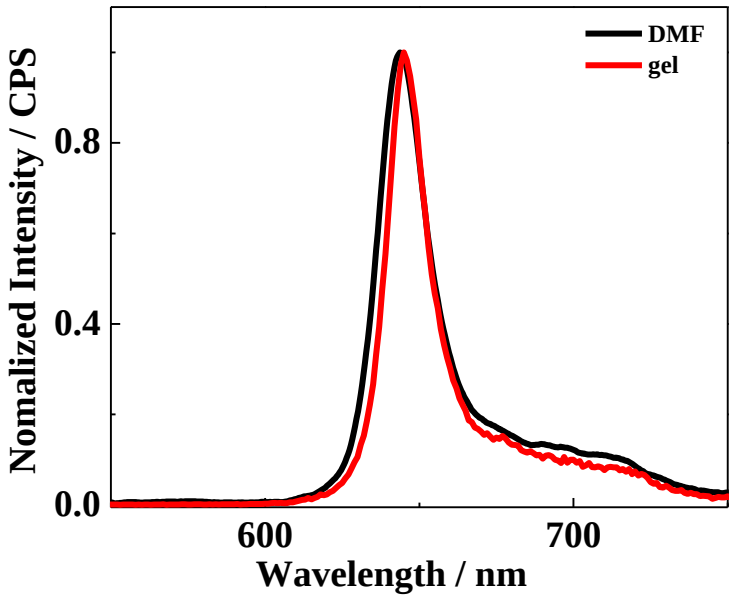

Fig. S64 Normalized emission spectra of **PtOEP** in XLG/PVP hydrogel (red) and in DMF (black). (λ_{ex} = 530 nm, **[PtOEP]** = 10 μM).

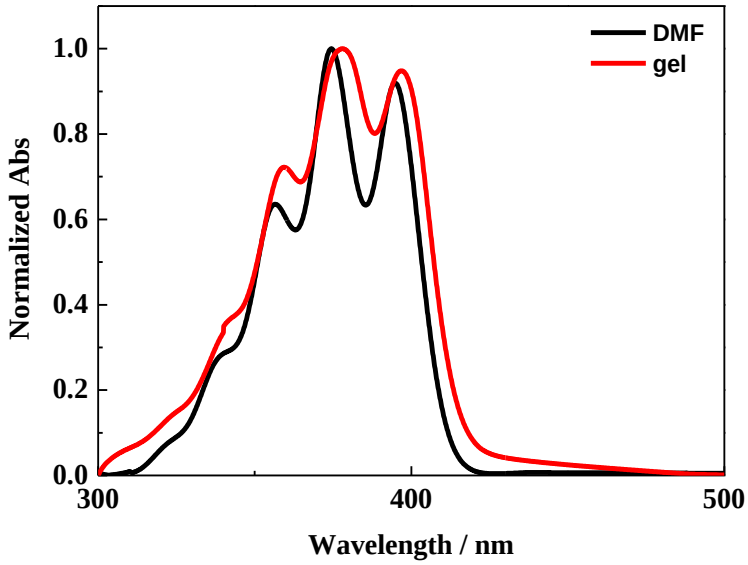

Fig. S65 Normalized absorption spectra of **DPAS** in XLG/PVP hydrogel (red) and in DMF (black). (**[DPAS]** = 0.2 mM)

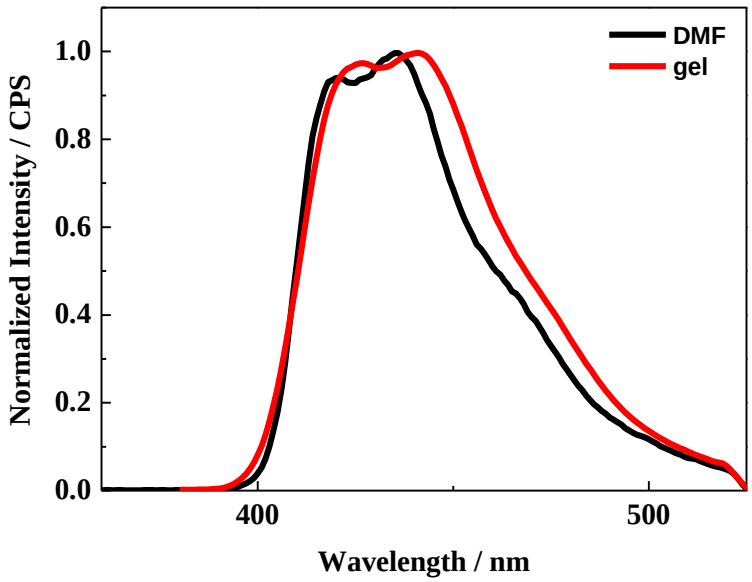

Fig. S66 Normalized emission spectra of **DPAS** in XLG/PVP hydrogel (red) and in DMF (black). (λ_{ex} = 370 nm, **[DPAS]** = 0.2 mM)

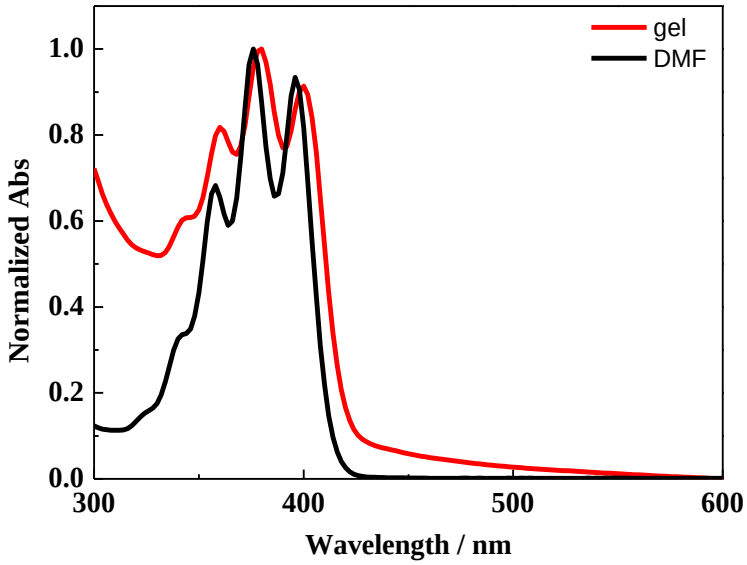

Fig. S67 Normalized absorption spectra of **A-1** in XLG/PVP hydrogel (red) and in DMF (black). (**[A-1]** = 0.2 mM)

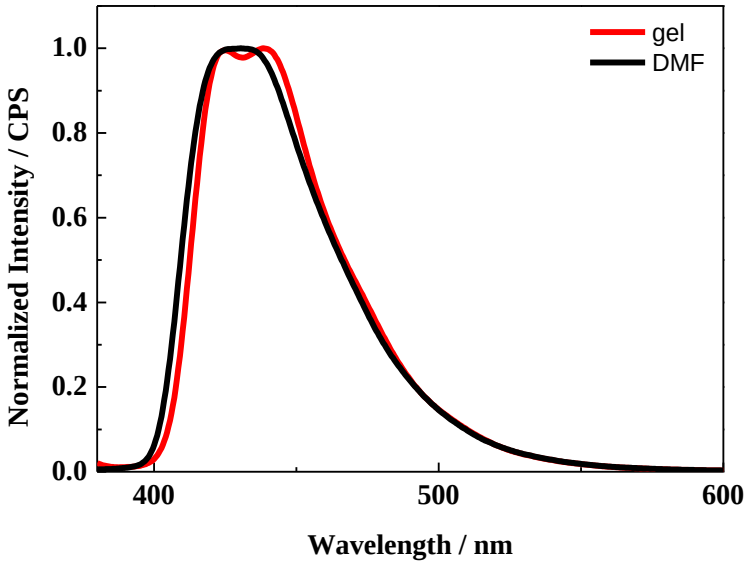

Fig. S68 Normalized emission spectra of **A-1** in XLG/PVP hydrogel (red) and in DMF (black). (λ_{ex} = 370 nm, **[A-1]** = 0.2 mM)

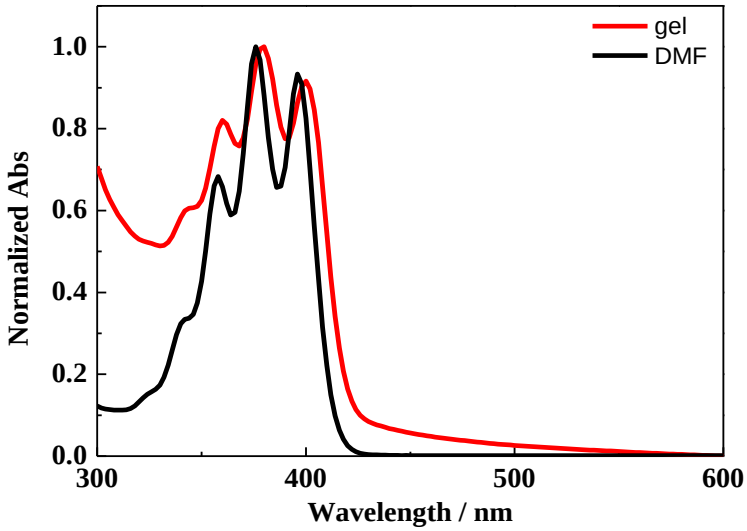

Fig. S69 Normalized absorption spectra of **A-2** in XLG/PVP hydrogel (red) and in DMF (black). (**[A-2]** = 0.2 mM)

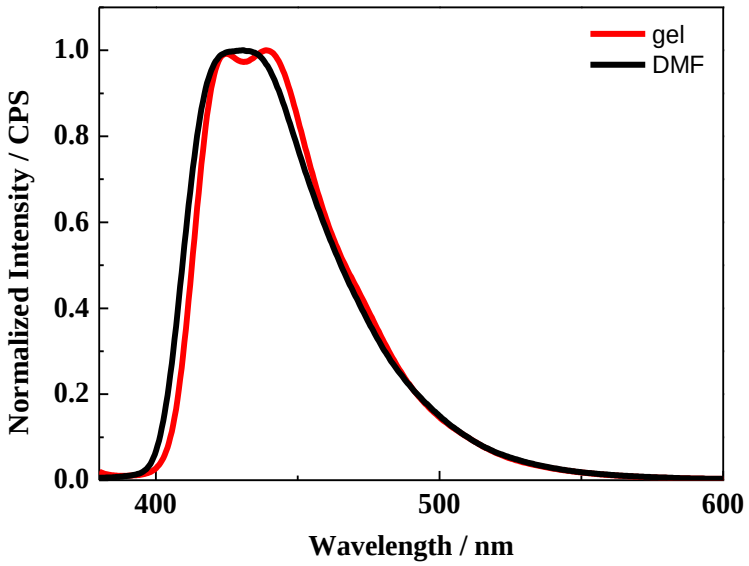

Fig. S70 Normalized emission spectra of **A-2** in XLG/PVP hydrogel (red) and in DMF (black). (λ_{ex} = 370 nm, **[A-2]** = 0.2 mM)

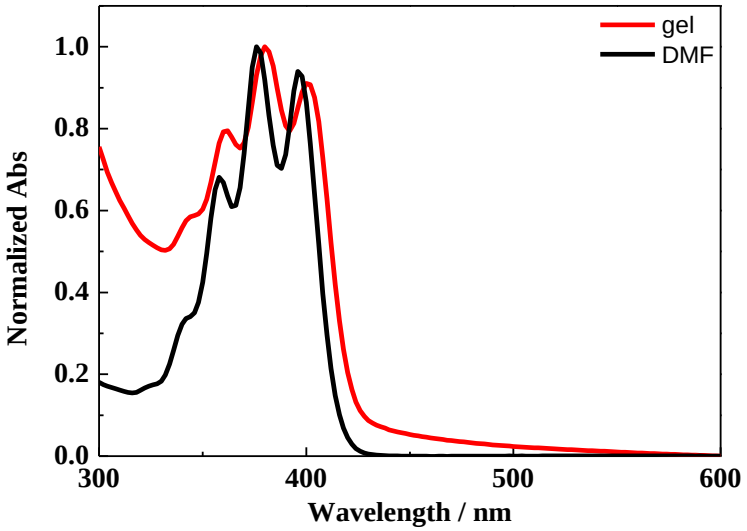

Fig. S71 Normalized absorption spectra of **A-3** in XLG/PVP hydrogel (red) and in DMF (black). (**[A-3]** = 0.2 mM)

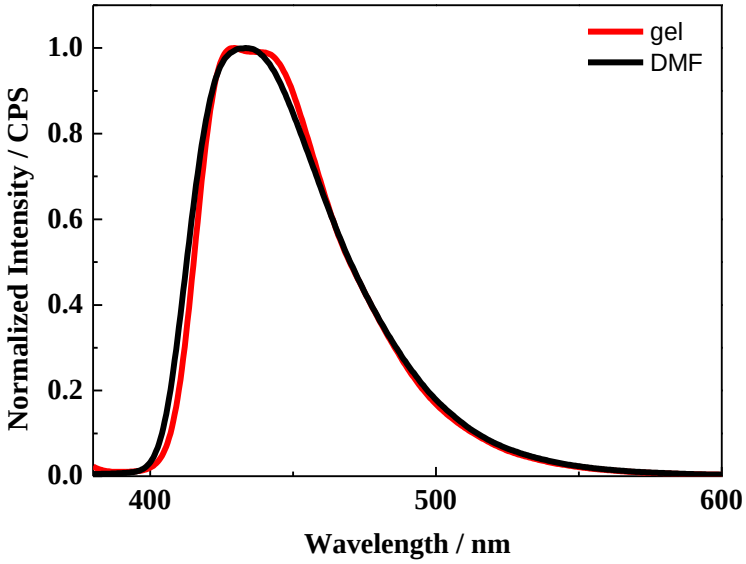

Fig. S72 Normalized emission spectra of **A-3** in XLG/PVP hydrogel (red) and in DMF (black). (λ_{ex} = 370 nm, **[A-3]** = 0.2 mM)

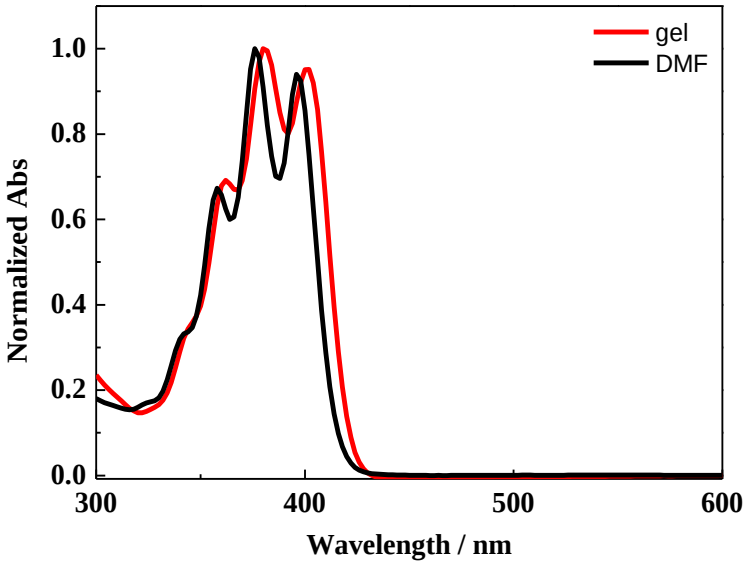

Fig. S73 Normalized absorption spectra of **A-4** in XLG/PVP hydrogel (red) and in DMF (black). (**[A-4]** = 0.2 mM)

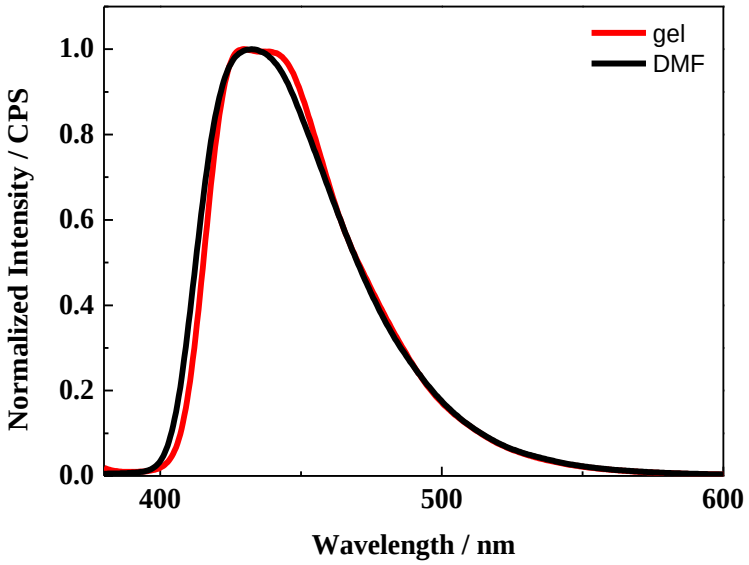

Fig. S74 Normalized emission spectra of **A-4** in XLG/PVP hydrogel (red) and in DMF (black). (λ_{ex} = 370 nm, **[A-4]** = 0.2 mM)

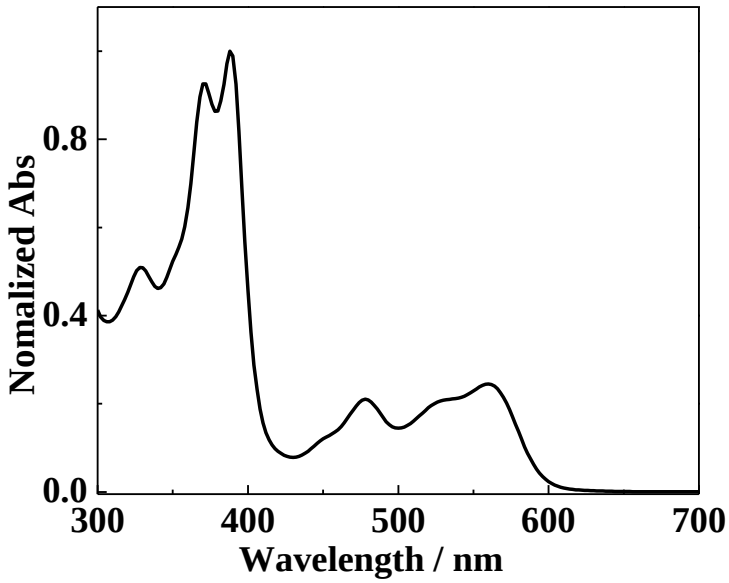

Fig. S75 Normalized absorption spectra of **Pt-1** in XLG/PVP hydrogel.

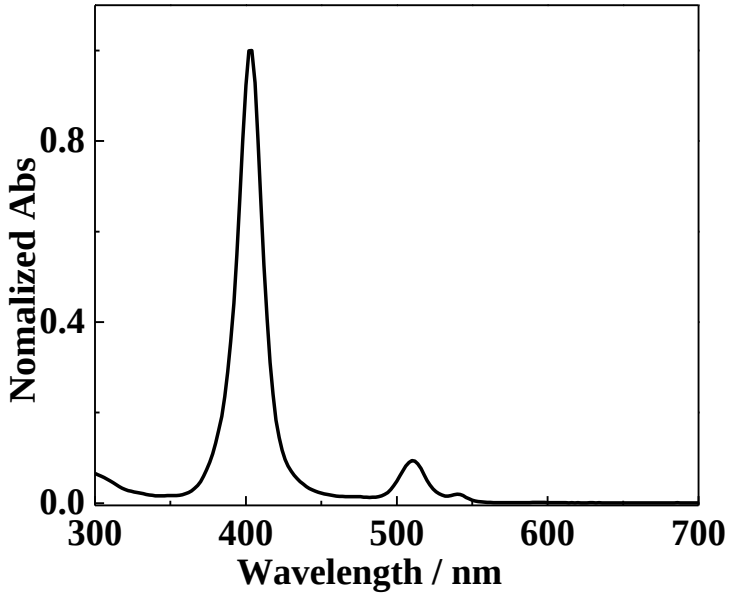

Fig. S76 Normalized absorption spectra of **PtTCPP** in XLG/PVP hydrogel.

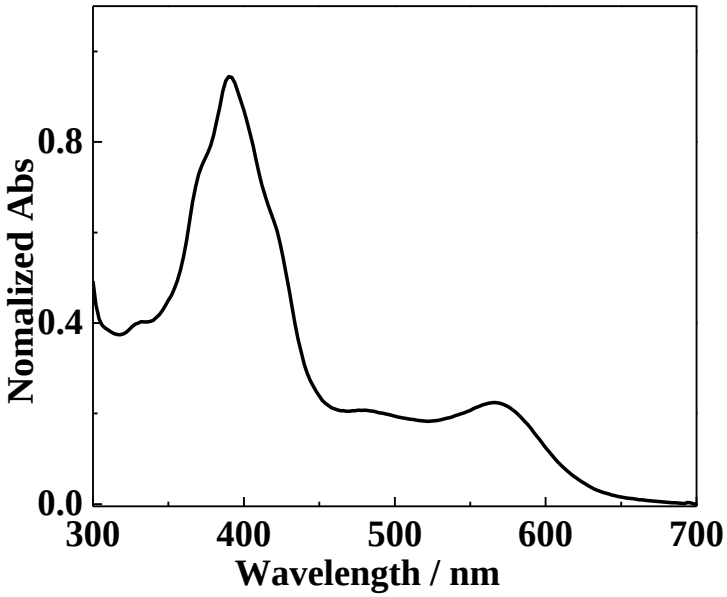

Fig. S77 Normalized absorption spectra of **Pt-2** in XLG/PVP hydrogel.

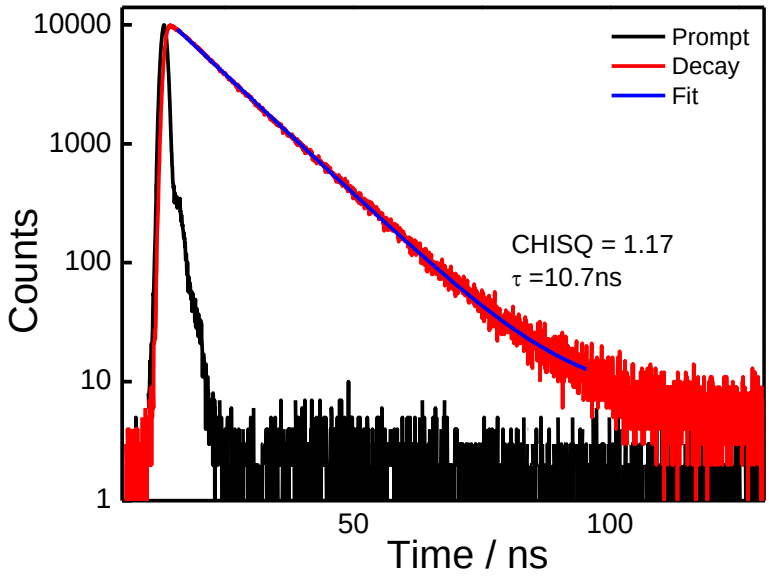

Fig. S78 The prompt emission decay of **DPAS** in the XLG/PVP hydrogel. The decay was monitored at 442 nm excited with 390 nm Nano LED. (**[DPAS]** = 2.5 mM)

7.0 Upconversion details in hydrogels

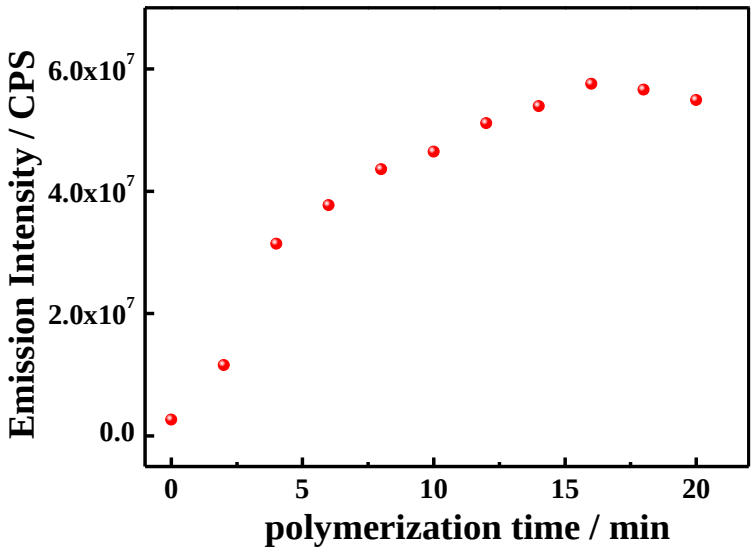

Fig. S79 Dependence of the integration of UC emission on different polymerization time. (**[PtOEP]** = 10 μM, **[DPAS]** = 2.5 mM)

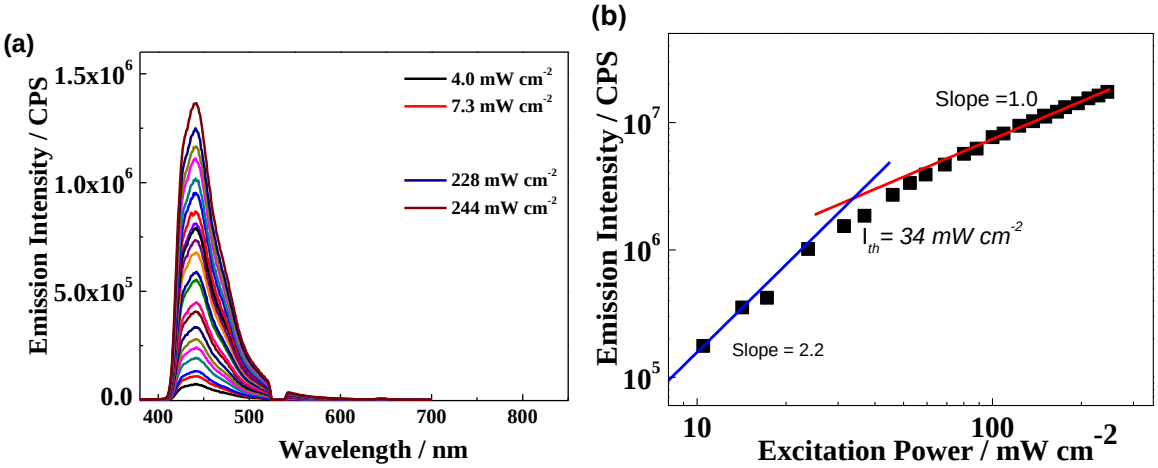

Fig. S80 (a) UC emission intensity of XLG/PVP gel doped with **PtOEP/DPAS** at different power under 532 nm laser (**[PtOEP]** = 10 μM, **[DPAS]** = 1.0 mM) **(b)** Dependence of the integration of UC emission on the incident power density. The TTA-UC threshold excitation intensity (I_{th}) was estimated to be 34 mW cm^{-2} from the intersection point of the two slopes.

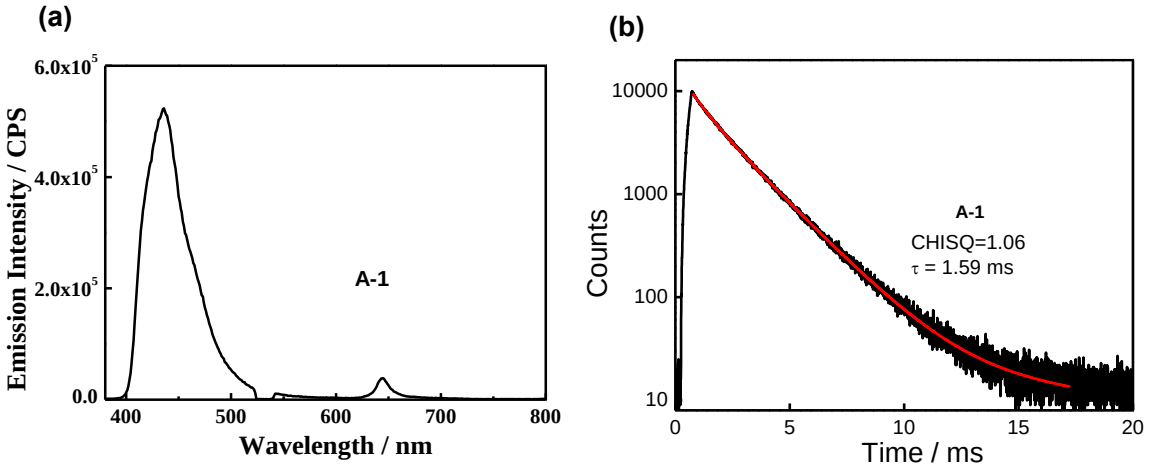

Fig. S81 (a) The UC emission spectra of the freshly prepared XLG/PVP hydrogel doped with 10 μM **PtOEP** and 2.5 mM **A-1.** (P.I. = 8.0 mW) **(b)** UC emission decay of the XLG/PVP hydrogel doped with **PtOEP/A-1** under 532 nm laser, the decay was monitored at 441 nm.

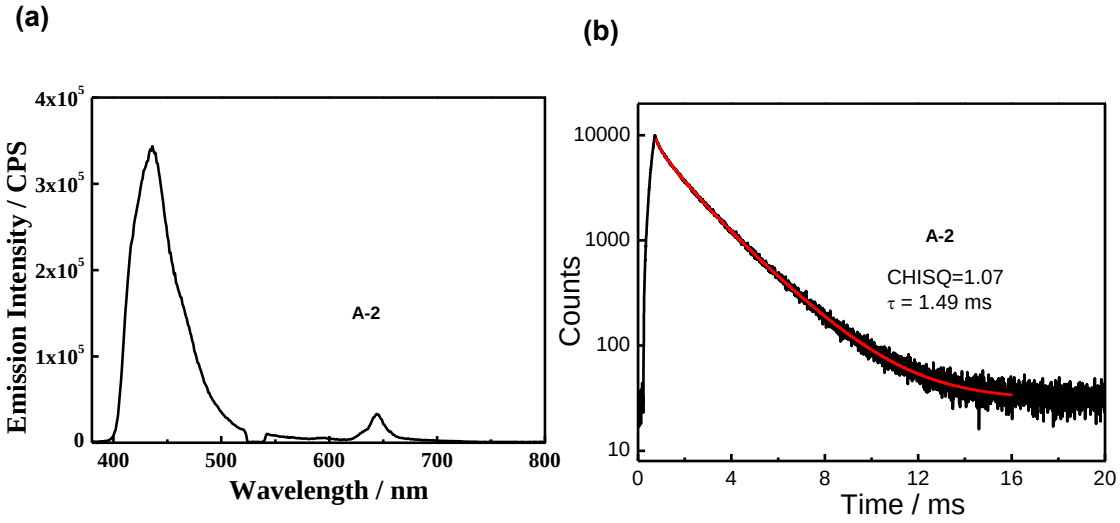

Fig. S82 (a) The UC emission spectra of the freshly prepared XLG/PVP hydrogel doped with 10 μM **PtOEP** and 2.5 mM **A-2.** (P.I. = 8.0 mW) **(b)** UC emission decay of XLG/PVP gel doped with **PtOEP/A-2** under 532 nm laser, the decay was monitored at 441 nm.

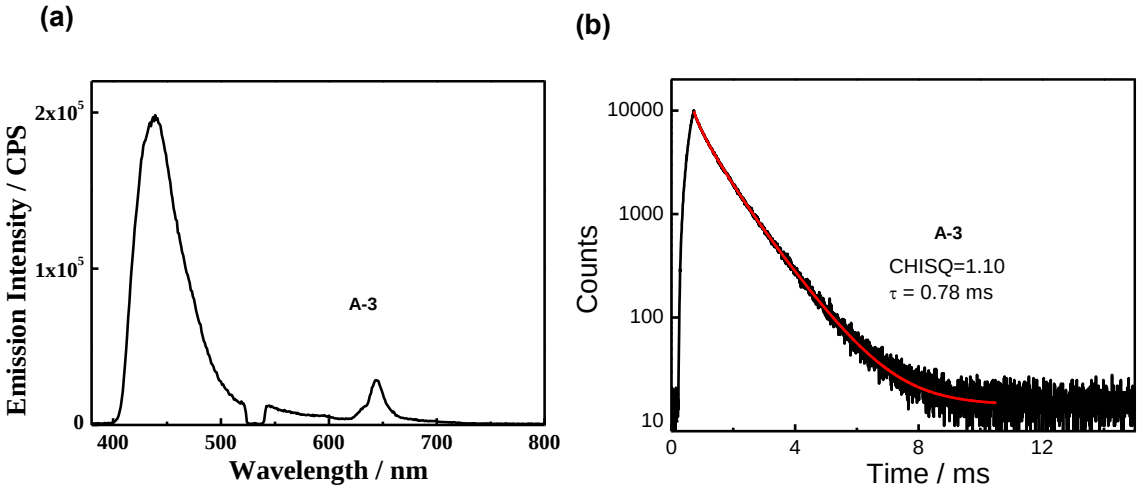

Fig. S83 (a) The UC emission spectra of the freshly prepared XLG/PVP hydrogel doped with 10 μM **PtOEP** and 2.5 mM **A-3.** (P.I. = 8.0 mW) **(b)** UC emission decay of XLG/PVP hydrogel doped with **PtOEP/A-3** under 532 nm laser, the decay of the emission was monitored at 441 nm.

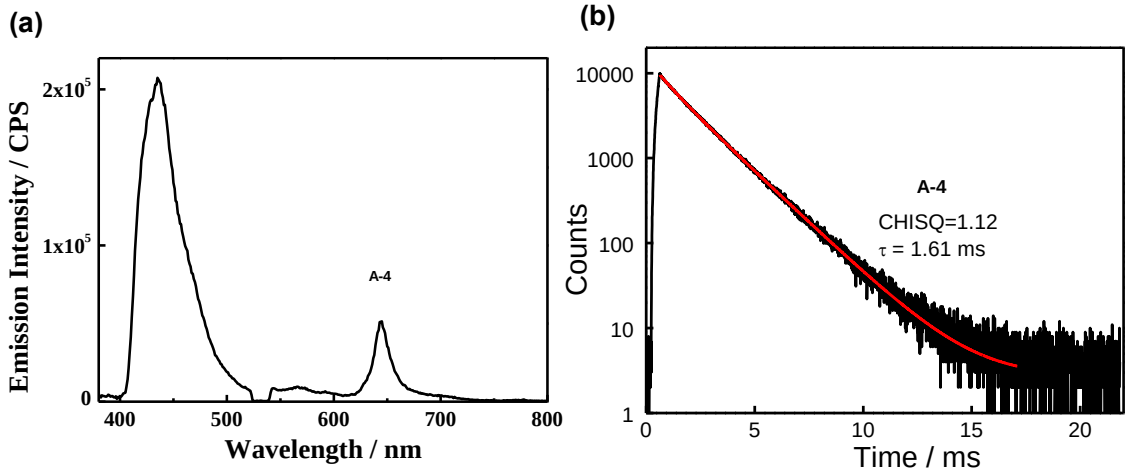

Fig. S84 (a) The UC emission spectra of the freshly prepared XLG/PVP hydrogel doped with 10 μM **PtOEP** and 2.5 mM **A-4** (P.I. = 8.0 mW); **(b)** UC emission decay curves of XLG/PVP hydrogel doped with **PtOEP/A-4** under 532 nm laser, the decay was monitored at 441 nm.

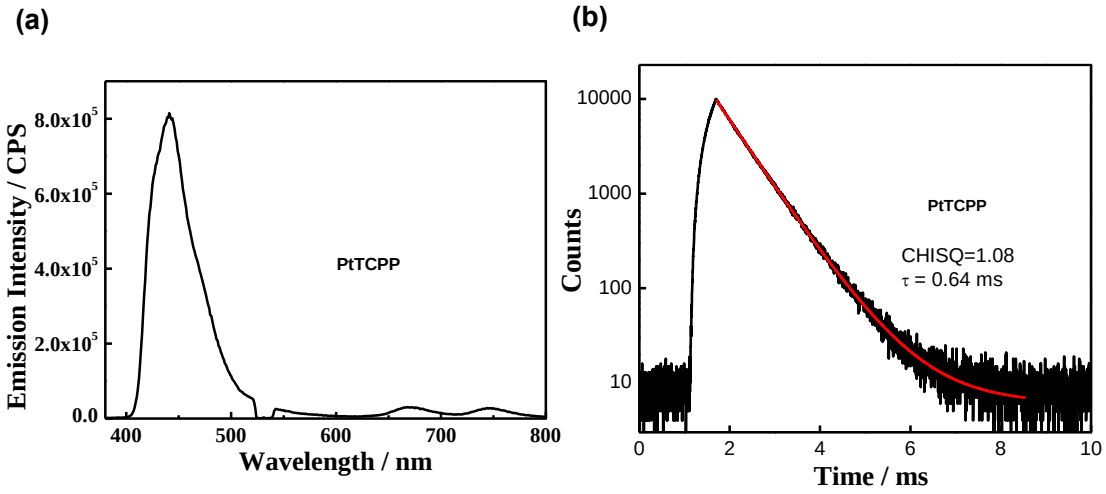

Fig. S85 (a) The UC emission spectra of the freshly prepared XLG/PVP hydrogel doped with 10 μM **PtTCPP** and 2.5 mM **DPAS** (P.I. = 8.0 mW); **(b)** UC emission decay of XLG/PVP hydrogel doped with **PtTCPP/DPAS** under 532 nm laser, the decay was monitored at 442 nm.

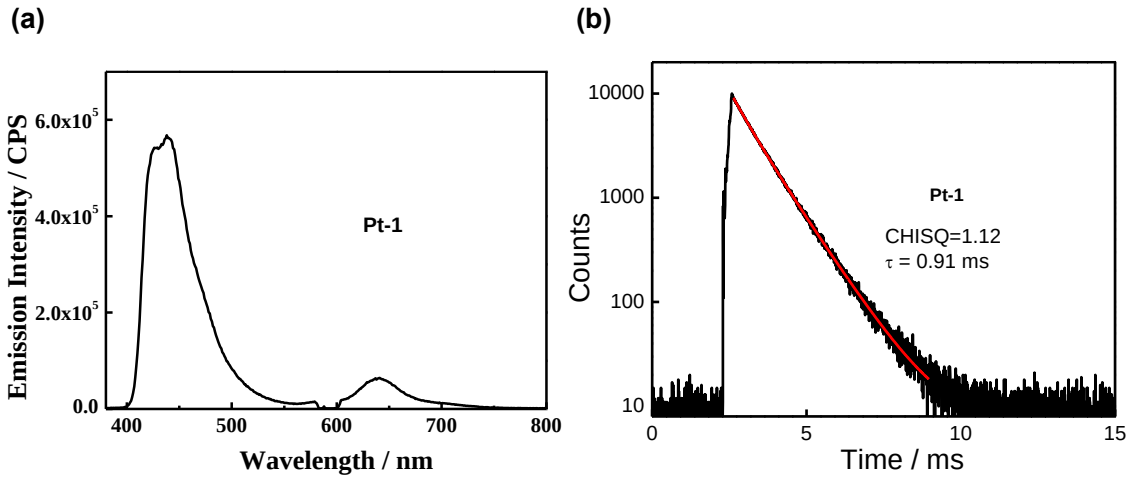

Fig. S86 (a) The UC emission spectra of the freshly prepared XLG/PVP hydrogel doped with 10 μM **Pt-1** and 2.5 mM **DPAS.** (P.I. = 8.0 mW) **(b)** UC emission decay of XLG/PVP hydrogel doped with **Pt-1/DPAS** under 589 nm laser, the decay was monitored at 442 nm.

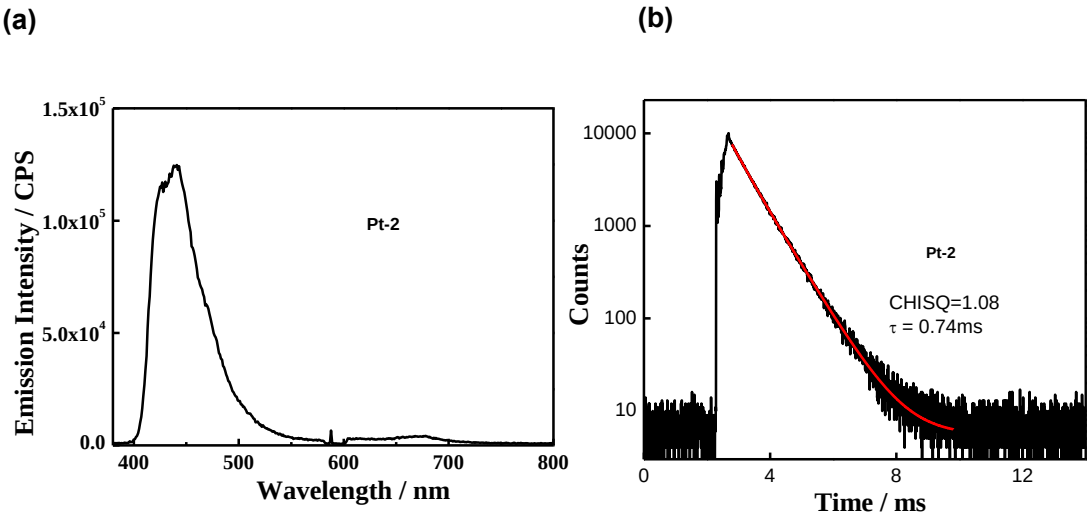

Fig. S87 (a) The UC emission spectra of the freshly prepared XLG/PVP hydrogel doped with 10 μM **Pt-2** and 2.5 mM **DPAS.** (P.I. = 8.0 mW) **(b)** UC emission decay of XLG/PVP hydrogel doped with **Pt-2/DPAS** under 589 nm laser, the decay was monitored at 442 nm.

Table S4 The UC emission related parameters of the XLG/PVP hydrogel doped different sensitizers[a]

Sensitizers	λ_{ex}[b]/ nm	λ_{em}[c]/ nm	τ[d]/ ms	Φ_{UC} %[e]	$\Delta\lambda$[h]/ nm	ΔE[i]/ eV
PtOEP	532	427	2.1	10.0[f]	-105	0.57
PtTCPP	532	427	0.64	5.1[f]	-105	0.57
Pt-1	589	427	0.91	4.6[g]	-162	0.80
Pt-2	589	427	0.74	3.3[g]	-162	0.80

[a] DPAS was used as acceptor. [b] Excitation wavelength. [c] Upconverted emission wavelength. [d] the lifetime of the UC emission monitored at 442 nm [e] Upconversion quantum yields. [f] with Rhodamine B as the standard (Φ_F = 89 % in ethanol). [g] with 3,3'-Diethyloxadicarbocyanine iodide (**C-5**) (Φ_F = 49 % in ethanol) as the standard. [h] $\Delta\lambda = \lambda_{em} - \lambda_{ex}$ [i] $\Delta E = 1240/\lambda_{em} - 1240/\lambda_{ex}$.

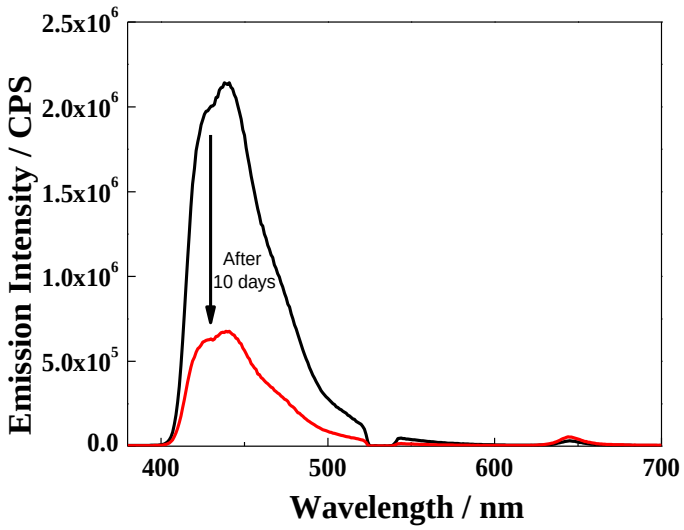

Fig. S88 UC emission spectra of the freshly prepared XLG/PVP hydrogel doped with 10 μM **PtOEP** and 2.5 mM **DPAS** (black line) and that after exposing to ambient atmosphere for 10 days. (P.I. = 4.8 mW)

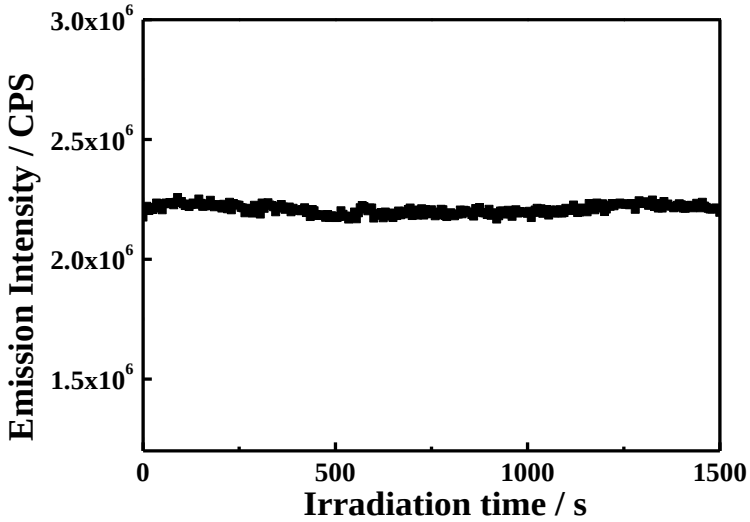

Fig. S89 Kinetics acquisition of the UC emission at 442 nm of a freshly prepared XLG/PVP hydrogel under continuous irradiation of 532 nm laser. (**[PtOEP]** = 10 μM, **[DPAS]** = 2.5 mM, P.I. = 4.8 mW).

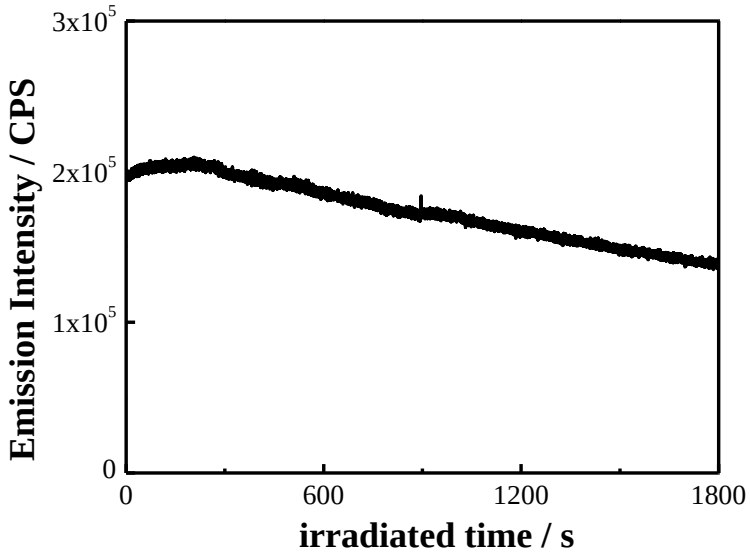

Fig. S90 Kinetics acquisition of the UC emission in the XLG/PMMA gel at 441 nm with continuous irradiation of 532 nm laser. (**[PtOEP]** = 10 μM, **[DPAS]** = 2.5 mM)

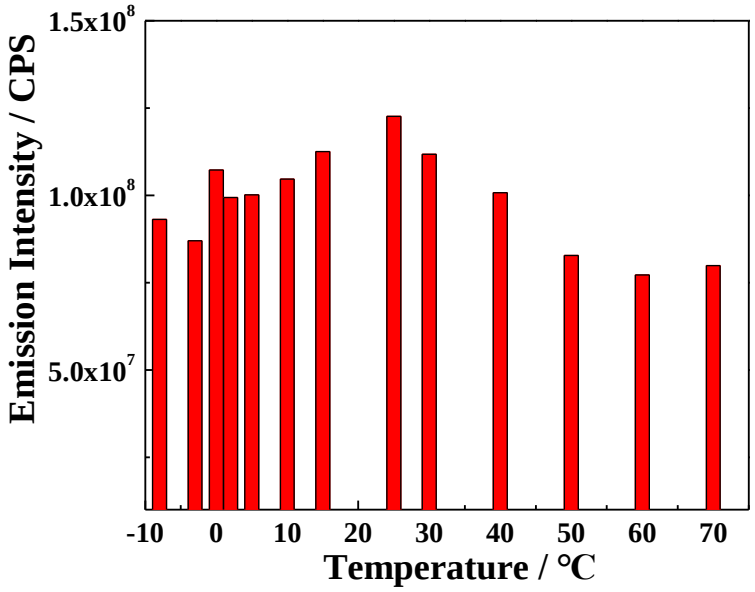

Fig. S91 Temperature dependence of the UC emission in XLG/PVP gel with 532 nm laser (**[PtOEP]** = 10 μM, **[DPAS]** = 2.5 mM)

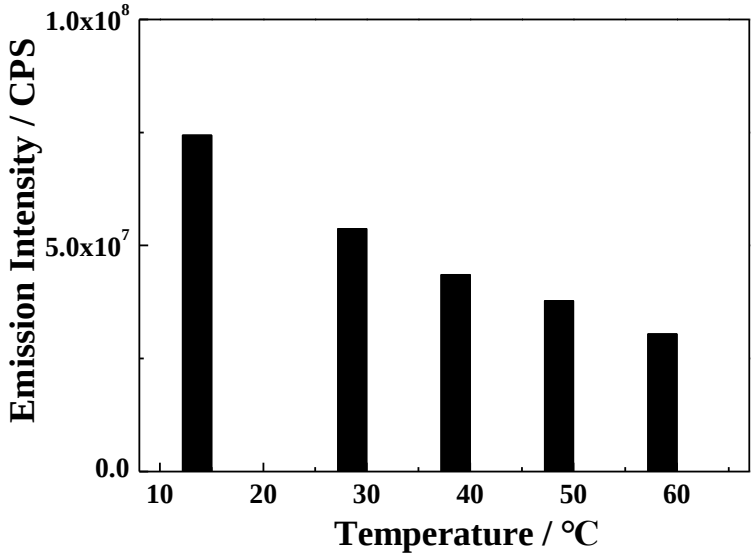

Fig. S92 Temperature dependence of the UC emission in DMF with 532 nm laser (**[PtOEP]** = 10 μM, **[DPAS]** = 2.5 mM)

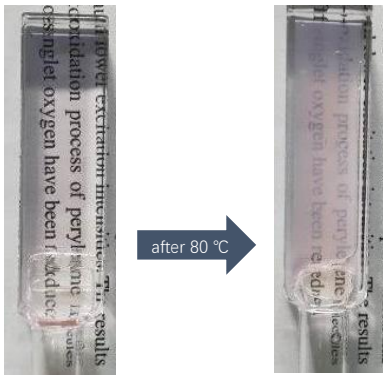

Fig. S93 Digital picture of XLG/PVP gel before and after heating at 80 °C.

8.0 Characterization of the dried gels.

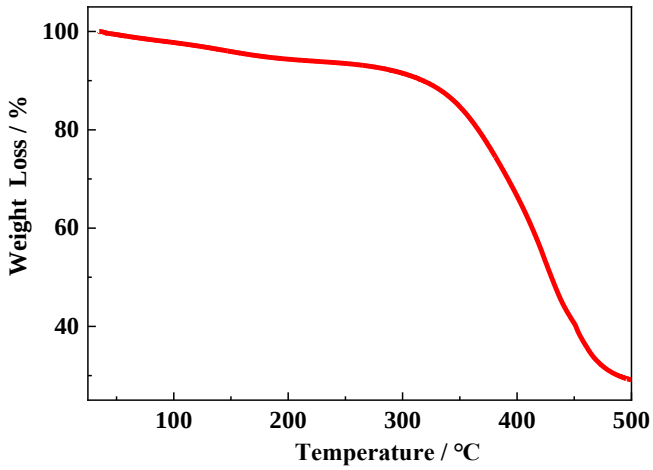

Fig. S94 Thermogravimetric analysis (TG) curve of XLG/PVP dry gel in the presence of **PtOEP** and **DPAS** dyes pair. (**[PtOEP]** = 10 μM, **[DPAS]** = 2.5 mM)

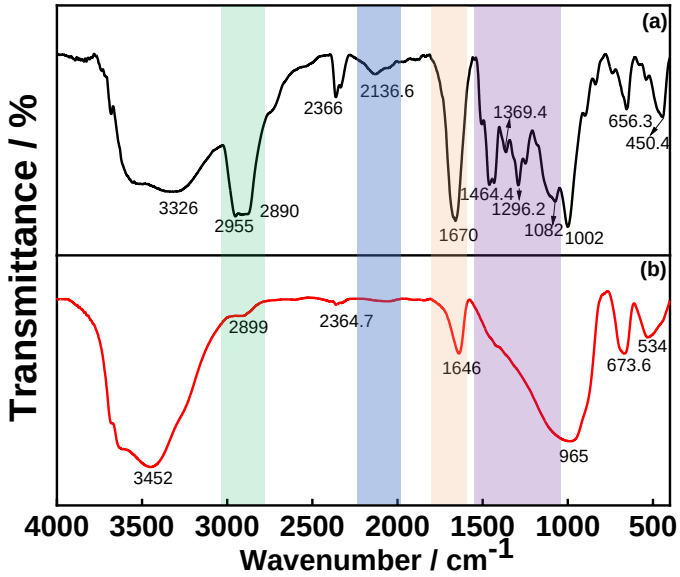

Fig.S95 The Fourier Transform Infrared (FTIR) spectra of (a) XLG/PVP dried gel in the presence of **PtOEP** and **DPAS** dyes pair ([**PtOEP**] = 10 μM, [**DPAS**] = 2.5 mM); (b) XLG Laponite powder.

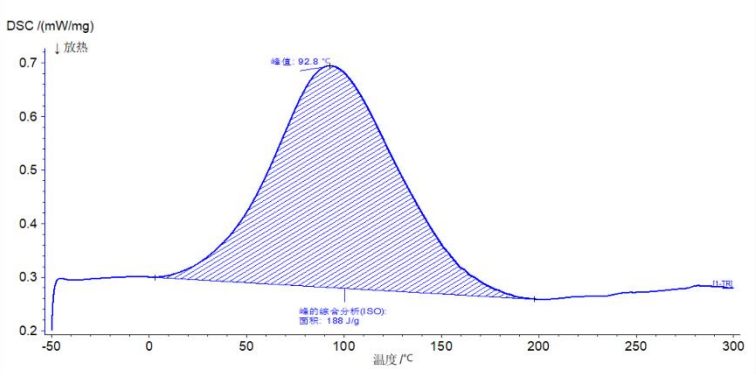

Fig.S96 Differential Scanning Calorimetry (DSC) curves of XLG/PVP hydrogel in the presence of **PtOEP** and **DPAS** dyes pair ([**PtOEP**] = 10 μM, [**DPAS**] = 2.5 mM).

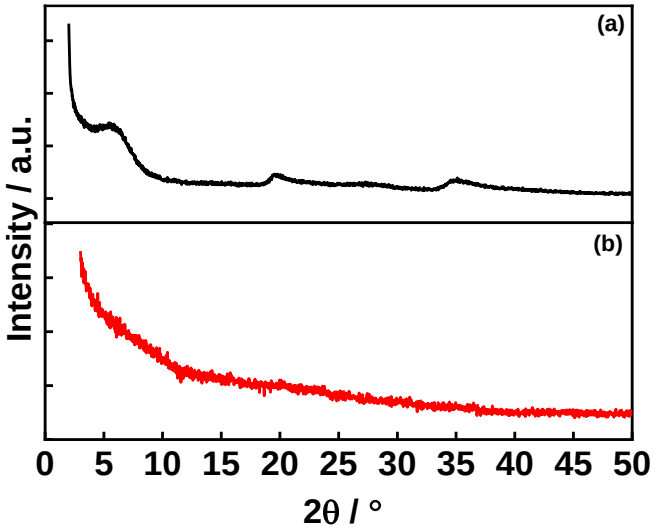

Fig. S97 X-ray diffraction patterns of (a) Laponite XLG powder; (b) XLG/PVP dried gel in the presence of **PtOEP** and **DPAS** dyes pair. (**[PtOEP]** = 10 μM, **[DPAS]** = 2.5 mM).

9.0 Upconversion details in dried gels

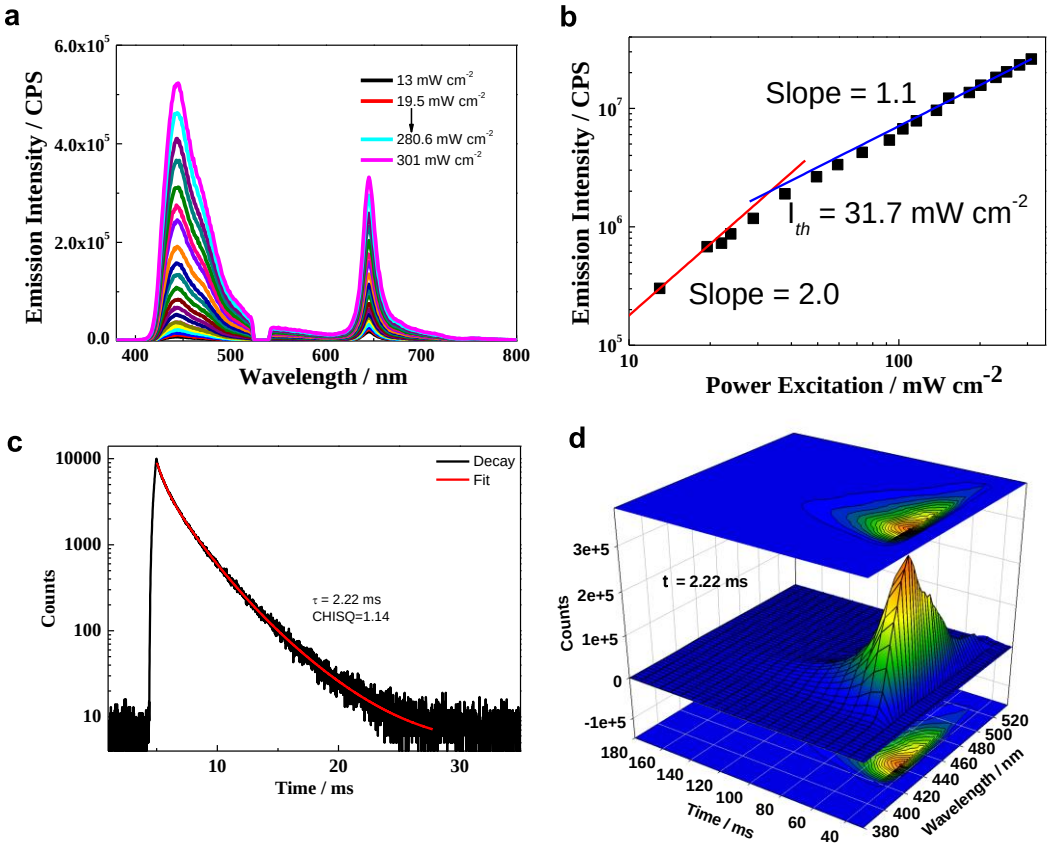

Fig. S98 (a) UC Intensity of dry gel dope with **PtOEP/DPAS** at different power under 532 nm laser; (b) Dependence of the integration of UC emission on the incident power density. The TTA-UC threshold excitation intensity (I_{th}) was estimated to be 31.7 mW cm^{-2} from the intersection point of the two slopes. (c) UC emission decay curves of XLG/PVP dry gel under 532 nm laser, the decay of the emission was monitored at 442 nm. (d) Time-resolved emission spectra (TRES) of the upconverted fluorescence of the UC dry gel at room temperature under 532 nm laser (**[PtOEP]** = 10 μM, **[DPAS]** = 2.5 mM).

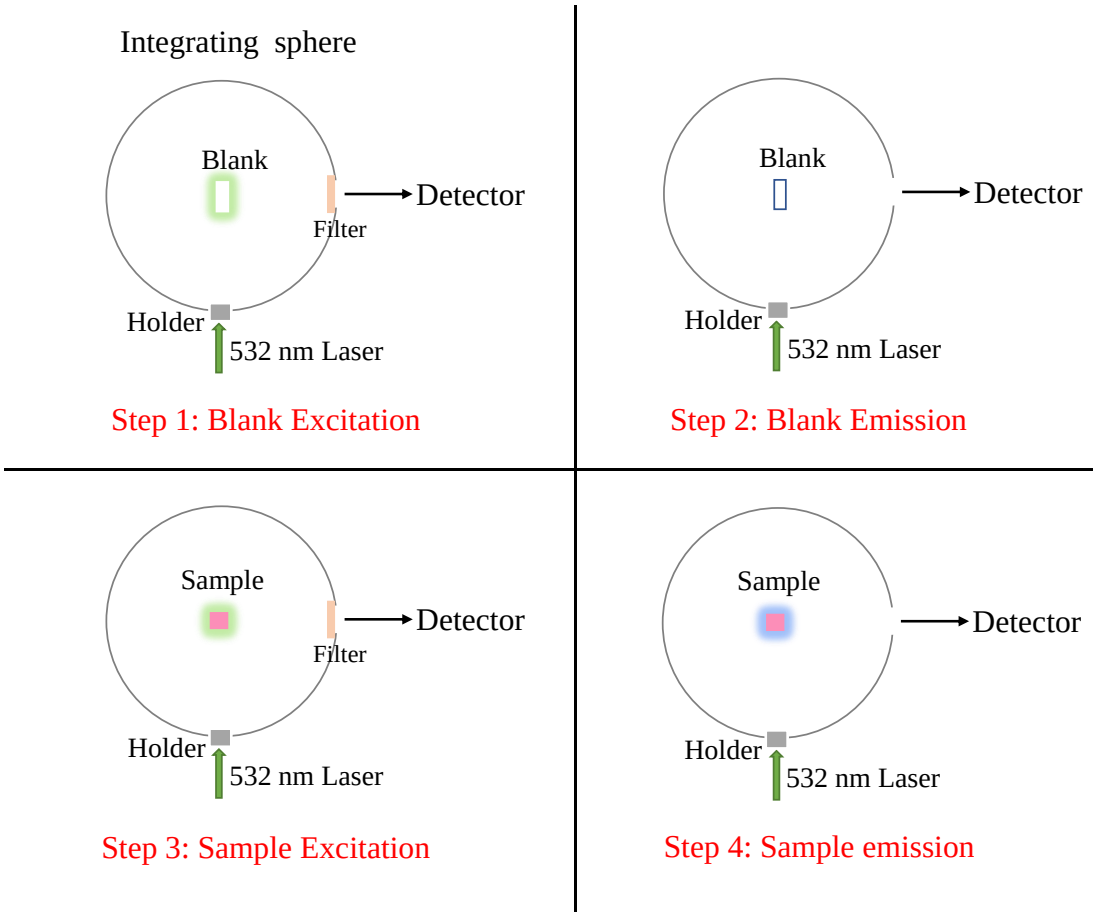

Fig. S99 Schematic diagram of absolute quantum efficiency measurements of TTA-UC system in dry gel. Four curve method is adopted in the experiments.

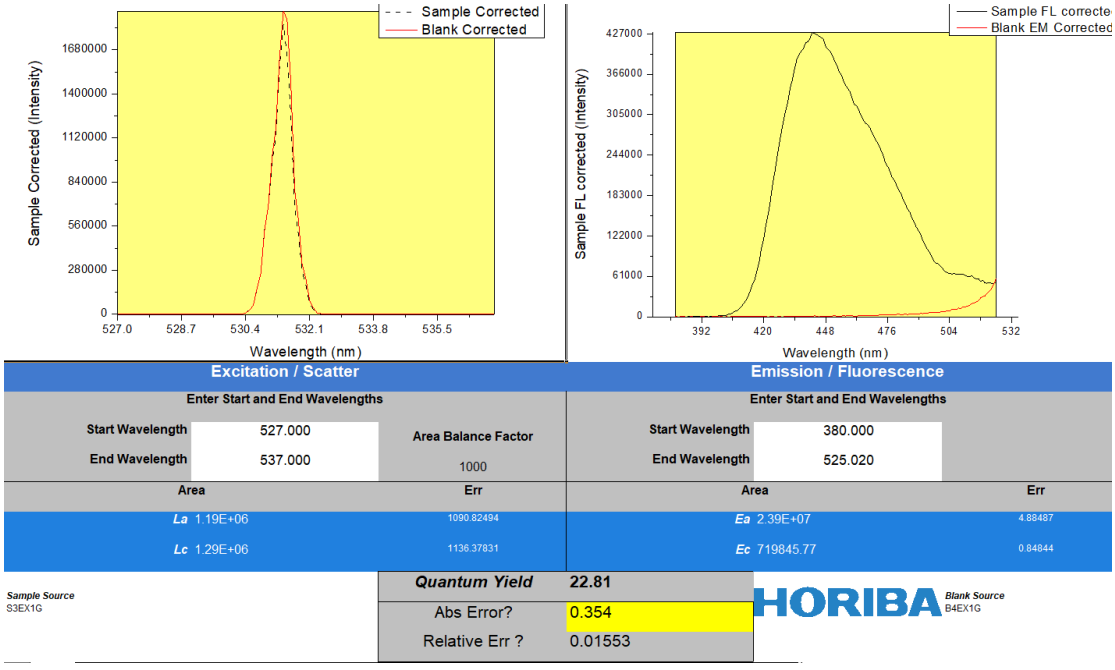

Fig. S100 The detailed calculation of quantum yields of UC dry gel with **PtOEP** as triplet photosensitizer and **DPAS** as triplet acceptor. Abs Error represents the absolute Error of this measurement; Relative Err refers the Relative error of this measurement.

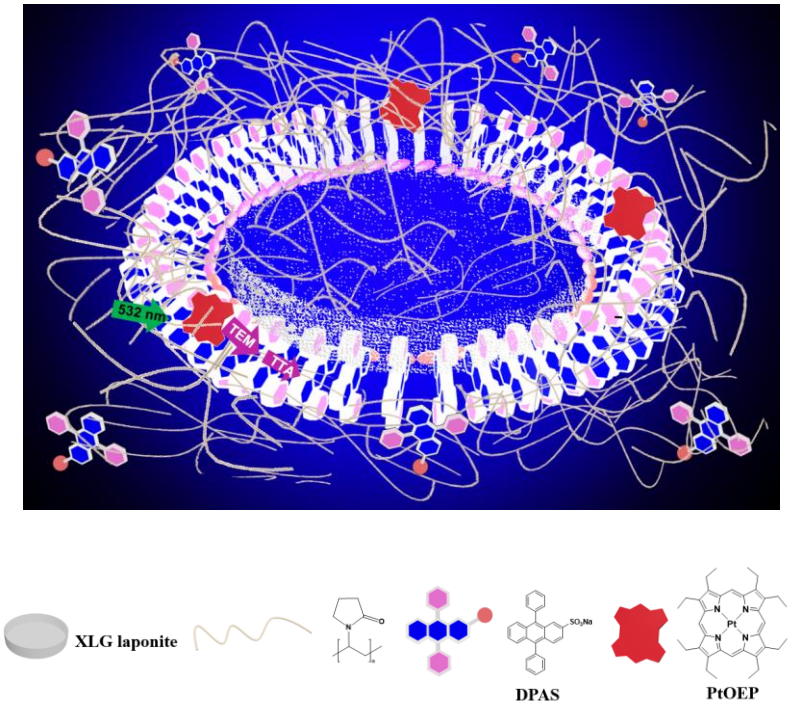

Fig. S101 Schematic diagram of the clay nanosheet act as an independent unit for TTA-UC.

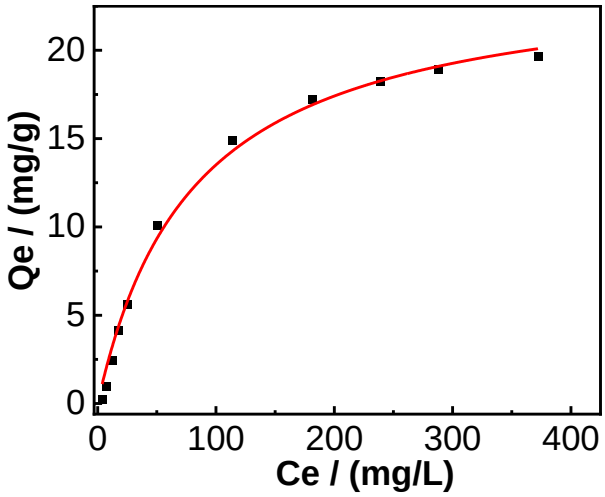

Fig. S102 Equilibrium adsorption isotherms of **DPAS** onto the Laponite surface at 1.5 mL of aqueous solution. Laponite concentration= 10.0 g L^{-1}. Black solid squares are experimental data, and red line represents the best fitting to the Langmuir adsorption model.

10.0 References

1. S. Hisamitsu, N. Yanai and N. Kimizuka, *Angew. Chem. Int. Ed. Engl.*, 2015, **54**, 11550-11554.
2. S. Kolemen, T. Ozdemir, D. Lee, G. M. Kim, T. Karatas, J. Yoon and E. U. Akkaya, *Angew. Chem. Int. Ed.*, 2016, **55**, 3606-3610.
3. C. Fan, L. Wei, T. Niu, M. Rao, G. Cheng, J. J. Chruma, W. Wu and C. Yang, *J. Am. Chem. Soc.*, 2019, **141**, 15070-15077.
4. R. P. Briñas, T. Troxler, R. M. Hochstrasser and S. A. Vinogradov, *J. Am. Chem. Soc.*, 2005, **127**, 11851-11862.
5. M. Hosoyamada, N. Yanai, T. Ogawa and N. Kimizuka, *Chemistry*, 2016, **22**, 2060-2067.
6. A. Abulikemu, Y. Sakagami, C. Heck, K. Kamada, H. Sotome, H. Miyasaka, D. Kuzuhara and H. Yamada, *ACS Appl. Mater. Interfaces*, 2019, **11**, 20812-20819.
7. E. Radiunas, M. Dapkevicius, S. Raisys, S. Jursenas, A. Jozeliunaite, T. Javorskis, U. Sinkeviciute, E. Orentas and K. Kazlauskas, *Phys. Chem. Chem. Phys.*, 2020, **22**, 7392-7403.
8. S. Raisys, K. Kazlauskas, S. Jursenas and Y. C. Simon, *ACS Appl. Mater. Interfaces*, 2016, **8**, 15732-15740.
9. M. Wu, D. N. Congreve, M. W. B. Wilson, J. Jean, N. Geva, M. Welborn, T. Van Voorhis, V. Bulović, M. G. Bawendi and M. A. Baldo, *Nat. Photonics*, 2015, **10**, 31-34.
10. M. Oldenburg, A. Turshatov, D. Busko, S. Wollgarten, M. Adams, N. Baroni, A. Welle, E. Redel, C. Wöll, B. S. Richards and I. A. H. *, *Adv. Mater.*, 2016, **28**, 8477-8482.
11. T.-A. Lin, C. F. Perkinson and M. A. Baldo, *Adv. Mater.*, 2020, **32**, 1908175.
12. X. Jiang, X. Guo, J. Peng, D. Zhao and Y. Ma, *ACS Appl. Mater. Interfaces*, 2016, **8**, 11441-11449.
13. F. Marsico, A. Turshatov, R. Pekoz, Y. Avlasevich, M. Wagner, K. Weber, D. Donadio, K. Landfester, S. Baluschev and F. R. Wurm, *J. Am. Chem. Soc.*, 2014, **136**, 11057-11064.
14. P. Mahato, A. Monguzzi, N. Yanai, T. Yamada and N. Kimizuka, *Nat. Mater.*, 2015, **14**, 924-930.
15. T. Kashino, M. Hosoyamada, R. Haruki, N. Harada, N. Yanai and N. Kimizuka, *ACS Appl. Mater. Interfaces*, 2021, **13**, 13676-13683.
16. M. Kinoshita, Y. Sasaki, S. Amemori, N. Harada, Z. Hu, Z. Liu, L. K. Ono, Y. Qi, N. Yanai and N. Kimizuka, *ChemPhotoChem*, 2020, **4**, 5271-5278.
17. A. Turshatov, D. Busko, N. Kiseleva, S. L. Grage, I. A. Howard and B. S. Richards, *ACS Appl. Mater. Interfaces*, 2017, **9**, 8280-8286.
18. T. Ogawa, N. Yanai, S. Fujiwara, T.-Q. Nguyen and N. Kimizuka, *J. Mater. Chem. C*, 2018, **6**, 5609-5615.
19. S. Raišys, O. Adomėnienė, P. Adomėnas, A. Rudnick, A. Köhler and K. Kazlauskas, *J. Phys. Chem. C*, 2021, **125**, 3764-3775.
20. T. Ogawa, M. Hosoyamada, B. Yurash, T. Q. Nguyen, N. Yanai and N. Kimizuka, *J. Am. Chem. Soc.*, 2018, **140**, 8788-8796.
21. K. Kamada, Y. Sakagami, T. Mizokuro, Y. Fujiwara, K. Kobayashi, K. Narushima, S. Hirata and M. Vacha, *Mater. Horiz.*, 2017, **4**, 83-87.
22. J.-H. Kim, F. Deng, F. N. Castellano and J.-H. Kim, *Chem. Mater.*, 2012, **24**, 2250-2252.
23. R. Enomoto, M. Hoshi, Y. Murakami, H. Oyama, H. Uekusa, H. Agata, S. Kurokawa, H.

Kuma and Y. Murakami, *Mater. Horiz.*, 2021, **8**, 3449-3456.
24. A. Monguzzi, F. Bianchi, A. Bianchi, M. Mauri, R. Simonutti, R. Ruffo, R. Tubino and F. Meinardi, *Adv. Energy Mater.*, 2013, **3**, 680-686.
25. A. Ronchi, C. Capitani, V. Pinchetti, G. Gariano, M. L. Zaffalon, F. Meinardi, S. Brovelli and A. Monguzzi, *Adv. Mater.*, 2020, **32**, 2002953.
26. P. Bharmoria, S. Hisamitsu, H. Nagatomi, T. Ogawa, M. A. Morikawa, N. Yanai and N. Kimizuka, *J. Am. Chem. Soc.*, 2018, **140**, 10848-10855.